

DYNAMICS OF MULTI-SPAN CATENARY SYSTEMS

MUHI CHANDRA BORGOHAIN

**Thesis submitted for the degree of
Doctor of philosophy**

University of Edinburgh

November 1970



ACKNOWLEDGEMENTS

The author wishes to acknowledge with gratitude the constant advice of his thesis supervisors, particularly Dr. G.T.S. Done and Dr. A.D.S. Barr.

Special thanks are due to Mr. George Smith for his skill and advice in constructing the experimental models, Miss A. Myles for her speed and accuracy in typing this thesis and colleagues for their constant cooperation throughout the research.

Finally acknowledgement is due to the Government of Assam (India) for awarding the author a scholarship for the three years of the research period.

Muhi C. Borgohain.

SUMMARY

In this Thesis the dynamics of multi-span catenary systems are studied in which all the suspension points are at the same level and the catenaries are shallow. The dynamics of single span catenaries have been previously studied by many researchers but the knowledge gained could be applied to multi-span cases only with difficulty.

It was found that the Rayleigh-Ritz method could be applied successfully in the multi-span case for finding normal modes and natural frequencies provided arbitrary modes were introduced to represent inter-span coupling. The particular case of equal spans coupled through suspension arms was examined. Also, the effect of tower flexibilities on the natural frequencies of a set of equal spans connected between two towers was investigated. For the latter case, flexibility matrices for inplane and lateral loads needed to be calculated and for this purpose an approximate procedure for calculating the flexibility matrices of any tower was devised.

Nonlinear dynamics of single span ends-fixed catenaries were considered and found to be very difficult to analyse. Nonlinear effects were observed in the laboratory by constructing simple models and the phenomena observed were explained on a physical basis.

A preliminary study of the nonlinear couplings in multi-span catenary systems was performed and from this it was concluded that nonlinear couplings were less important than in single span catenaries.

CONTENTS

	Page No.
Principal Notations	i
<u>Chapter 1 - Introduction</u>	
1.1 Summary of previous works	1
1.2 Observations at Red Moss Test Line	3
1.3 Purpose of the present research	6
1.4 Summary of various models of aerodynamic excitation	7
<u>Chapter 2 - Critical Assessment of the Methods of Obtaining Normal Modes and Natural Frequencies of Single Span Fixed-Fixed Catenary</u>	
2.1 Resume' of Saxon and Cahn's Asymptotic method	11
2.2 Resume' of Simpson's Lumped-parameter method	15
2.3 Rayleigh-Ritz method	25
2.4 ^a Comparative Study of the above three methods	33
<u>Chapter 3 - Natural Frequencies and Normal Modes of Multi-span Catenary Systems</u>	
3.1 Inplane Modes	42
3.2 Lateral Modes	48
3.3 Calculation for Red Moss Test Line	54
<u>Chapter 4 - Natural Frequencies and Normal Modes of Systems Composed of Equal Subsystems</u>	
4.1 Coupling of equal spans through suspension arms	73
4.2 Coupling of equal spans through tower flexibility	78

<u>Chapter 5 - Nonlinear Coupling Between Inplane and Lateral Modes of an Inextensible Catenary</u>	89
<u>Chapter 6 - Nonlinear Coupling Between Inplane and Lateral Modes of Multi-span Catenaries</u>	114
6.1 Single span free-free catenary	114
6.2 Nonlinear effects in multi-span catenary systems	120
6.3 Comments about Red Moss Test Line excitation system	121
<u>Chapter 7</u>	128
7.1 Discussion	128
7.2 Areas of Further Studies	130
References	133
Appendix A - Catenaries with various end conditions	138
Appendix B - Flexibility of towers	144
Appendix C - Analytical methods applied to (5.13)	156
Appendix D - Digital computer program for solving nonlinear differential equations	167
Appendix E - Normal modes and natural frequencies of a catenary with three extra point masses	171
Appendix F - Design of the catenary model	177

PRINCIPAL NOTATIONS(i) Important Matrix Symbols

D, V, W	Displacement vector (various suffices)
E	Stiffness matrix
F	Force vector
Fl_i	Inplane flexibility matrix
G	Transposition matrix associated with inplane inertia matrix (Simpson's method)
I	Unit matrix
J	Transposition matrix
M	Inertia matrix (various suffices)
Q	Transformation matrix associated with inplanemotion
V	Potential energy
T	Kinetic energy
Ψ	Modal matrix (various suffices)

(ii) Other Important Symbols (scalar)

d	Dip of a catenary
E	Young's modulus of elasticity
f	Frequency in Hz
g	Acceleration due to gravity
H	Horizontal component of cable tension
H_i	Non-dimensionalised horizontal co-ordinate, h_i/A
h_i	Horizontal point co-ordinate
K	Stiffness of the elastic band
L	Length of cable, half span of a catenary

l	Length of links comprising an inextensible catenary
l_s	Length of suspension arms
M_s	Mass of suspension arms
m	Point mass, mass/unit length of the cable
N	Number of point masses per span
R	Non dimensionalised elongation of one elastic band, r/l
r	Elongation of one elastic band
S_i	See θ_i
t_i	Tan θ_i
u	Horizontal displacement at the cable end point (various subscripts), normal displacement
v	General vertical deformation of a cable tangential displacement
V_i	Non-dimensionalised vertical co-ordinate, v_i/l
v_i	Vertical point co-ordinate
W	Weight carried by the suspension arm
X	Non-dimensionalised co-ordinate, x/l
x	Vertical deflection of the mass on two elastic bands
Z_i	Non-dimensionalised lateral co-ordinate, z_i/l
z_i	Lateral point co-ordinate
α	Angle made by a point on the catenary to the horizontal
ϵ	Small parameter

- λ An eigenvalue, frequency parameter is Saxon and Cahn's method, Lagrange multiplier
- ω Circular frequency (rad/sec)

(iii) Suffices

- e Denotes value at equilibrium
- v Denotes vertical motion or displacement i.e. D_V
denotes vector of vertical displacement
- v_S Vertical symmetrical modes in spans
- v_{AS} Vertical antisymmetrical modes in spans
- z Denotes lateral motion or displacement
- h Denotes horizontal motion or displacement
- t Denotes transformation i.e. D_{Vt} is derived from D_V
by omitting one of the elements in the latter
- i,j Denote the element in the ith row and jth column of
the matrix to which they are attached

(iv) Brackets

- { } Denotes a column vector
- [] Denotes a row vector
- [] Denotes a square matrix or a rectangular matrix
- [] Denotes a diagonal matrix

Transposition is denoted by a "dash"

Numbers in [] denote references at the back of the main thesis.

INTRODUCTION1.1 SUMMARY OF PREVIOUS WORK

The subject of oscillating catenaries has been frequently discussed in the technical literature for the last hundred years. Rohrs, in the mid-nineteenth century formulated a set of differential equations for inplane motions of a single uniform catenary and obtained approximate solutions for the case where the catenary was considered 'flat' [27]. Routh devoted a complete chapter in his famous book "Advanced Rigid Dynamics" to the problem of the oscillating suspension chain and formed the following equations for inplane motions.

$$\left. \begin{aligned} m(s) \frac{\partial^2 x}{\partial t^2} &= \frac{\partial}{\partial s} \left(T \frac{\partial x}{\partial s} \right) \\ m(s) \frac{\partial^2 y}{\partial t^2} &= \frac{\partial}{\partial s} \left(T \frac{\partial y}{\partial s} \right) - m(s)g \\ \left(\frac{\partial x}{\partial s} \right)^2 + \left(\frac{\partial y}{\partial s} \right)^2 &= 1 \end{aligned} \right\} \quad (1.1)$$

where $x(s,t)$ and $y(s,t)$ are the space coordinates of any point on the chain, s is the distance along the chain to this point from the vertex, $m(s)$ is the mass per unit length of the chain and $T(s,t)$ is the dynamical tension at this point at time t .

Routh found (1.1) to be analytically intractable for a uniform chain and proceeded to solve artificially for the particular case where the mass distribution was such that it hung in equilibrium in the form of a cycloid [28].

Many approximate solutions to (1.1) have been put forward since the initial work of Routh. The most notable solutions are those of Saxon and Cahn [29] and Goodey [10]. Saxon and Cahn formed a fourth order differential equation in tangential displacement and obtained approximate solutions by an asymptotic method. Goodey simplified the Saxon and Cahn's procedure by changing the axes of reference in (1.1) to tangent - normal form and obtained approximate solutions by a modified asymptotic method.

Engineers have long been interested in the statical and dynamical problems of suspended cables chiefly because of their wide use in suspension bridges and electrical power transmission line systems. Sir Alfred Pugsley was the first to put forward some semi-empirical formulae for the first three natural frequencies of a flat uniform suspension chain which are widely used in suspension bridge and transmission line design [23]. Reissner used the Rayleigh-Ritz method to obtain an approximate solution for the lowest frequency of an entire suspension bridge system [26]. Much work on finite difference technique applied to cables and bridges was carried out at the N.P.L. (National Physical Laboratory) by Frazer and Scruton [8]. Some recent advancements towards the transmission line oscillation problem have been made by R.A. Scriven of the C.E.R.L. (Central Electricity Research Laboratory) who succeeded in generalising (1.1) to three dimensions and obtained approximate solutions for the case where the boundary conditions involved end relaxations. He also successfully derived the equations for inplane motion of an elastic catenary but did not provide any solution [30, 31, 32]. More recently Simpson used the lumped parameter method and found it very successful. He represented a cable by a series of lumped masses connected by weightless strings and used matrix methods for the normal mode analysis with the aid of a digital computer.

He also successfully generalised his lumped parameter method to the case of elastic and multi-span catenary systems [35].

Although nonlinear effects are known to be important in catenary dynamics, relatively little work has been done on the subject. Poskitt formulated a nonlinear equation of motion for large transverse oscillations of sagging cables and obtained approximate solutions by substituting a combination of assumed modes [22]. Simpson, [35], described the effect of nonlinear coupling between inplane and lateral modes and compared the system with the elastic pendulum of Minorsky [20, 21] which can exhibit autoparametric excitation.

1.2 OBSERVATIONS AT RED MOSS TEST LINE

As a result of a contract with the S.S.E.B. (South of Scotland Electricity Board) the writer spent most of his research period on problems concerning the Red Moss Test Line. The line is situated at Douglas Moor, Lanarkshire. A profile of the test line is given in Fig. 3.2 while the assumed test line configuration, which will be used in a later part of this Thesis (Chapter 3), is represented in Fig. 3.3. It comprises five spans, erected on 400-KV suspension towers, with anchor towers at each end. The top and bottom phases of the 275-KV circuit (on the West) are strung with normally stranded 0.175 sq. inch copper equivalent S.C.A. (Steel cured aluminium) conductor, but the middle phase is strung with smooth bodied conductor with a copper equivalent of 0.225 sq. inch. Similarly on the 400-KV (on the east) circuit, the top and bottom phases comprise quadruple bundles of 0.4 sq. inch copper equivalent S.C.A. conductor but the middle phase is strung with a smooth bodied conductor of the same copper equivalent area. A plane view of the experimental line with directions is given in Fig. 1.1.

Construction of the line was completed in May 1963, although modifications are continually being made. The above specifications of the Test Line were being extracted from an unspecified C.E.R.L. circulation.

On 27th November 1964, vertical galloping of top and bottom phases of 400-KV and 275-KV circuits was observed at Red Moss. The salient features of the observations were obtained through private communications with the S.S.E.B. and are summarised below.

- a) Oscillation on the top and bottom phases of the 400-KV circuit involved spans 3-4 and 4-5 in anti-phase with an insulator movement of ± 15 deg. at tower 4, the insulator moving away from the rising span. The numbering of the spans is shown in Fig. 1.1. The middle phase was steady. A double amplitude of 14 to 16 ft. on the top and bottom phases was estimated. The mode of vibration was fundamental with a frequency of $\frac{1}{4}$ to $\frac{1}{5}$ HZ.
- b) A maximum movement of 2 ft. double amplitude occurred on the bottom phase, span 3-4 of the 275-KV circuit, with little on the top phase and none on the middle. The movement on span 3-4, bottom phase, was not in the fundamental mode but at a higher order accompanied by subconductor oscillation and including both vertical and horizontal (lateral) components. Movement on the top phase was of lower order.

Galloping was again observed on the twin earth wire of the Red Moss experimental line on 17th December 1968. The oscillation involved spans 3-4 and 4-5 with a vertical amplitude of ± 1 ft. and a torsional amplitude of ± 45 deg. on span 4-5 and a vertical amplitude of ± 1 ft. and torsional amplitude of 0-90 deg. on span 3-4.

Both the vertical and torsional modes were fundamental with a frequency of $\frac{1}{4}$ HZ., but not in phase, the vertical leading the torsional by less than half of a cycle.

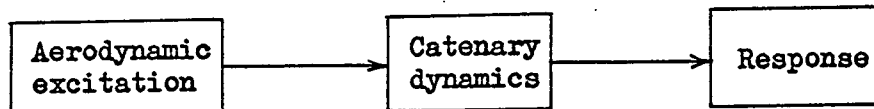
The writer with Dr. G.T.S. Done and Dr. A.D.S. Barr went to the site and observed the natural and forced vibration of the Test Line. To facilitate forcing the line is fitted with a hydraulic exciter (made by Dowty - Rotol) at tower 4, the exciter being controlled from a control hut (see Fig. 1.1) which is situated some 300 ft. from tower 4. The displacement and force produced at the excitation point were fed back to a pen recorder at the control hut and visual observation of the conductor movements was made. A preliminary theoretical calculation for the normal modes and natural frequencies was performed of which the results are given in Chapter 3. In addition to the normal modes, some unusual oscillations were observed which are summarised below.

Forcing Frequency	Description of Conductor Movements
0.15 HZ.	Spans 4-5 and 5-6 are in phase at 0.4 HZ.
0.17 HZ.	Spans 3-4, 4-5 are in anti-phase at exciting frequency and span 2-3 moving at double the exciting frequency.
0.36 HZ.	Span 5-6 vibrating first in fundamental and later span 3-4 building up to fundamental at 0.17 HZ.
0.39 HZ.	Span 4-5, 5-6 are in phase in fundamental, span 5-6 having large amplitude, span 3-4 in fourth fundamental at 0.85 HZ.

The traces from the pen recorder were observed and in most cases it was seen that force produced was of double the frequency of the displacement at the excited point.

1.3 PURPOSE OF THE PRESENT RESEARCH

The overall problem of galloping can be expressed as a simple block diagram as given below.



The various models of aerodynamics excitation which have so far been postulated and used are given in the succeeding section. The object of the present research is to study catenary dynamics which is still not fully understood, meanwhile ignoring models of aerodynamic excitation. The methods of solving the oscillating catenary problem, mentioned in section 1.1, have certain limitations; for example, none of the methods is easily applicable to multi-span cases. The method of Saxon and Cahn as well as Goodey becomes cumbersome even when the case of a simple uniform catenary with relaxed ends is considered [32]. Pugsley's procedure based on elementary wave theory is not applicable to multi-span cases. This is because little is known regarding wave reflection and restitution at the points of span-interconnection. Reissner's Rayleigh-Ritz method is of course applicable to the multi-span case, but, as pointed out by Pugsley in [23], the expressions become so vastly complicated that one may lose insight into the physical problem. The finite difference technique introduced by Frazer and Scruton, although free from the above limitations, were never used explicitly to solve for the modes and the frequencies of catenaries.

The Simpson's lumped parameter method is also free from all the limitations and applicable to multi-span cases. But, here too, the ultimate matrices become so large that it does not appear that the method can be conveniently used to deal with five, six or more spans simply because the total number of degrees of freedom becomes too great for straightforward solution on a digital computer. Less cumbersome is the Simpson's transfer function method [37], but this is only used for inplane modes. Thus although the dynamics of the single span are well understood, there is no really satisfactory method of analysing a multi-span catenary system.

1.4 SUMMARY OF VARIOUS MODELS OF AERODYNAMIC EXCITATION

There have been many mechanisms of excitation postulated to explain certain galloping phenomena and it is reasonable to say that this area of interest has been well investigated. All the models of excitation which are given below depend basically on an instability mechanism.

Vibration due to sleet [11, 12]

When the wind blows past a cable of circular cross-section, it exerts a mean force on the cable having the same direction as the wind. In the case where the cross-section of the cable becomes unsymmetric due to accretion of ice, this will no longer hold true, and an angle will be included between the direction of the wind and that of the force. As a result there will be a force component normal to the wind (lift) as well as the component in the direction of the wind (drag). These lift and drag forces provide a damping term in the equation of motion of the cable normal to the wind and when this term becomes negative, any vibration, however small, will be increased in amplitude.

The condition for negative damping is achieved when the effect of the negative slope of the lift curve is greater than the damping action due to the drag. This is also known as "Den-Hartog Instability".

Variation of Separation Points on Helically Wrapped Stranded Cables [30]

Results of Aerodynamic tests (see Davis, Richards and Scriven [6]) showed the existence of a region of wind speed in which there was a negative rate of change of drag force with increase of wind speed. Also in this region for a yawed wind, a very substantial lift force existed which varied rapidly with increase of wind speed, even changing sign. The drag force characteristics gave rise to a Den-Hartog type instability but this time in the lateral sense. Scriven suggested that catenary modes excited laterally would cause a fluctuating lift force and so excite the inplane modes. Since the antisymmetric lateral and inplane modes have nearly equal frequencies for shallow catenaries, then it would appear that excitation of the inplane antisymmetric modes is at resonance and large amplitudes can be expected. The characteristics of the lift and drag variations are, of course, associated with the separation phenomena of the flow over the surface of the conductor [6].

Frozen Raindrops in Twin Power Transmission Lines [38]

Simpson and Lawson, using quasi-static aerodynamic forces, formed the equations of motion for a single span catenary oscillating fundamentally in vertical, lateral and torsional antisymmetric modes. Using an approach similar to that used in aircraft aeroelasticity they studied the stability of the three constituent binary systems over a wide range parameter (including the positioning of an ice ridge on each conductor).

They showed that flutter leading to large amplitude oscillation occurs in predominantly vertical modes. This can happen for a certain configuration of wind speed and incidence, equilibrium configuration of twin line and when thin ridges of ice in the form of frozen raindrops are present on the conductors.

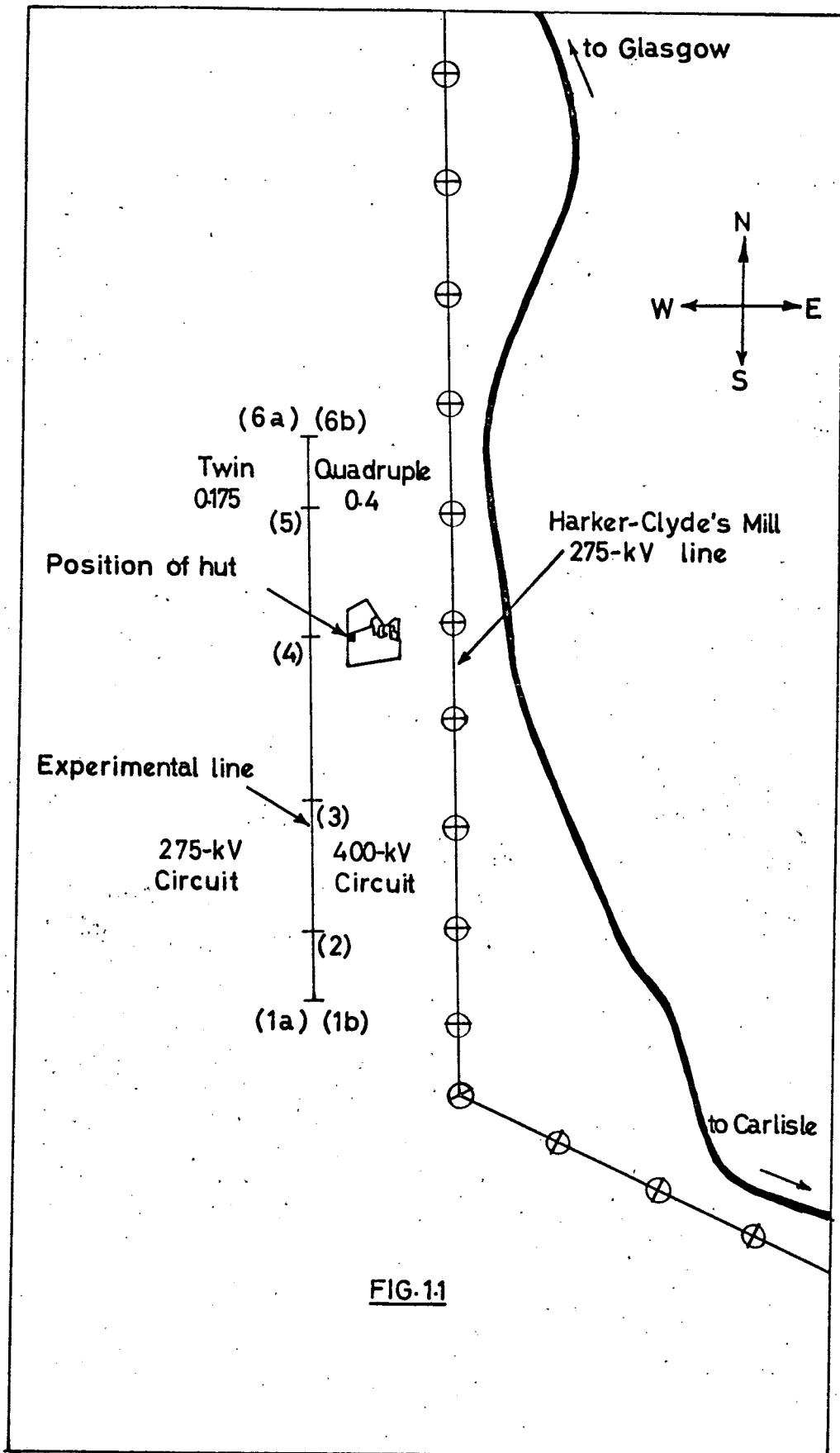


FIG. 1.1

CHAPTER 2CRITICAL ASSESSMENT OF THE METHODS OF OBTAINING NORMAL
MODES AND NATURAL FREQUENCIES OF SINGLE SPAN FIXED-FIXED
CATENARIES2.1 RESUME' OF SAXON AND CAHN'S ASYMPTOTIC METHOD [29]

Consider an inextensible cable of length L suspended from two fixed points at the same level at a distance $a(\leq L)$ apart. Let s be the arc length measured along the cable to a given point from the mid-point of the cable and $x(s,t)$ and $y(s,t)$ be the space coordinates of this point, where x and y are referred to the lowest point of the equilibrium catenary as origin, as shown in Fig. 2.1. If $T(s,t)$ is the tension per unit mass per unit length of the chain, the equations for inplane motions of the cable can be written as -

$$\frac{\partial^2 x}{\partial t^2} = \frac{\partial}{\partial s} \left(T \frac{\partial x}{\partial s} \right) \quad (2.1)$$

$$\frac{\partial^2 y}{\partial t^2} = \frac{\partial}{\partial s} \left(T \frac{\partial y}{\partial s} \right) - g \quad (2.2)$$

To ensure conservation of length during motion, the cable is subject to an equation of constraint given by

$$\left(\frac{\partial x}{\partial s} \right)^2 + \left(\frac{\partial y}{\partial s} \right)^2 = 1 \quad (2.3)$$

The equations (2.1) - (2.3) are to be solved for small departures from the equilibrium position.

Equilibrium Values

To obtain the equations describing the equilibrium catenary, the time derivatives in (2.1) - (2.3) are set equal to zero. When these static equations are solved and expressed in terms of the angle α , which the tangent to the catenary at s makes with the x -axis, they yield the following well known equations

$$x \cancel{X}' = L \frac{\sinh^{-1}(\tan \alpha)}{2 \tan \alpha_0} \quad (2.4)$$

$$y \cancel{Y}' = L \frac{\sec \alpha - 1}{2 \tan \alpha_0} \quad (2.5)$$

$$T = \frac{9L}{2 \tan \alpha_0} \frac{1}{\cos \alpha} \quad (2.6)$$

$$s = \frac{L}{2} \frac{\tan \alpha}{\tan \alpha_0} \quad (2.7)$$

where α_0 is the value of α at the ends of the cable corresponding to $s = \pm \frac{L}{2}$.

Small Amplitude Approximation

Assume a solution differing little from the equilibrium catenary, such that

$$\left. \begin{aligned} x \cancel{X}' &= X_e + \xi(s, t) \\ y \cancel{Y}' &= Y_e + \eta(s, t) \\ T &= T_e + \tau(s, t) \end{aligned} \right\} \quad (2.8)$$

where the subscript e refers to the equilibrium values. Substituting (2.8) into (2.1) - (2.3) and neglecting quadratic terms in the small quantities ξ , η and τ they find

$$\left. \begin{aligned} \frac{\partial^2 \xi}{\partial t^2} &= \frac{\partial}{\partial s} \left(T_e \frac{\partial \xi}{\partial s} + \tau \frac{dx_e}{ds} \right) \\ \frac{\partial^2 \eta}{\partial t^2} &= \frac{\partial}{\partial s} \left(T_e \frac{\partial \eta}{\partial s} + \tau \frac{dy_e}{ds} \right) \\ \frac{dx_e}{ds} \frac{\partial \xi}{\partial s} + \frac{dy_e}{ds} \frac{\partial \eta}{\partial s} &= 0 \end{aligned} \right\} \quad (2.9)$$

Changing the space variable from s to α by use of (2.7) and assuming that

ξ , η and τ are proportional to $\exp(-i\omega t)$, (2.9) become

$$-\lambda^2 \xi = \cos^2 \alpha \frac{d}{d\alpha} \left(\cos \alpha \frac{d\xi}{d\alpha} + \tau \cos \alpha \right) \quad (2.10)$$

$$-\lambda^2 \eta = \cos^2 \alpha \frac{d}{d\alpha} \left(\cos \alpha \frac{d\eta}{d\alpha} + \tau \sin \alpha \right) \quad (2.11)$$

$$\cos \alpha \frac{d\xi}{d\alpha} + \sin \alpha \frac{d\eta}{d\alpha} = 0 \quad (2.12)$$

$$\text{where} \quad \lambda^2 = \frac{L \omega^2}{2 g \tan \alpha_0} \quad (2.13)$$

Saxon and Cahn now introduce new variables u and v , locally perpendicular and tangential to the equilibrium catenary as shown in Fig. 2.2, so that

$$\left. \begin{aligned} \xi &= v \cos \alpha - u \sin \alpha \\ \eta &= u \sin \alpha + v \cos \alpha \end{aligned} \right\} \quad (2.14)$$

Substituting (2.14) into (2.10) - (2.12) they obtain

$$\frac{\lambda^2}{\cos^2 \alpha} v = v \cos \alpha - u' \cos \alpha - \tau \quad (2.15)$$

$$\frac{\lambda^2}{\cos^2 \alpha} u = -u'' \cos \alpha + u' \sin \alpha - u \cos \alpha - \tau + v \sin \alpha \quad (2.16)$$

$$v' = u \quad (2.17)$$

where the primes denote differentiation with respect to α . Elimination of τ from (2.15) - (2.17) gives the following fourth order differential equation for v :

$$(v'''' + v'')\cos\alpha - 2(v''' + v')\sin\alpha + \frac{\lambda^2}{\cos^3\alpha}(v''\cos\alpha + 2v'\sin\alpha - v\cos\alpha) = 0 \quad (2.18)$$

The factor λ^2 is large and so Saxon and Cahn solve (2.18) to order $1/\lambda^2$ by writing

$$v = \sum v_n \lambda^{-2n} \quad (2.19)$$

Thus they find

$$v = \frac{A}{i\lambda} \cos^{7/4}\alpha e^{i(\lambda f + g/\lambda)} - \frac{B}{i\lambda} \cos^{7/4}\alpha e^{-i(\lambda f + g/\lambda)} + C \sin\alpha + D(\cos\alpha + \alpha \sin\alpha) \quad (2.20)$$

with four arbitrary constants A, B, C, D and where

$$f(\alpha) = \int_0^\alpha \frac{d\alpha}{\cos^{3/2}\alpha} \quad (2.21)$$

$$g(\alpha) = \frac{11}{8} \int_0^\alpha (1 + \frac{1}{44} \tan^2\alpha) \cos^{3/2}\alpha d\alpha \quad (2.22)$$

working back for u , they find

$$u = A \cos^{1/4}\alpha e^{i(\lambda f + g/\lambda)} + B \cos^{1/4}\alpha e^{-i(\lambda f + g/\lambda)} + C \cos\alpha + D\alpha \cos\alpha \quad (2.23)$$

Manipulation of their formulae gives

$$\tau = A(2\cos^{5/4}\alpha + \frac{\cos^{7/4}\alpha \sin\alpha}{i\lambda}) e^{i(\lambda f + g/\lambda)} + B(2\cos^{5/4}\alpha - \frac{\cos^{7/4}\alpha \sin\alpha}{i\lambda}) e^{-i(\lambda f + g/\lambda)} - \frac{\lambda^2 C}{\cos\alpha} - D(\frac{\lambda^2 \alpha}{\cos\alpha} - 4 \sin\alpha \cos\alpha) \quad (2.24)$$

Under the requirements that u and v vanish at $\alpha = \pm \alpha_0$, the solutions decompose into odd and even pairs which lead immediately to the following transcendental equations for λ :

Odd modes (u odd about $\alpha = 0$, v even)

$$\tan(\lambda f + g/\lambda) = -\frac{1}{\lambda} \frac{\alpha \cos^{5/2} \alpha}{\cos \alpha + \alpha \sin \alpha} = -\frac{1}{\lambda} h(\alpha) \quad (2.25)$$

Even modes (u even about $\alpha = 0$, v odd)

$$\cot(\lambda f + g/\lambda) = \frac{1}{\lambda} \frac{\cos^{5/2} \alpha}{\sin \alpha} = \frac{1}{\lambda} k(\alpha) \quad (2.26)$$

If $\lambda \gg 1$, for odd and even modes respectively

$$\lambda f = n\pi, \quad n = 1, 2, \dots \quad (2.27)$$

$$\lambda f = (n + \frac{1}{2})\pi, \quad n = 1, 2, \dots \quad (2.28)$$

Expanding (2.25) and (2.26) to order $1/\lambda^2$, the explicit solutions are:

Odd modes

$$\lambda = \frac{n\pi}{f} \left[1 - \frac{f(g+h)}{(n\pi)^2} \right], \quad n = 1, 2, \dots \quad (2.29)$$

Even modes

$$\lambda = \frac{(n+\frac{1}{2})\pi}{f} \left[1 - \frac{f(g+k)}{\{(n+\frac{1}{2})\pi\}^2} \right], \quad n = 1, 2, \dots \quad (2.30)$$

Equations (2.29) and (2.30) give the explicit expressions for λ and hence by (2.13) the characteristic frequencies of the cable.

2.2 RESUME OF SIMPSON'S LUMPED PARAMETER METHOD [35]

For small oscillations of a catenary, the inplane and lateral modes are uncoupled. Hence in analysing the normal modes of vibration of a catenary, the motions normal to the vertical plane of equilibrium can be treated separately from the vertical and cross-span motions.

The catenary is represented by a system of N lumped masses connected together by $N+1$ weightless inextensible links as shown in Fig.

2.3. The span and dip of the lumped-mass catenary are kept equal to those of the actual catenary. As the links are inextensible, the system possesses $2N-1$ ($= 3N - N - 1$) degrees of freedom, $N-1$ in vertical plane and N in lateral plane.

Inplane Motion

Consider the five-mass catenary shown in Fig. 2.4.

Equilibrium Conditions

In the absence of any force other than that due to gravity the system hangs vertically in equilibrium and the funicular polygon of Fig. 2.5 is easily drawn. It is clear from Fig. 2.5 that H , the horizontal component of tension is constant across the span and is given by

$$H = \frac{mg}{2 \tan\theta_1} \quad (2.31)$$

Also from Fig. 2.5, it is clear that

$$\tan\theta_1 = \frac{\tan\theta_3}{3} = \frac{\tan\theta_5}{5} \quad (2.32)$$

Link Kinematics for a General Inplane Displacement

Consider a link between the i th and the j th masses as shown in Fig. 2.6. In a general displacement h_i , v_i , h_j and v_j of the masses, the condition of inextensibility for the link is simply

$$(h_i - h_j + l\cos\theta_i)^2 + (v_i - v_j + l\sin\theta_i)^2 = l^2 \quad (2.33)$$

where l is the length of the link and θ_i is the inclination of the link to the horizontal.

Solving (2.33) for $(h_i - h_j)$ up to $(v_i - v_j)^2$

$$(h_i - h_j) = -\tan\theta_i(v_i - v_j) - \frac{\sec^3\theta_i}{2l}(v_i - v_j)^2 \quad (2.34)$$

After non-dimensionalisation by writing $V_i = \frac{v_i}{l}$ and $H_i = \frac{h_i}{l}$, (2.34)

becomes

$$H_i - H_j = -\tan\theta_i(V_i - V_j) - \frac{\sec^3\theta_i}{2}(V_i - V_j)^2 \quad (2.35)$$

Referring to Fig. 2.4, (2.35) holds true for i odd and $j = i + 2$.

A similar equation can be obtained for i even and $j = i + 2$ by replacing θ_i in (2.35) by $180 - \theta_i$ to give

$$H_i - H_j = \tan\theta_i(V_i - V_j) + \frac{\sec^3\theta_i}{2}(V_i - V_j)^2 \quad (2.36)$$

where $\theta_0 = \theta_1$, $\theta_2 = \theta_3$, $\theta_4 = \theta_5$; since the system has been assumed symmetrical.

Potential Energy in a General Displacement

Equations (2.35) and (2.36) may be written for each link comprising the system of Fig. 2.4, so that

$$\left. \begin{aligned} H_5 &= -t_5 V_5 - \frac{s_5^3}{2} V_5^2 \\ H_3 - H_5 &= -t_3 (V_3 - V_5) - \frac{s_3^3}{2} (V_3 - V_5)^2 \\ H_1 - H_3 &= -t_1 (V_1 - V_3) - \frac{s_1^3}{2} (V_1 - V_3)^2 \\ H_2 - H_1 &= -t_1 (V_1 - V_2) - \frac{s_1^3}{2} (V_1 - V_2)^2 \\ H_4 - H_2 &= -t_3 (V_2 - V_4) - \frac{s_3^3}{2} (V_2 - V_4)^2 \\ -H_4 &= -t_5 V_4 - \frac{s_5^3}{2} V_4^2 \end{aligned} \right\} \quad (2.37)$$

where the compatibility relations $H_0 = H_1$, $V_0 = V_1$ have been used and $t_i = \tan\theta_i$, $S_i = \sec\theta_i$.

Adding (2.37) and using (2.32) to give

$$\begin{aligned} (v_5 + v_3 + v_1 + v_2 + v_4) + \frac{1}{4t_1} [S_5^3 v_5^2 + S_3^3 (v_3 - v_5)^2 + S_1^3 (v_1 - v_3)^2 + S_1^3 (v_1 - v_2)^2 + \\ S_3^3 (v_2 - v_4)^2 + S_5^3 v_4^2] = 0 \end{aligned} \quad (2.38)$$

Solution of (2.38) for V_1 up to second order gives

$$\begin{aligned} V_1 = -(v_5 + v_3 + v_2 + v_4) - \frac{1}{4t_1} [S_5^3 v_5^2 + S_3^3 (v_3 - v_5)^2 + S_1^3 (v_5 + 2v_3 + v_2 + v_4)^2 + \\ + S_1^3 (v_5 + v_3 + 2v_2 + v_4)^2 + S_3^3 (v_2 - v_4)^2 + S_5^3 v_4^2] \end{aligned} \quad (2.39)$$

The system has no spring stiffnesses and hence the potential energy consists wholly of gravitational terms. In fact

$$V = -mg \sum_{i=1}^5 v_i = -mgl \sum_{i=1}^5 v_i \quad (2.40)$$

Substitution of V_1 from (2.39) in (2.40) gives

$$\begin{aligned} V = \frac{mglS_1^3}{4t_1} [(S_5/S_1)^3 v_5^2 + (S_3/S_1)^3 (v_3 - v_5)^2 + (v_5 + 2v_3 + v_2 + v_4)^2 \\ + (v_5 + v_3 + 2v_2 + v_4)^2 + (S_3/S_1)^3 (v_2 - v_4)^2 + (S_5/S_1)^3 v_4^2] \end{aligned} \quad (2.41)$$

In matrix form, the potential energy becomes

$$V = \frac{1}{2} D_{Vt}' E_V D_{Vt} \quad (2.42)$$

with

$$D_{Vt} = \{v_5, v_3, v_2, v_4\} \quad (2.43)$$

$$E_V = \frac{mglS_1^3}{2t_1} [\bar{T}' \Delta \bar{T} + C_1 C_1' + J C_1 C_1' J] \quad (2.44)$$

where

$$\bar{T} = \begin{bmatrix} 1 & 0 & 0 & 0 \\ -1 & 1 & 0 & 0 \\ 0 & 0 & 1 & -1 \\ 0 & 0 & 0 & 1 \end{bmatrix} \quad (2.45)$$

$$\Delta = \left[\left(\frac{s_5}{s_1} \right)^3, \left(\frac{s_3}{s_1} \right)^3, \left(\frac{s_3}{s_1} \right)^3, \left(\frac{s_5}{s_1} \right)^3 \right] \quad (2.46)$$

$$c_1 = \{1, 2, 1, 1\} \quad (2.47)$$

$$J = \begin{bmatrix} 0 & 0 & 0 & 1 \\ 0 & 0 & 1 & 0 \\ 0 & 1 & 0 & 0 \\ 1 & 0 & 0 & 0 \end{bmatrix} \quad (2.48)$$

Kinetic Energy in a General Inplane Displacement

The kinetic energy is given by

$$T = \frac{1}{2} \sum_{i=1}^5 m(\dot{v}_i^2 + \dot{h}_i^2) = \frac{m l^2}{2} (\dot{D}'_V \dot{D}_V + \dot{D}'_H \dot{D}_H) \quad (2.49)$$

where

$$D_V = \{v_5, v_3, v_1, v_2, v_4\} \quad (2.50)$$

$$D_H = \{h_5, h_3, h_1, h_2, h_4\} \quad (2.51)$$

From (2.39) and (2.37) the matrix relations are

$$D_V = \begin{bmatrix} v_5 \\ v_3 \\ v_1 \\ v_2 \\ v_4 \end{bmatrix} = \begin{bmatrix} 1 & 0 & 0 & 0 \\ 0 & 1 & 0 & 0 \\ -1 & -1 & -1 & -1 \\ 0 & 0 & 1 & 0 \\ 0 & 0 & 0 & 1 \end{bmatrix} \begin{bmatrix} v_5 \\ v_3 \\ v_2 \\ v_4 \end{bmatrix} = G D_{Vt} \quad (2.52)$$

$$\text{and } D_H = \begin{bmatrix} H_5 \\ H_3 \\ H_1 \\ H_2 \\ H_4 \end{bmatrix} = t_1 \begin{bmatrix} -5 & 0 & 0 & 0 & 0 \\ -2 & -3 & 0 & 0 & 0 \\ -2 & -2 & -1 & 0 & 0 \\ 0 & 0 & 0 & 3 & 2 \\ 0 & 0 & 0 & 0 & 5 \end{bmatrix} \begin{bmatrix} V_5 \\ V_3 \\ V_1 \\ V_2 \\ V_4 \end{bmatrix} \quad (2.53)$$

Through (2.52), (2.53) becomes

$$D_H = t_1 Q D_V t \quad (2.54)$$

where

$$Q = \begin{bmatrix} -5 & 0 & 0 & 0 & 0 \\ -2 & -3 & 0 & 0 & 0 \\ -2 & -2 & -1 & 0 & 0 \\ 0 & 0 & 0 & 3 & 2 \\ 0 & 0 & 0 & 0 & 5 \end{bmatrix} \begin{bmatrix} 1 & 0 & 0 & 0 \\ 0 & 1 & 0 & 0 \\ -1 & -1 & -1 & -1 \\ 0 & 0 & 1 & 0 \\ 0 & 0 & 0 & 1 \end{bmatrix} = \begin{bmatrix} -5 & 0 & 0 & 0 \\ -2 & -3 & 0 & 0 \\ -1 & -1 & 1 & 1 \\ 0 & 0 & 3 & 2 \\ 0 & 0 & 0 & 5 \end{bmatrix}$$

Hence using (2.52) and (2.54) in (2.49) the kinetic energy becomes

$$T = \frac{ml^2}{2} \dot{D}'_{Vt} (G'G + t_1^2 Q'Q) \dot{D}_{Vt} = \frac{1}{2} \dot{D}'_{Vt} A \dot{D}_{Vt} \quad (2.56)$$

Using Lagrange's equations and using the condition for a normal mode of frequency ω the equations of motion for the simple five-mass catenary can be written as

$$\omega^2 A_V D_{Vt} = E_V D_{Vt} \quad (2.57)$$

The natural modes and frequencies may be obtained by matrix iteration on

$$E_V^{-1} A_V D_{Vt} = \lambda^2 D_{Vt} \quad (2.58)$$

$$\begin{aligned}
 v_5 &= -\frac{z_5^2}{2l_5} \\
 v_3 &= -\frac{z_5^2}{2l_5} - \frac{(z_3 - z_5)^2}{2l_3} \\
 v_1 &= -\frac{z_5^2}{4l_5} - \frac{(z_3 - z_5)^2}{4l_5} - \frac{(z_1 - z_3)^2}{4l_1} - \frac{(z_1 - z_2)^2}{4l_1} - \frac{(z_2 - z_4)^2}{4l_3} - \frac{z_4^2}{4l_5} \\
 v_2 &= -\frac{z_4^2}{2l_5} - \frac{(z_2 - z_4)^2}{2l_3} \\
 v_4 &= -\frac{z_4^2}{2l_5}
 \end{aligned}
 \tag{2.67}$$

where $l_i = l \sin \theta_i$

The potential energy is given by

$$V = -mg \sum_{i=1}^5 v_i \tag{2.68}$$

Through (2.67), (2.68) becomes

$$\begin{aligned}
 V = \frac{mg}{4} \left[\frac{5z_5^2}{l_5} + \frac{3(z_3 - z_5)^2}{l_3} + \frac{(z_1 - z_3)^2}{l_1} + \frac{(z_1 - z_2)^2}{l_1} + \frac{3(z_1 - z_2)^2}{l_3} + \right. \\
 \left. + \frac{5z_4^2}{l_5} \right] \tag{2.69}
 \end{aligned}$$

Writing $l_i = it_1 \cos \theta_i l$, $i = 5, 3, 1$, (2.69) in matrix form becomes

$$V = \frac{1}{2} D_z' E_z D_z \tag{2.70}$$

with

$$D_z = \{z_5, z_3, z_1, z_2, z_4\} \tag{2.71}$$

$$\text{and } E_Z = \frac{mg}{2lt_1} \begin{bmatrix} S_5+S_3 & -S_3 & 0 & 0 & 0 \\ -S_3 & S_3+S_1 & -S_1 & 0 & 0 \\ 0 & -S_1 & 2S_1 & -S_1 & 0 \\ 0 & 0 & -S_1 & S_1+S_3 & -S_3 \\ 0 & 0 & 0 & -S_3 & S_5+S_3 \end{bmatrix} \quad (2.72)$$

Since the coordinates are taken at the mass points the kinetic energy is simply given by

$$T = \frac{m}{2} \sum_{i=1}^5 \dot{z}_i^2 \quad (2.73)$$

In matrix form (2.73) is written as

$$T = \frac{1}{2} \dot{D}'_Z A_Z \dot{D}_Z \quad (2.74)$$

$$\text{where } A_Z = m \times (5 \times 5 \text{ unit matrix}) \quad (2.75)$$

The extensions of (2.71), (2.72) and (2.75) for a general N-mass system (N = odd) are obvious.

On application of Lagrange's equations and the condition for a normal mode of frequency ω

$$E_Z D_Z = \omega^2 A_Z D_Z \quad (2.76)$$

As before the frequencies and modes can be obtained by matrix iteration on

$$E^{-1}_Z A_Z D_Z = \lambda^2 D_Z \quad (2.77)$$

$$\text{where } \lambda^2 = \frac{1}{\omega^2}$$

2.3 RAYLEIGH - RITZ METHOD [3, 19]

It is mentioned earlier in section 1.3 that although the dynamics of single span fixed-fixed catenary are well understood, there is no really satisfactory way of applying this knowledge to multi-span systems. It seemed to the author that here was a good case for applying the Rayleigh-Ritz method to the problem of oscillating catenaries. To assess the applicability we apply the method first to single span fixed-fixed catenary.

Let us consider an inextensible cable suspended from two fixed points at the same level, distant $2L$ apart, as shown in Fig. 28. Let $x(s,t)$, $y(s,t)$, $z(s,t)$ be the spatial coordinates of a point at arc length s , measured along the cable from the midpoint of the cable as origin and time t . Let us assume that the equilibrium shape of the cable, hanging vertically under the influence of gravity only, is parabolic. Then if m is the mass per unit length of the cable and d is the dip of the catenary formed by the cable, the static horizontal component of tension, H , is given by

$$H = \frac{mgL^2}{2d} \quad (2.78)$$

Small Amplitude Approximation

Let us perturb the position of the point (X_e, Y_e, Z_e) by small amount (u, v, w) such that

$$\left. \begin{aligned} X &= X_e + u \\ Y &= Y_e + v \\ Z &= Z_e + w \end{aligned} \right\} \quad (2.79)$$

where the subscript e refers to the equilibrium values.

As the cable is assumed inextensible, the geometrical equation ensuring conservation of length during motion is:

$$\left(\frac{\partial x}{\partial s}\right)^2 + \left(\frac{\partial y}{\partial s}\right)^2 + \left(\frac{\partial z}{\partial s}\right)^2 = 1 \quad (2.80)$$

Substituting (2.79) in (2.80) and using equilibrium conditions, we obtain

$$\left(\frac{\partial u}{\partial s}\right)^2 + 2 \frac{dx_e}{ds} \frac{\partial u}{\partial s} + \left(\frac{\partial v}{\partial s}\right)^2 + 2 \frac{dy_e}{ds} \frac{\partial v}{\partial s} + \left(\frac{\partial w}{\partial s}\right)^2 = 0 \quad (2.81)$$

If the catenary is considered flat, ds in (2.81) can well be replaced by dx_e . Thus we arrive at

$$\left(\frac{\partial u}{\partial x}\right)^2 + \left(\frac{\partial v}{\partial x}\right)^2 + \left(\frac{\partial w}{\partial x}\right)^2 + 2 \frac{\partial u}{\partial x} + 2 \frac{dy}{dx} \frac{\partial v}{\partial x} = 0 \quad (2.82)$$

For convenience, the subscript e has been dropped from dy_e and dx_e in (2.82). Solving (2.82) for $\frac{\partial u}{\partial x}$ to second order we obtain

$$\frac{\partial u}{\partial x} = -\frac{dy}{dx} \frac{\partial v}{\partial x} - \frac{1}{2} \left(\frac{\partial v}{\partial x}\right)^2 - \frac{1}{2} \left(\frac{\partial w}{\partial x}\right)^2 \quad (2.83)$$

For a parabolic catenary, we can write

$$\frac{dy}{dx} = \frac{mgx}{H} \quad (2.84)$$

The equation (2.83), through (2.84) becomes

$$\frac{\partial u}{\partial x} = -\frac{mg}{H} x \frac{\partial v}{\partial x} - \frac{1}{2} \left(\frac{\partial v}{\partial x}\right)^2 - \frac{1}{2} \left(\frac{\partial w}{\partial x}\right)^2 \quad (2.85)$$

Integrating (2.85) between the limits $-L$ and L we obtain

$$mg \int_{-L}^L v dx = \frac{H}{2} \int_{-L}^L \left(\frac{\partial v}{\partial x}\right)^2 dx + \frac{H}{2} \int_{-L}^L \left(\frac{\partial w}{\partial x}\right)^2 dx \quad (2.86)$$

0(2)

As the cable is assumed inelastic, the potential energy is wholly due to gravity and is given by

$$V = mg \int_{-L}^L v dx \quad (2.87)$$

Substituting from (2.86) in (2.87)

$$V = \frac{H}{2} \int_{-L}^L \left(\frac{\partial v}{\partial x}\right)^2 dx + \frac{H}{2} \int_{-L}^L \left(\frac{\partial w}{\partial x}\right)^2 dx \quad (2.88)$$

Neglecting the small cross-span movements of the cable elements, kinetic energy is simply

$$T = \frac{m}{2} \int_{-L}^L \dot{v}^2 dx + \frac{m}{2} \int_{-L}^L \dot{w}^2 dx \quad (2.89)$$

In view of (2.86), the cable is subject to an equation of constraint given by

$$\int_{-L}^L v dx = 0 + o(2) \quad (2.90)$$

From (2.88) - (2.90), it is seen that the inplane and lateral modes are uncoupled for small oscillations of a catenary and hence they can be treated separately from each other.

Inplane Modes

The potential energy is

$$V = \frac{H}{2} \int_{-L}^L \left(\frac{\partial v}{\partial x}\right)^2 dx \quad (2.91)$$

and the kinetic energy

$$T = \frac{m}{2} \int_{-L}^L \dot{v}^2 dx \quad (2.92)$$

The equation of constraint given by (2.90).

Assuming for v a combination of trigonometric or string modes, so called because the mode shapes of elastic string are of this form, we write

$$v = V_1 \cos \frac{\pi x}{2L} + V_2 \sin \frac{\pi x}{L} + V_3 \cos \frac{3\pi x}{2L} + V_4 \sin \frac{2\pi x}{L} + V_5 \cos \frac{5\pi x}{2L} + V_6 \sin \frac{3\pi x}{L} + V_7 \cos \frac{7\pi x}{2L} \quad (2.93)$$

where in (2.93) it is understood that only seven string modes are used.

Substituting the assumed series (2.93) in (2.91) we obtain respectively

$$V = \frac{\pi^2 H}{8L} (V_1^2 + 4V_2^2 + 9V_3^2 + 16V_4^2 + 25V_5^2 + 36V_6^2 + 49V_7^2) \quad (2.94)$$

$$T = \frac{mL}{2} (\dot{V}_1^2 + \dot{V}_2^2 + \dot{V}_3^2 + \dot{V}_4^2 + \dot{V}_5^2 + \dot{V}_6^2 + \dot{V}_7^2) \quad (2.95)$$

$$V_1 - V_3/3 + V_5/5 - V_7/7 = 0 \quad (2.96)$$

From (2.94) - (2.96) it is also observed that the assumed symmetrical and antisymmetrical string modes are uncoupled and can be treated separately.

Symmetrical Inplane Modes

$$V = \frac{\pi^2 H}{8L} (V_1^2 + 9V_3^2 + 25V_5^2 + 49V_7^2) \quad (2.97)$$

$$T = \frac{mL}{2} (\dot{V}_1^2 + \dot{V}_3^2 + \dot{V}_5^2 + \dot{V}_7^2) \quad (2.98)$$

and the equation of constraint is given by (2.96).

In matrix form

$$V = \frac{1}{2} V'_S E_{VS} V_S \quad (2.99)$$

$$T = \frac{1}{2} \dot{V}'_S M_{VS} \dot{V}_S \quad (2.100)$$

where $V_S = \{V_1, V_3, V_5, V_7\}$ (2.101)

$$E_{VS} = \frac{\pi^2 H}{4L} \begin{bmatrix} 1 & & & 0 \\ & 9 & & \\ & & 25 & \\ 0 & & & 49 \end{bmatrix} \quad (2.102)$$

$$M_{VS} = mL \begin{bmatrix} 1 & & & 0 \\ & 1 & & \\ & & 0 & 1 \\ & & & 1 \end{bmatrix} \quad (2.103)$$

From (2.96), we obtain the matrix relation

$$V_S = \begin{bmatrix} V_1 \\ V_3 \\ V_5 \\ V_7 \end{bmatrix} = \begin{bmatrix} 1/3 & -1/5 & 1/7 \\ 1 & 0 & 0 \\ 0 & 1 & 0 \\ 0 & 0 & 1 \end{bmatrix} \begin{bmatrix} V_3 \\ V_5 \\ V_7 \end{bmatrix} = Q V_{st} \quad (2.104)$$

Performing singular transformations of (2.99) and (2.100) we arrive at

$$V = \frac{1}{2} V'_{st} Q' E_{VS} Q V_{st} = \frac{1}{2} V'_{st} E_{Vst} V_{st} \quad (2.105)$$

$$T = \frac{1}{2} \dot{V}'_{st} Q' M_{VS} Q \dot{V}_{st} = \frac{1}{2} \dot{V}'_{st} M_{Vst} \dot{V}_{st} \quad (2.106)$$

Applying Lagrange's equations and the condition for a normal mode of frequency ω

$$E_{VSt} V_{St} = \omega^2 M_{VSt} V_{St} \quad (2.107)$$

Equation (2.107) defines the symmetrical inplane motions of a simple inextensible catenary. The frequencies and the mode shapes may be obtained by matrix iteration on

$$E_{VSt}^{-1} M_{VSt} V_{St} = \lambda^2 V_{St} \quad (2.108)$$

where $\lambda^2 = \frac{1}{\omega^2}$

If a frequency, ω_i , and its associated vector, V_{St}^i , have been determined, we may use (2.104) to give the actual vector corresponding to the normal mode shape. Thus we obtain

$$V_S^i = Q V_{St}^i \quad (2.109)$$

Antisymmetrical Inplane Modes

From (2.94) and (2.95) we can write

$$V = \frac{\pi^2 H}{8L} (4V_2^2 + 16V_4^2 + 36V_6^2) \quad (2.110)$$

$$T = \frac{mL}{2} (\dot{V}_2^2 + \dot{V}_4^2 + \dot{V}_6^2) \quad (2.111)$$

In view of the assumed antisymmetrical motions, the constraint relation $\int_{-L}^L v \, dx = 0$ is automatically satisfied.

In matrix form

$$V = \frac{1}{2} V'_{AS} E_{VAS} V_{AS} \quad (2.112)$$

$$T = \frac{1}{2} \dot{V}'_{AS} M_{VAS} \dot{V}_{AS} \quad (2.113)$$

where E_{VAS} and M_{VAS} are diagonal matrices and are given by

$$E_{VAS} = \frac{\pi^2 H}{L} \begin{bmatrix} 1 & & 0 \\ & 4 & \\ 0 & & 9 \end{bmatrix} \quad (2.114)$$

$$M_{VAS} = mL \begin{bmatrix} 1 & & 0 \\ & 1 & \\ 0 & & 1 \end{bmatrix} \quad (2.115)$$

Applying Lagrange's equations, we obtain the equations for inplane antisymmetrical motions of a simple inextensible catenary.

$$M_{VAS} \ddot{V}_{AS} + E_{VAS} V_{AS} = 0 \quad (2.116)$$

The equation (2.116) represents a set of uncoupled equations and applying the condition for a normal mode of frequency, ω , we obtain

$$\omega_i = \frac{i\pi}{L} \sqrt{H/m} \quad (2.117)$$

In the above application of the Rayleigh-Ritz method we have used a total of seven string modes-four symmetrical and three antisymmetrical. In fact, the generalisation to any number of symmetrical and antisymmetrical string modes is obvious and self-explanatory from the above procedure.

Lateral Modes

Referring to (2.88) and (2.89) we obtain respectively for the potential and the kinetic energy expressions

$$V = \frac{H}{2} \int_{-L}^L \left(\frac{\partial w}{\partial x} \right)^2 dx \quad (2.118)$$

and

$$T = \frac{m}{2} \int_{-L}^L \dot{w}^2 dx \quad (2.119)$$

Since no first order term in w is involved in (2.86), there is no equation of constraint like (2.90). Hence (2.118) and (2.119) are sufficient to define the lateral modes of a simple inextensible catenary. As before, assuming a linear combination of string modes for w , satisfying all the geometric boundary conditions, we write

$$w = W_1 \cos \frac{\pi x}{2L} + W_2 \sin \frac{\pi x}{L} + W_3 \cos \frac{3\pi x}{2L} + W_4 \sin \frac{2\pi x}{L} \quad (2.120)$$

Substituting the assumed series (2.120) in (2.118) and (2.120) we obtain

$$V = \frac{\pi^2 H}{8L} (W_1^2 + 4 W_2^2 + 9 W_3^2 + 16 W_4^2) \quad (2.121)$$

$$T = \frac{mL}{2} (\dot{W}_1^2 + \dot{W}_2^2 + \dot{W}_3^2 + \dot{W}_4^2) \quad (2.122)$$

In matrix form

$$V = \frac{1}{2} W_z' E_z W_z \quad (2.123)$$

and

$$T = \frac{1}{2} \dot{W}_z' M_z \dot{W}_z \quad (2.124)$$

where

$$W_z = \{W_1, W_2, W_3, W_4\} \quad (2.125)$$

and E_z and M_z are diagonal matrices and are given by

$$E_z = \frac{2\pi H}{4L} \begin{bmatrix} 1 & & & 0 \\ & 4 & & \\ & & 9 & \\ 0 & & & 16 \end{bmatrix} \quad (2.126)$$

$$M_z = mL \times (4 \times 4 \text{ unit matrix}) \quad (2.127)$$

Applying Lagrange's equations and the condition for a normal mode of frequency, ω , we obtain

$$\omega_i = \frac{i\pi}{2L} \sqrt{\frac{H}{m}}, \quad i = 1, 2, 3 \quad (2.128)$$

From the above analysis, it is seen the lateral modes and frequencies of a simple fixed-fixed catenary can be very well represented by the stretched string counterparts.

2.4 COMPARATIVE STUDY OF THE ABOVE THREE METHODS

The method of Saxon and Cahn is not easily applicable to the multi-span cases, it becomes too mathematically involved even when the case of the catenary with relaxed ends is considered. The method is mathematically sound but complex from the engineers' point of view. The accuracy increases with the increase in mode number or with the increase in the span/dip ratio. The Simpson's lumped parameters method, on the other hand, is easily applicable to the multi-span cases, although the sizes of the matrices become very large. The method is very straightforward but lengthy.

The accuracy of the results depends on the number of masses and the type of mass-distribution used to represent the catenary. The writer's Rayleigh-Ritz approach is very simple and straightforward from the Engineers' points of view and is easily applicable to multi-span cases (see Chapters 3 and 4). Although matrices are involved, these are small in size. The accuracy of the method increases as the dip/span ratio becomes small. Although the method is approximate, the numerical results, compare very favourably with the experimental results and those of the other methods described.

For the purposes of comparison, the centre span of the "Severn Crossing" is taken and the frequencies, obtained from each of the above three methods and the experiment are given in the Table 1. Perhaps a few words at this point about the Severn crossing would be appropriate. Although the writer was involved with problems concerning the "Red Moss Test Line", the dimensions of the test line were not in possession at the beginning of this research. The writer gathered the following specifications, as applied to this calculation, from reference [35].

Specification of Severn Centre Span

Span	=	5310 ft.
Sag	=	265 ft.
Mass/unit length of the cable	=	$22850 / (5310 \times 32.2)$ slugs/ft.

Experiment on Single Span (Fixed-fixed) Catenary Model

For this purpose a model consisting of 21 masses was built in the laboratory (for design details see Appendix-F). The resonance tests were performed by attaching an electromagnetic exciter to one of the end masses.

The selection of this particular point of excitation was because no nodes occurred at this point in low-frequency modes; higher frequency modes could not be excited anyway. The frequencies for the four lowest inplane modes obtained from the experiment were scaled by the factor, $\sqrt{d_m/d}$, where d_m is the dip of the catenary model and these are given in the last column of Table - 1.

Table I

Mode No.	Saxon and Cahn Hz	Simpson Hz	Rayleigh-Ritz Hz	Experimental Hz
1	0.12094	0.12145	0.12319	0.12
2	0.17468	0.17463	0.17609	0.17
3	0.24358	0.24213	0.24639	0.25
4	0.30012	0.29637	0.30276	0.31
5	0.36584	0.35748	0.36958	-
6	0.42364	0.40983	0.42734	-
7	0.48801	0.46545	0.49277	-
8	0.54652	0.51420	0.55124	-
9	0.61014	0.56389	0.61596	-
10	0.66911	0.60773	0.67486	-
11	0.73225	0.65083	0.73916	-
12	0.79153	0.68867	0.79803	-
13	0.85435	0.72450	0.86235	-
14	0.91387	0.75543	0.92174	-
15	0.97645	0.78339	0.98554	-
16	1.03614	0.80669	1.04499	-
17	1.09854	0.82629	1.10873	-
18	1.15837	0.89133	1.16750	-
19	1.22062	0.85221	1.23193	-
20	1.28057	0.85750	1.29201	-

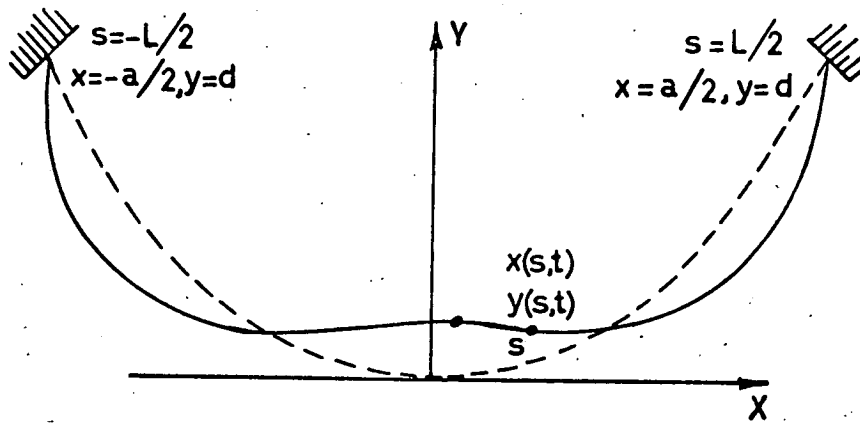


FIG. 2.1.

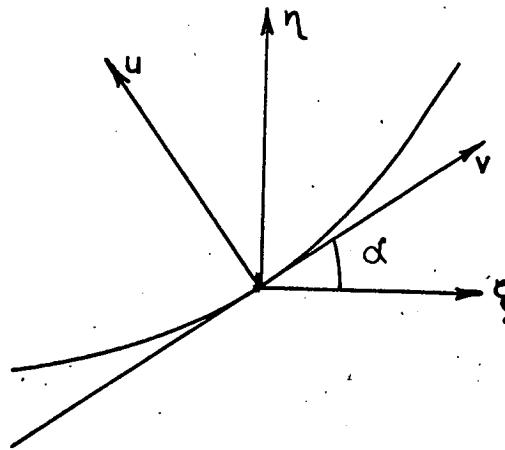


FIG. 2.2

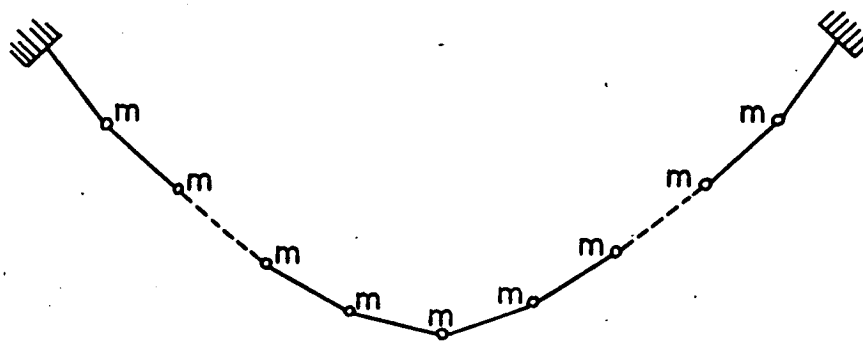


FIG. 2.3

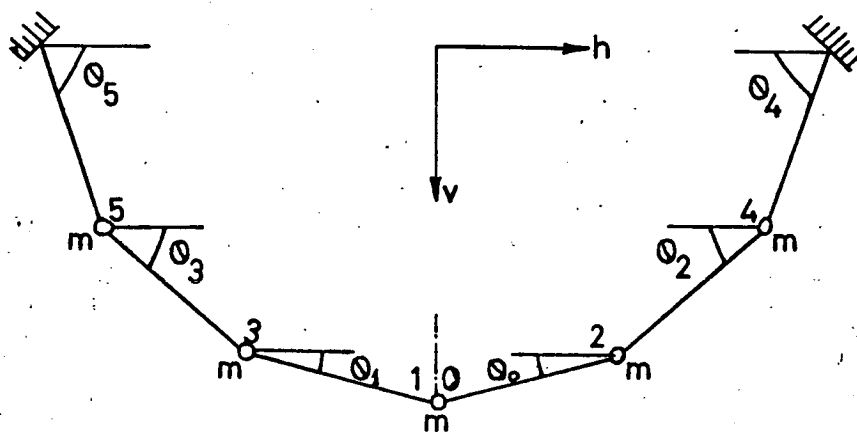


FIG. 2.4

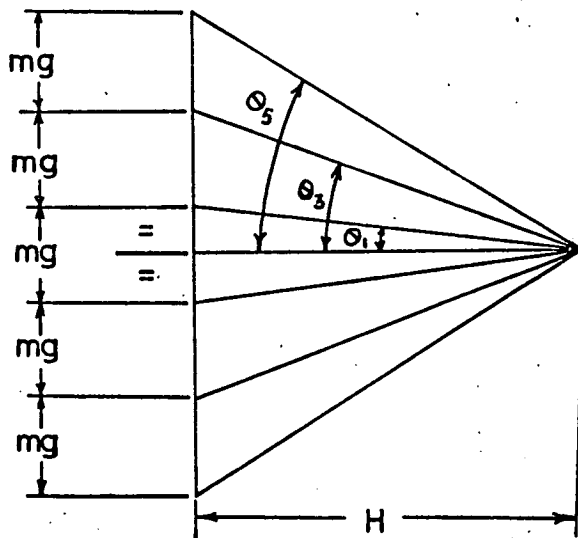


FIG. 2.5

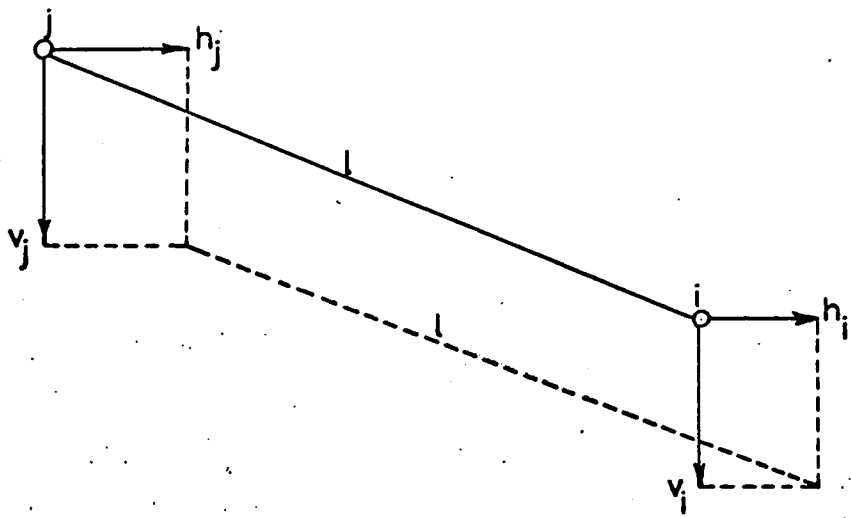


FIG. 2.6

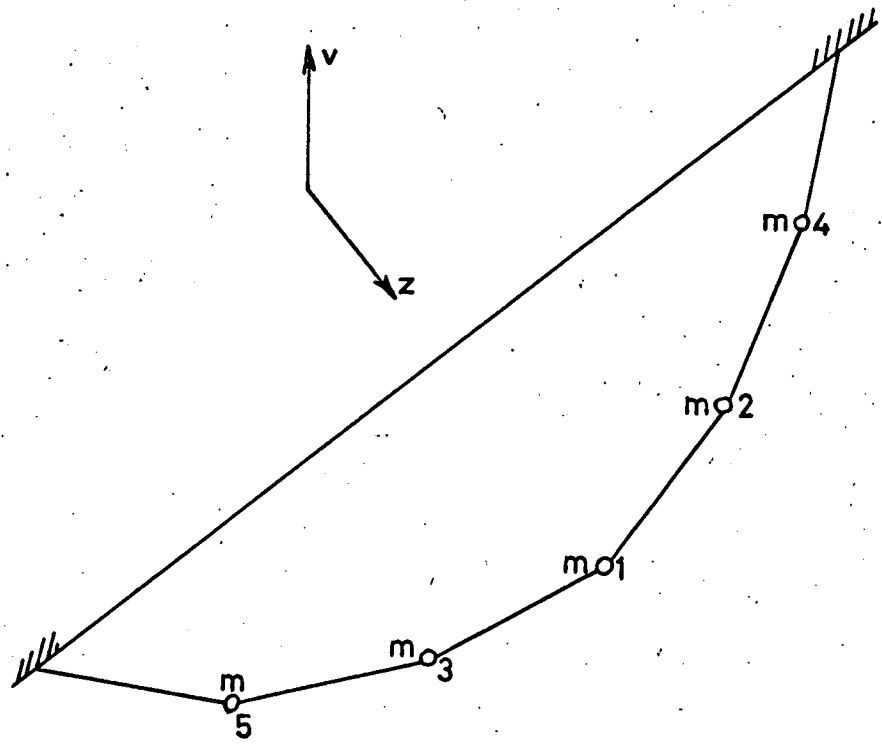


FIG. 2.7

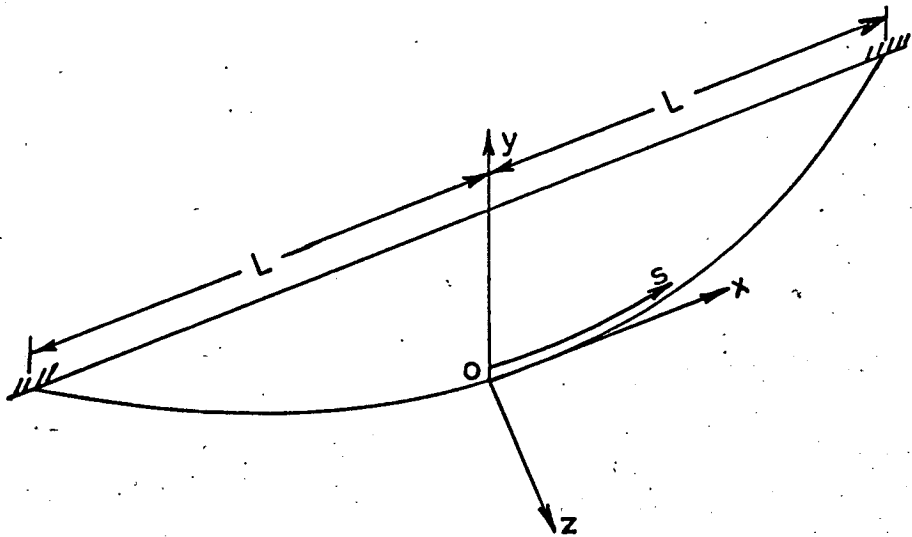


FIG. 2.8

CHAPTER 3NATURAL FREQUENCIES AND NORMAL MODES OF MULTI-SPANCATENARY SYSTEMS

It was shown in section 2.3 that the method of Rayleigh-Ritz can efficiently be applied to the problem of the oscillating single span fixed-fixed catenary.. The method will now be employed to deal with the case of multi-span systems. But before going into the detail of multi-span systems, it was thought useful to consider one or two basic catenaries of which a multi-span system is comprised; these are given in Appendix-A. In fact, the equation of motion for the basic catenaries can subsequently be applied to construct the equations of motion for the complex multi-span systems.

The analysis discussed in the present section is based on the following assumptions:-

- a) cable elasticity effects are insignificant
- b) cables are suspended from the same horizontal level
- c) the extremities of the outermost spans are rigidly fixed
- d) tower flexibility and inertia effects are negligible
- e) catenaries are flat and the equilibrium shapes are parabolic

Three Span System

Consider the three span system shown in Fig. 3.1. Referring to the fixed-fixed, fixed-free and free-free catenaries (fixed-free and free-free catenaries are discussed in the Appendix-A), it was demonstrated that for small oscillations of a catenary, the inplane and lateral modes are uncoupled.

This fact will be used in the following analysis since it is convenient to set up separate equations of motion for the vertical and lateral planes.

3.1 INPLANE MODES

The potential energy in a general inplane displacement can be written as

$$V = \frac{H}{2} \int_{-L_1}^{L_1} \left(\frac{\partial v_1}{\partial x} \right)^2 dx + \frac{H}{2} \int_{-L_2}^{L_2} \left(\frac{\partial v_2}{\partial x} \right)^2 dx + \frac{H}{2} \int_{-L_3}^{L_3} \left(\frac{\partial v_3}{\partial x} \right)^2 dx + \frac{2mg(L_1 + L_2) + M_s g}{4l_s} u_{12}^2 + \frac{2mg(L_2 + L_3) + M_s g}{4l_s} u_{23}^2 \quad (3.1)$$

and the kinetic energy takes the form

$$T = \frac{m}{2} \int_{-L_1}^{L_1} \dot{v}_1^2 dx + \frac{m}{2} \int_{-L_2}^{L_2} \dot{v}_2^2 dx + \frac{m}{2} \int_{-L_3}^{L_3} \dot{v}_3^2 dx + \frac{M_s}{8} (\dot{u}_{12}^2 + \dot{u}_{23}^2) \quad (3.2)$$

The equations of constraint ensuring compatibility at the common-span points are given by

$$\left. \begin{aligned} u_{12} &= \frac{mg}{H} \int_{-L_1}^{L_1} v_1 dx \\ u_{23} - u_{12} &= \frac{mg}{H} \int_{-L_2}^{L_2} v_2 dx \\ -u_{23} &= \frac{mg}{H} \int_{-L_3}^{L_3} v_3 dx \end{aligned} \right\} \quad (3.3)$$

Solution by the Rayleigh-Ritz Method [3, 19]

The method of Rayleigh-Ritz consists of selecting a trial family of functions satisfying all the boundary conditions of the problem and constructing a linear combination of these functions.

As in the practical catenary systems, there are very little vertical movements at the suspension points, we write

$$\left. \begin{aligned} v_1 &= V_{11} \cos \frac{\pi x}{2L_1} + V_{12} \sin \frac{\pi x}{L_1} + V_{13} \cos \frac{3\pi x}{2L_1} + V_{14} \sin \frac{2\pi x}{L_1} + V_{15} \cos \frac{5\pi x}{2L_1} + V_{16} \sin \frac{3\pi x}{L_1} \\ v_2 &= V_{21} \cos \frac{\pi x}{2L_2} + V_{22} \sin \frac{\pi x}{L_2} + V_{23} \cos \frac{3\pi x}{2L_2} + V_{24} \sin \frac{2\pi x}{L_2} + V_{25} \cos \frac{5\pi x}{2L_2} + V_{26} \sin \frac{3\pi x}{L_2} \\ v_3 &= V_{31} \cos \frac{\pi x}{2L_3} + V_{32} \sin \frac{\pi x}{L_3} + V_{33} \cos \frac{3\pi x}{2L_3} + V_{34} \sin \frac{2\pi x}{L_3} + V_{35} \cos \frac{5\pi x}{2L_3} + V_{36} \sin \frac{3\pi x}{L_3} \end{aligned} \right\} (3.4)$$

where in (3.4) it is understood that six modes per span are considered.

If we substitute (3.4) into (3.1) - (3.3), we respectively obtain

$$\begin{aligned} V &= \frac{\pi^2 H}{8L_1} (v_{11}^2 + 4v_{12}^2 + 9v_{13}^2 + 16v_{14}^2 + 25v_{15}^2 + 36v_{16}^2) + \\ &+ \frac{\pi^2 H}{8L_2} (v_{21}^2 + 4v_{22}^2 + 9v_{23}^2 + 16v_{24}^2 + 25v_{25}^2 + 36v_{26}^2) + \\ &+ \frac{\pi^2 H}{8L_3} (v_{31}^2 + 4v_{32}^2 + 9v_{33}^2 + 16v_{34}^2 + 25v_{35}^2 + 36v_{36}^2) + \frac{K_1}{2} u_{12}^2 + \frac{K_2}{2} u_{23}^2 \end{aligned} \quad (3.5)$$

$$\begin{aligned} T &= \frac{mL_1}{2} (\dot{v}_{11}^2 + \dot{v}_{12}^2 + \dot{v}_{13}^2 + \dot{v}_{14}^2 + \dot{v}_{15}^2 + \dot{v}_{16}^2) + \\ &+ \frac{mL_2}{2} (\dot{v}_{21}^2 + \dot{v}_{22}^2 + \dot{v}_{23}^2 + \dot{v}_{24}^2 + \dot{v}_{25}^2 + \dot{v}_{26}^2) + \\ &+ \frac{mL_3}{2} (\dot{v}_{31}^2 + \dot{v}_{32}^2 + \dot{v}_{33}^2 + \dot{v}_{34}^2 + \dot{v}_{35}^2 + \dot{v}_{36}^2) + \frac{M_s}{8} (\dot{u}_{12}^2 + \dot{u}_{23}^2) \end{aligned} \quad (3.6)$$

and the equations of constraint are -

$$\left. \begin{aligned} \bar{u}_{12} &= \frac{4mgL_1}{\pi H} \left(v_{11} - \frac{v_{13}}{3} + \frac{v_{15}}{5} \right) \\ \bar{u}_{23} - \bar{u}_{12} &= \frac{4mgL_2}{\pi H} \left(v_{21} - \frac{v_{23}}{3} + \frac{v_{25}}{5} \right) \\ -\bar{u}_{23} &= \frac{4mgL_3}{\pi H} \left(v_{31} - \frac{v_{33}}{3} + \frac{v_{35}}{5} \right) \end{aligned} \right\} \quad (3.7)$$

where in (3.5), $K_1 = \frac{2mg(L_1 + L_2) + M_s g}{2l_s}$ and $K_2 = \frac{2mg(L_2 + L_3) + M_s g}{2l_s}$

Equations (3.5) - (3.7) imply that the constraining relations (3.3) being automatically satisfied, the individual span antisymmetric modes can exist by themselves and for these modes we obtain

$$r_i^j = \frac{i}{2L_j} \sqrt{\frac{H}{m}}, \quad i = 1, 2, \dots \quad (3.8)$$

where $j = 1, 2, 3$ in our present case. On the other hand the inter-span coupling occurs through the individual span assumed symmetric modes and for this case we can write

$$\begin{aligned} v &= \frac{\pi^2 H}{8L_1} (v_{11}^2 + 9v_{13}^2 + 25v_{15}^2) + \frac{\pi^2 H}{8L_2} (v_{21}^2 + 9v_{23}^2 + 25v_{25}^2) + \\ &+ \frac{\pi^2 H}{8L_3} (v_{31}^2 + 9v_{33}^2 + 25v_{35}^2) + \frac{K_1}{2} \bar{u}_{12}^2 + \frac{K_2}{2} \bar{u}_{23}^2 \end{aligned} \quad (3.9)$$

$$\begin{aligned} T &= \frac{mL_1}{2} (\dot{v}_{11}^2 + \dot{v}_{13}^2 + \dot{v}_{15}^2) + \frac{mL_2}{2} (\dot{v}_{21}^2 + \dot{v}_{23}^2 + \dot{v}_{25}^2) + \frac{mL_3}{2} (\dot{v}_{31}^2 + \dot{v}_{33}^2 + \dot{v}_{35}^2) + \\ &+ \frac{M_s}{8} (\dot{\bar{u}}_{12}^2 + \dot{\bar{u}}_{23}^2) \end{aligned} \quad (3.10)$$

and the equations of constraint are still given by (3.7).

Using Lagrange's equations and the condition for a normal mode of frequency, ω , we obtain the equations for inplane motion for the three span system

$$\omega^2 M_{Vt} D_{Vt} = E_{Vt} D_{Vt} \quad (3.20)$$

The matrices M_{Vt} and E_{Vt} are well conditioned and hence the frequencies and the modes may be determined in increasing order of magnitude by various standard methods.

If a frequency, ω_i , and its associated vector, D_{Vt}^i , have been determined, we may use (3.17) to give the coordinates, D_V^i , corresponding to the normal mode shape. Thus

$$D_V^i = Q D_{Vt}^i \quad (3.21)$$

Finally the natural modes may be calculated through (3.4).

3.2 LATERAL MODES

The potential energy in a general lateral displacement is given by

$$V = \frac{H}{2} \int_{-L_1}^{L_1} \left(\frac{\partial w_1}{\partial x} \right)^2 dx + \frac{H}{2} \int_{-L_2}^{L_2} \left(\frac{\partial w_2}{\partial x} \right)^2 dx + \frac{H}{2} \int_{-L_3}^{L_3} \left(\frac{\partial w_3}{\partial x} \right)^2 dx + \frac{2mg(L_1 + L_2) + M_s g}{4I_s} w_{12}^2 + \frac{2mg(L_2 + L_3) + M_s g}{4I_s} w_{23}^2 \quad (3.22)$$

and the kinetic energy becomes

$$T = \frac{m}{2} \int_{-L_1}^{L_1} \dot{w}_1^2 dx + \frac{m}{2} \int_{-L_2}^{L_2} \dot{w}_2^2 dx + \frac{m}{2} \int_{-L_3}^{L_3} \dot{w}_3^2 dx + \frac{M_s}{8} (\dot{w}_{12}^2 + \dot{w}_{23}^2) \quad (3.23)$$

Solutions by Rayleigh-Ritz and Rauscher Modes [3]

The method described in the following analysis consists of selecting a combination of sinusoidal deformation modes per span and a linear interpolation function mode for each pair of spans adjacent to a suspension point. This interpolation function permits the expression for the deformation in terms of a set of ordinates at specified points. Rauscher conceived the idea of the interpolation functions as a refinement of the lumped mass type of analysis, taking the continuous mass distribution into account but retaining the simplicity of a finite set of ordinates as a generalised coordinates. In their simplest form, interpolation functions are constructed from the deflection curves due to concentrated loads at selected points along the system.

To apply the Rayleigh-Ritz method together with the station functions, we write

$$\begin{aligned}
 w_1 &= \bar{w}_{12} \left(\frac{L_1 + x}{2L_1} \right) + W_{11} \cos \frac{\pi x}{2L_1} + W_{12} \sin \frac{\pi x}{L_1} + W_{13} \cos \frac{3\pi x}{2L_1} + W_{14} \sin \frac{2\pi x}{L_1} + \\
 &\quad + W_{15} \cos \frac{5\pi x}{2L_1} + W_{16} \sin \frac{3\pi x}{L_1} \\
 w_2 &= \bar{w}_{12} \left(\frac{L_2 - x}{2L_2} \right) + W_{21} \cos \frac{\pi x}{2L_2} + W_{22} \sin \frac{\pi x}{L_2} + W_{23} \cos \frac{3\pi x}{2L_2} + W_{24} \sin \frac{2\pi x}{L_2} + \\
 &\quad + W_{25} \cos \frac{5\pi x}{2L_2} + W_{26} \sin \frac{3\pi x}{L_2} + \bar{w}_{23} \left(\frac{L_2 + x}{2L_2} \right) \\
 w_3 &= \bar{w}_{23} \left(\frac{L_3 - x}{2L_3} \right) + W_{31} \cos \frac{\pi x}{2L_3} + W_{32} \sin \frac{\pi x}{L_3} + W_{33} \cos \frac{3\pi x}{2L_3} + W_{34} \sin \frac{2\pi x}{L_3} + \\
 &\quad + W_{35} \cos \frac{5\pi x}{2L_3} + W_{36} \sin \frac{3\pi x}{2L_3}
 \end{aligned} \quad (3.24)$$

Introducing (3.24) in (3.22) and (3.23) we eventually obtain

$$\begin{aligned}
 V = & \frac{\pi^2 H}{8L_1} (W_{11}^2 + 4W_{12}^2 + 9W_{13}^2 + 16W_{14}^2 + 25W_{15}^2 + 36W_{16}^2) + \\
 & + \frac{\pi^2 H}{8L_2} (W_{21}^2 + 4W_{22}^2 + 9W_{23}^2 + 16W_{24}^2 + 25W_{25}^2 + 36W_{26}^2) + \\
 & + \frac{\pi^2 H}{8L_3} (W_{31}^2 + 4W_{32}^2 + 9W_{33}^2 + 16W_{34}^2 + 25W_{35}^2 + 36W_{36}^2) + \\
 & + \frac{b_1}{2} \bar{w}_{12}^2 + \frac{b_2}{2} \bar{w}_{23}^2 - \frac{H}{2L_2} \bar{w}_{12} \bar{w}_{23} \quad (3.25)
 \end{aligned}$$

$$\begin{aligned}
 T = & \frac{m}{2} [L_1 (\dot{w}_{11}^2 + \dot{w}_{12}^2 + \dot{w}_{13}^2 + \dot{w}_{14}^2 + \dot{w}_{15}^2 + \dot{w}_{16}^2) + \\
 & + L_2 (\dot{w}_{21}^2 + \dot{w}_{22}^2 + \dot{w}_{23}^2 + \dot{w}_{24}^2 + \dot{w}_{25}^2 + \dot{w}_{26}^2) + \\
 & + L_3 (\dot{w}_{31}^2 + \dot{w}_{32}^2 + \dot{w}_{33}^2 + \dot{w}_{34}^3 + \dot{w}_{35}^2 + \dot{w}_{36}^2) + \\
 & + \frac{4L_1}{\pi} (\dot{\bar{w}}_{12} \dot{w}_{11} - \dot{\bar{w}}_{12} \dot{w}_{13}/3 + \dot{\bar{w}}_{12} \dot{w}_{15}/5) + \frac{4L_2}{\pi} (\dot{\bar{w}}_{12} \dot{w}_{21} - \dot{\bar{w}}_{12} \dot{w}_{23}/3 + \\
 & + \dot{\bar{w}}_{12} \dot{w}_{25}/5 + \dot{\bar{w}}_{23} \dot{w}_{21} - \dot{\bar{w}}_{23} \dot{w}_{23}/3 + \dot{\bar{w}}_{23} \dot{w}_{25}/5) + \\
 & + \frac{4L_3}{\pi} (\dot{\bar{w}}_{23} \dot{w}_{31} - \dot{\bar{w}}_{23} \dot{w}_{33}/3 + \dot{\bar{w}}_{23} \dot{w}_{35}/5) + c_1 \dot{\bar{w}}_{12}^2 + c_2 \dot{\bar{w}}_{23}^2 + \frac{2L_2}{3} \dot{\bar{w}}_{12} \dot{\bar{w}}_{23}] \quad (3.26)
 \end{aligned}$$

where in (3.25) and (3.26)

$$\begin{aligned}
 b_1 = & \frac{H}{2(L_1 + L_2)} + \frac{2mg(L_1 + L_2) + M_s g}{2l_s}, \quad b_2 = \frac{H}{2(L_2 + L_3)} + \frac{2mg(L_2 + L_3) + M_s g}{2l_s} \\
 c_1 = & \frac{2}{3} (L_1 + L_2) + \frac{M_s}{4m}, \quad c_2 = \frac{2}{3} (L_2 + L_3) + \frac{M_s}{4m}
 \end{aligned}$$

From (3.25) and (3.26) it is seen that the individual span assumed antisymmetric modes can again exist by themselves and for these modes we get

$$f_i^j = \frac{i}{2L_j} \sqrt{\frac{H}{m}}, \quad i = 1, 2, \dots \quad (3.27)$$

where $j = 1, 2, 3$. On the other hand for the coupled individual span symmetric modes we obtain.

$$\begin{aligned} V = & \frac{\pi^2 H}{8L_1} (W_{11}^2 + 9W_{13}^2 + 25W_{15}^2) + \frac{\pi^2 H}{8L_2} (W_{21}^2 + 9W_{23}^2 + 25W_{25}^2) + \\ & + \frac{\pi^2 H}{8L_3} (W_{31}^2 + 9W_{33}^2 + 25W_{35}^2) + \frac{b_1}{2} \bar{w}_{12}^2 + \frac{b_2}{2} \bar{w}_{23}^2 + \frac{H}{2L_2} \bar{w}_{12} \bar{w}_{23} \end{aligned} \quad (3.28)$$

$$\begin{aligned} T = & \frac{m}{2} [L_1 (\dot{w}_{11}^2 + \dot{w}_{13}^2 + \dot{w}_{15}^2) + L_2 (\dot{w}_{21}^2 + \dot{w}_{23}^2 + \dot{w}_{25}^2) + \\ & + L_3 (\dot{w}_{31}^2 + \dot{w}_{33}^2 + \dot{w}_{35}^2) + \frac{4L_1}{\pi} (\dot{w}_{12} \dot{w}_{11} - \dot{w}_{12} \dot{w}_{13}/3 + \dot{w}_{12} \dot{w}_{15}/5) + \\ & + \frac{4L_2}{\pi} (\dot{w}_{12} \dot{w}_{21} - \dot{w}_{12} \dot{w}_{23}/3 + \dot{w}_{12} \dot{w}_{25}/5 + \dot{w}_{23} \dot{w}_{21} - \dot{w}_{23} \dot{w}_{23}/3 + \dot{w}_{23} \dot{w}_{25}/5) + \\ & + \frac{4L_3}{\pi} (\dot{w}_{23} \dot{w}_{31} - \dot{w}_{23} \dot{w}_{33}/3 + \dot{w}_{23} \dot{w}_{35}/5) + C_1 \dot{w}_{12}^2 + C_2 \dot{w}_{23}^2 + \frac{2L_2}{3} \dot{w}_{12} \dot{w}_{23}] \end{aligned} \quad (3.29)$$

No reduction relation of the type (3.17) is required in this case because the number of coordinates is equal to the number of degrees of freedom.

In matrix form V and T can respectively be written as

$$V = \frac{1}{2} D'_z E_z D_z \quad (3.30)$$

$$T = \frac{1}{2} \dot{D}'_z M_z \dot{D}_z \quad (3.31)$$



The matrices M_z and E_z are well conditioned and hence the frequencies and modes may be determined by any standard method.

If a frequency, ω_i , and its associated vector, D_z^i , are determined, we can use (3.24), after dropping the antisymmetric modes, to calculate the natural mode shape corresponding to the frequency, ω_i .

3.3 CALCULATION FOR THE RED MOSS TEST LINE

The theory discussed in the previous sections will now be employed to calculate the natural frequencies and the normal modes of vibration of the Red Moss Test Line with which the writer was mainly concerned. The profile of the actual test line is given in Fig. 3.2, while the writer's assumed test line configuration is shown in Fig. 3.3. The assumptions given at the beginning of the present chapter are involved.^k

The characteristic matrices for the inplane and lateral modes are shown on separate sheets at the end of this chapter where it is also understood that only two symmetrical modes in each span are considered.

The Pattern of Computation

An outline of the computational procedure is given below -

- a) a Desk Calculator was used to calculate all the non-standard data required to specify the matrices for the whole system.

The required information was -

- i) the length of each span
- ii) the dip of one span
- iii) the mass per unit length of the cable
- iv) the length of one suspension arm

- v) the mass of one suspension arm
- b) the stiffness and inertia matrices of the system were formed by standard Atlas Autocode routines.
- c) the inverse of the stiffness matrix was computed and the dynamical matrix was formed.
- d) the eigenvalues and the vectors of the dynamical matrix were determined by a standard routine.

Comparison of Theory with Experiment

INPLANE MODES:- The natural frequencies of the inplane modes from the numerical analysis together with those from the tests performed at the site are given in Table-2, while the normal mode shapes are shown separately under an appropriate heading at the end of the present chapter. Inspection of Table-2 shows that there is a remarkable agreement between the calculated and the measured frequencies. The slight discrepancies may be due to the approximation that the cables are hung from the same horizontal level or due to the lack of the exact dip/span ratio. The dip was measured from one tower only and the distance between towers was known but for a system in which the towers are at differing altitude, this information is not enough. What is required, is the knowledge of all the dips or alternatively, one dip and the relative altitudes of the suspension points on the towers. Also due to positioning of the Dowty-Rotol exciter, some modes in which a node appears at or near the excitation point, cannot be excited. These modes which cannot be excited by the Dowty-Rotol would need to be excited by some other way e.g. by pulling periodically on a rope thrown over the line at an estimated anti-node (the third vertical mode was excited in this manner).

The modes which could be excited without great difficulty and those which could not are listed in Table-4.

LATERAL MODES:- The numerical analysis for the lateral modes was performed in the same way as for the inplane modes and the results are given in Table-3. No tests were performed at the site and hence no comparison of the calculated results could be made.

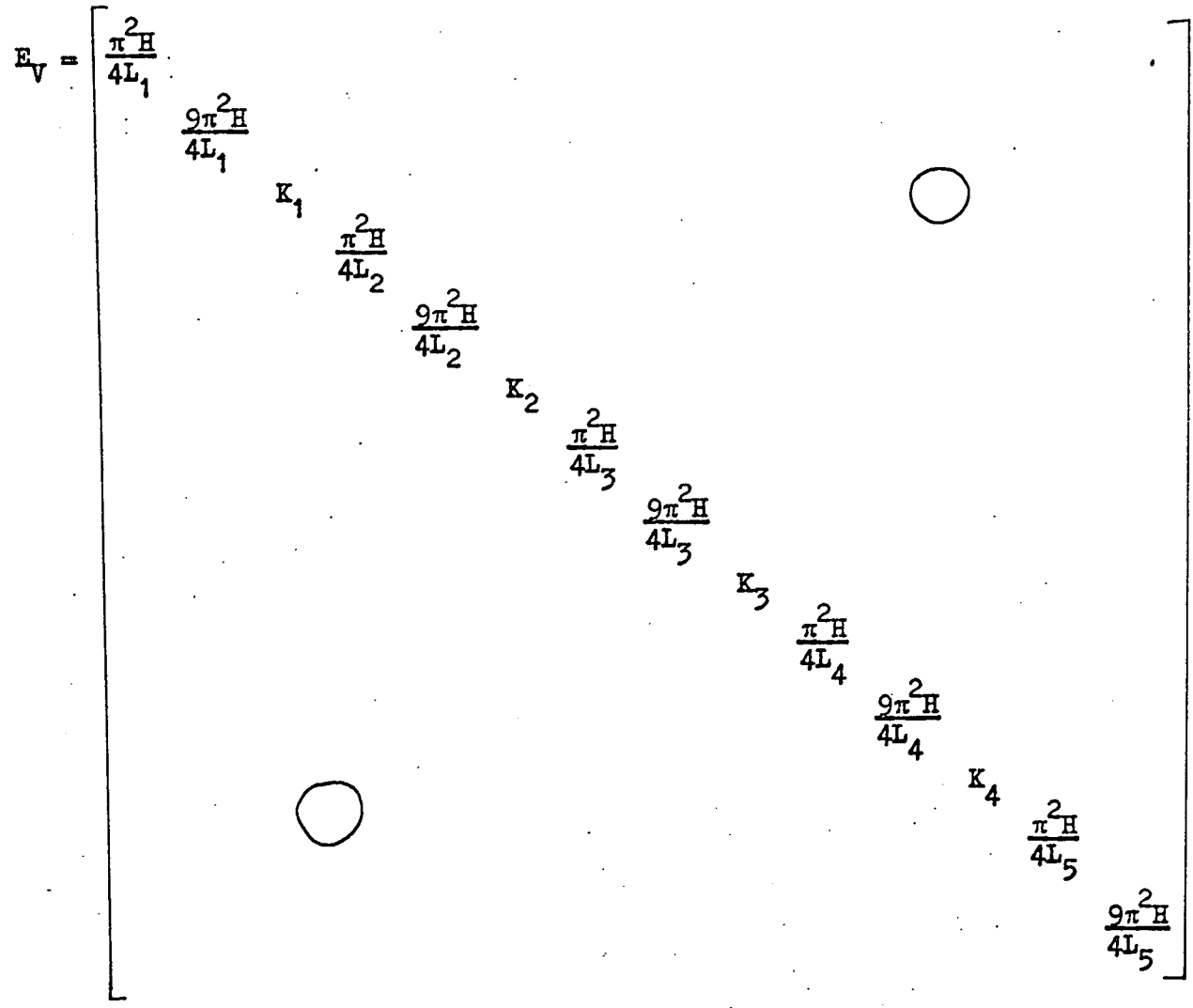
Interpolation of Results

Sketches of the normal mode shapes are given under the appropriate heading at the end of the present chapter in order of increasing natural frequencies. For the lateral modes, the displacement shown is the lateral horizontal component and may be readily visualised. Not quite so easy to visualise are the inplane modes for which the displacement shown is the vertical component; this component is satisfactory for describing the motion in the middle of a span but near the suspension points, the horizontal component of motion predominates. Thus, the inplane mode shapes shown do not adequately picture the insulator movements in the way the lateral mode shapes do.

THE CHARACTERISTIC MATRICES FOR THE RED MOSS TEST LINE

INPLANE MODES

$$D_{vt} = \{ v_{13} \bar{u}_{12} v_{23} \bar{u}_{23} v_{33} \bar{u}_{34} v_{43} \bar{u}_{45} v_{53} \}$$



$$M_Z = \begin{matrix} m \\ \begin{bmatrix} L_1 & 0 & \frac{2L_1}{\pi} \\ 0 & L_1 & \frac{-2L_1}{3\pi} \\ \frac{2L_1}{\pi} & \frac{-2L_1}{3\pi} & C_1 & \frac{2L_2}{\pi} & \frac{-2L_2}{3\pi} & \frac{L_2}{3} \\ & \frac{2L_2}{\pi} & L_2 & 0 & \frac{2L_2}{\pi} \\ & \frac{-2L_2}{3\pi} & 0 & L_2 & \frac{-2L_2}{3\pi} \\ \frac{L_2}{3} & \frac{2L_2}{\pi} & \frac{-2L_2}{3\pi} & C_2 & \frac{2L_3}{\pi} & \frac{-2L_3}{3\pi} & \frac{L_3}{3} \\ & \frac{2L_3}{\pi} & L_3 & 0 & \frac{2L_3}{\pi} \\ & \frac{-2L_3}{3\pi} & 0 & L_3 & \frac{-2L_3}{3\pi} \\ \frac{L_3}{3} & \frac{2L_3}{\pi} & \frac{-2L_3}{3\pi} & C_3 & \frac{2L_4}{\pi} & \frac{-2L_4}{3\pi} & \frac{L_4}{3} \\ & \frac{2L_4}{\pi} & L_4 & 0 & \frac{2L_4}{\pi} \\ & \frac{-2L_4}{3\pi} & 0 & L_4 & \frac{-2L_4}{3\pi} \\ \frac{L_4}{3} & \frac{2L_4}{\pi} & \frac{-2L_4}{3\pi} & C_4 & \frac{2L_5}{\pi} & \frac{-2L_5}{3\pi} \\ & \frac{2L_5}{\pi} & L_5 & 0 \\ & \frac{-2L_5}{3\pi} & 0 & L_5 \end{bmatrix} \end{matrix}$$

Table 2

Mode Number	Calculated Frequencies HZ	Experimental Frequencies HZ
1	0.17741	0.18
2	0.19921	0.20
3	0.32640	0.33
4	0.35021	0.35
5	0.37130	-
6	0.38780	-
7	0.40700	0.42
8	0.48442	0.50
9	0.55081	0.56
10	0.57742	0.58
11	0.75340	-
12	0.83340	-
13	1.12251	1.15
14	1.24325	1.28

Table 3

Mode Number	Calculated Frequency HZ
1	0.15057
2	0.17087
3	0.17759
4	0.32640
5	0.33369
6	0.35868
7	0.37130
8	0.38780
9	0.44671
10	0.49312
11	0.52662
12	0.55576
13	0.63963
14	0.75340
15	0.78611
16	0.83340
17	0.91929
18	1.18161
19	1.29820

Table 4

Inplane Modes		Lateral Modes	
Yes	No	Yes	No
1	-	1	-
2	-	2	-
-	3	-	3
4	-	-	4
-	5	-	5
-	6	-	6
7	-	-	7
8	-	-	8
9	-	9	-
10	-	10	-
-	11	11	-
-	12	12	-
13	-	13	-
14	-	-	14
		15	-
		-	16
		17	-
		-	18
		-	19

Yes = can be excited by the Dowty Rotol

No = cannot be excited by the Dowty Rotol

THREE SPAN SYSTEM

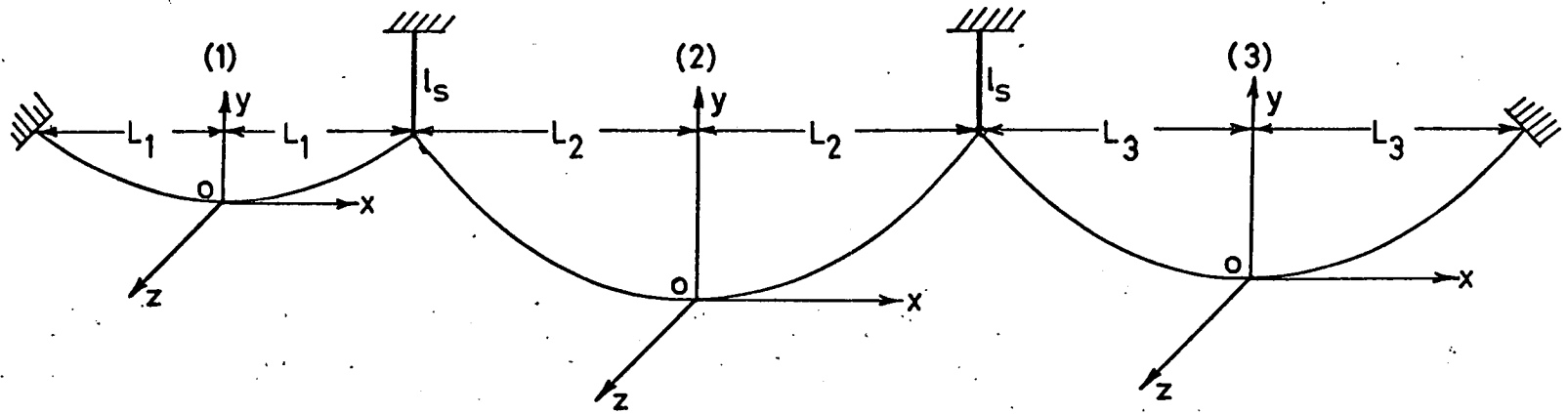


FIG. 3.1

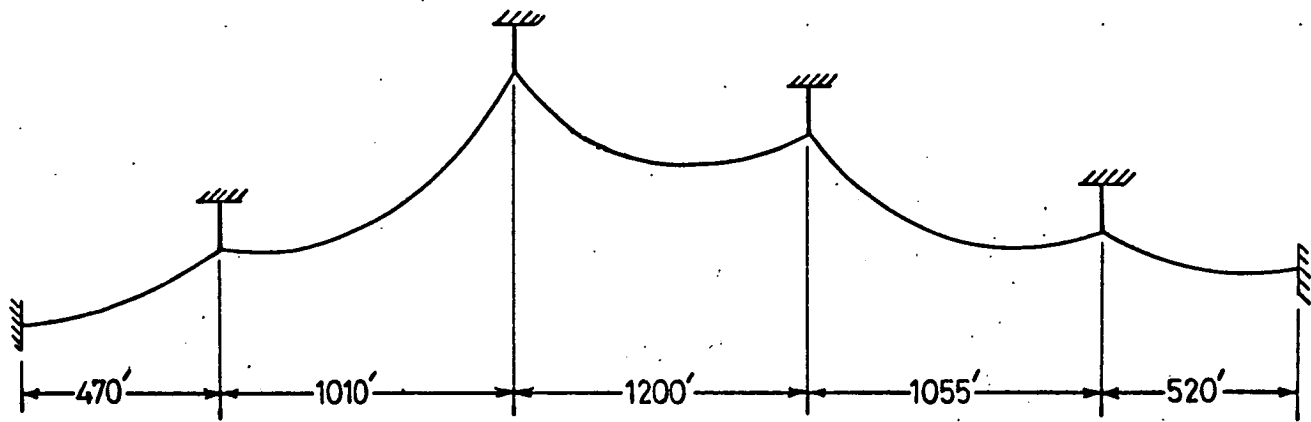


FIG. 3.2—ACTUAL TEST LINE

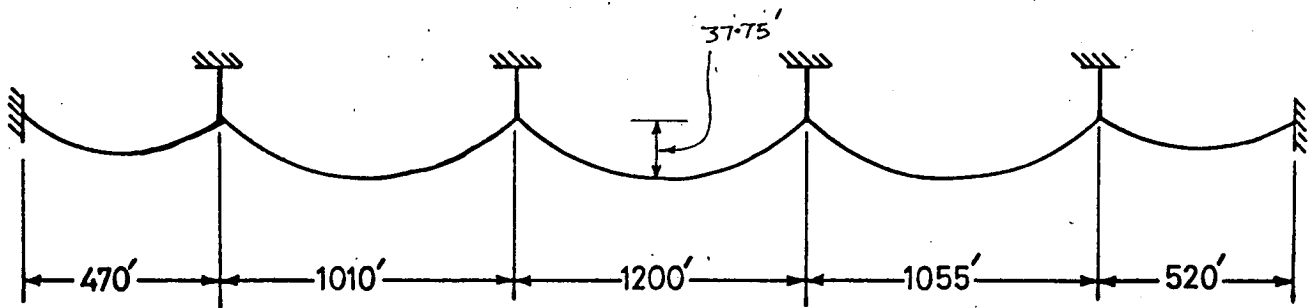


FIG. 3.3—ASSUMED TEST LINE CONFIGURATION

Quad bundle, weight of a single conductor is 1.008 lb/ft; length of suspension arm is 10 ft; weight of a single suspension arm is 500 lbs. and two are used at each support point.

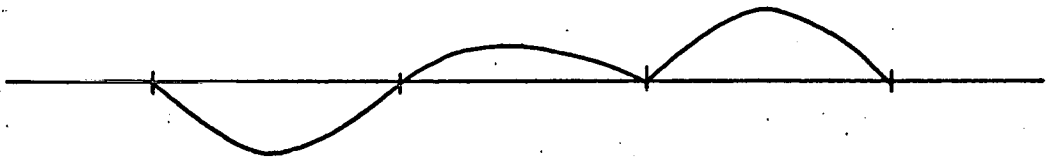
INPLANE NORMAL MODES OF VIBRATION FOR
RED MOSS TEST LINE

MODE NO.

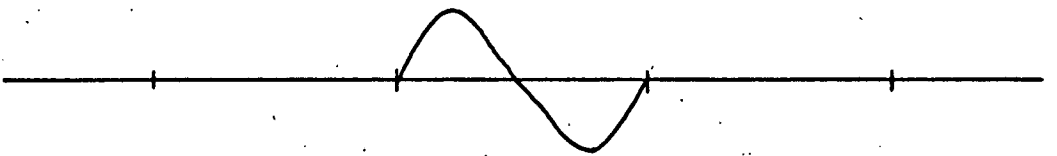
(1)



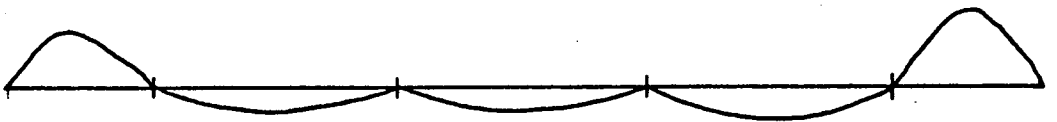
(2)



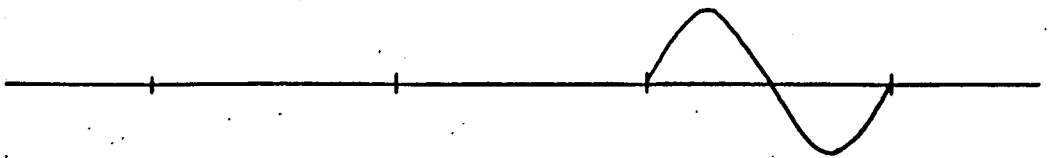
(3)



(4)

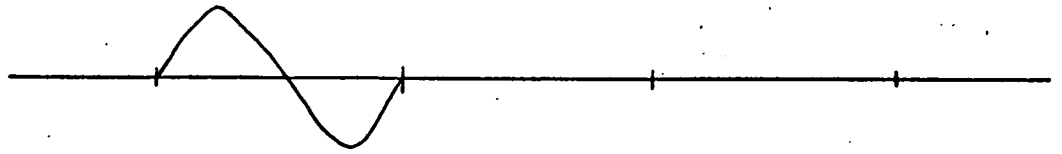


(5)

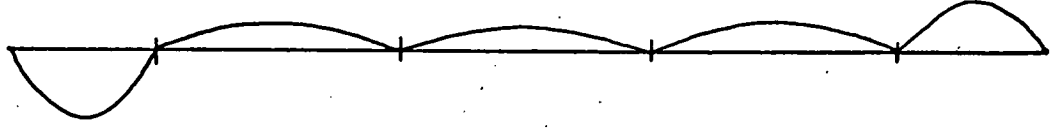


CONTD.

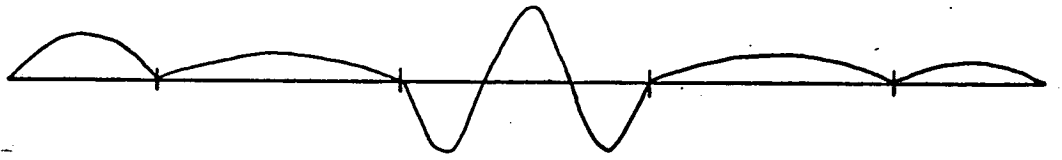
(6)



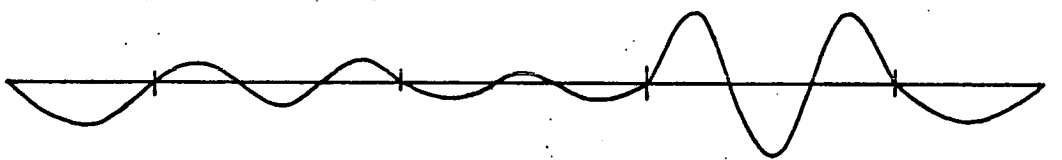
(7)



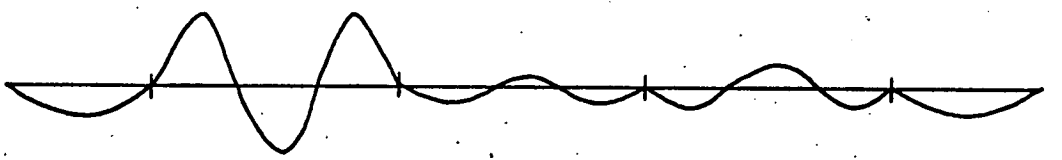
(8)



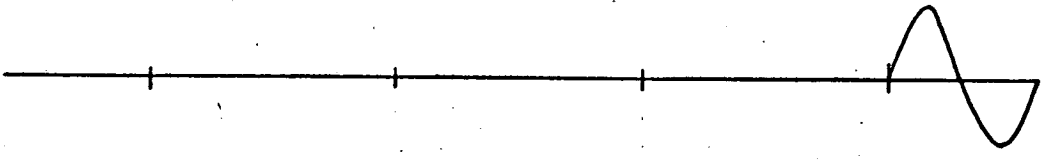
(9)



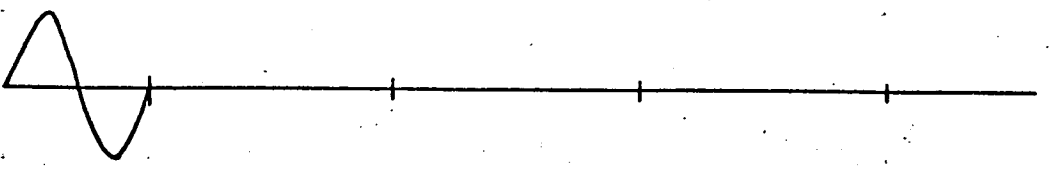
(10)



(11)



(12)

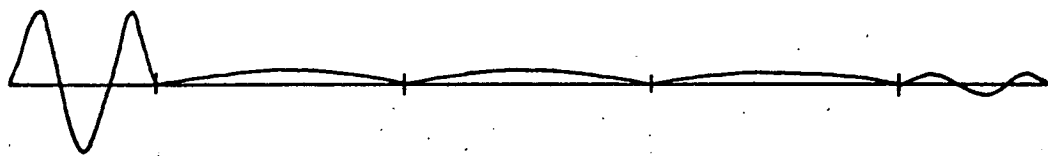


CONTD.

(13)

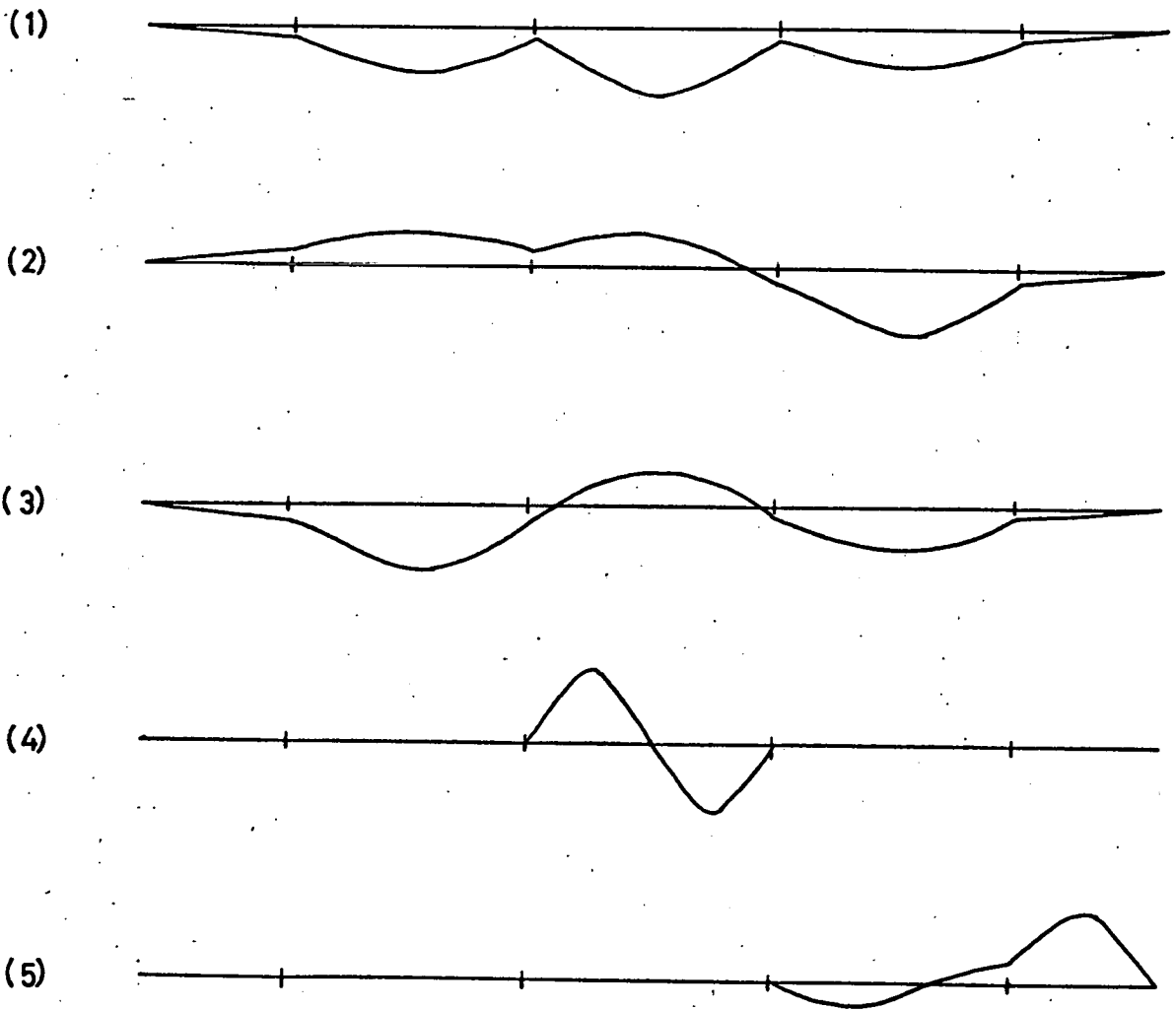


(14)



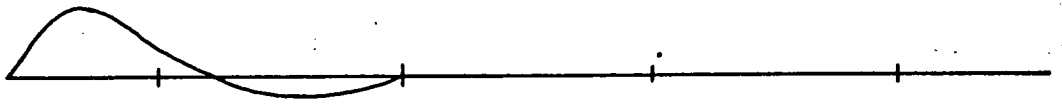
LATERAL NORMAL MODES OF VIBRATION FOR
RED MOSS TEST LINE

MODE NO.

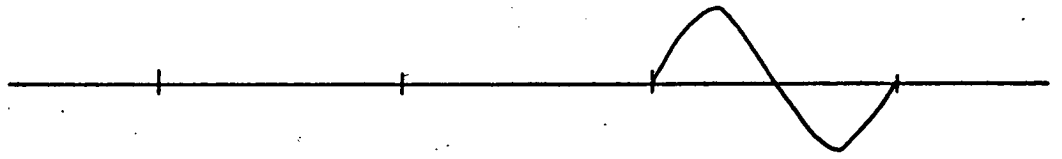


CONTD.

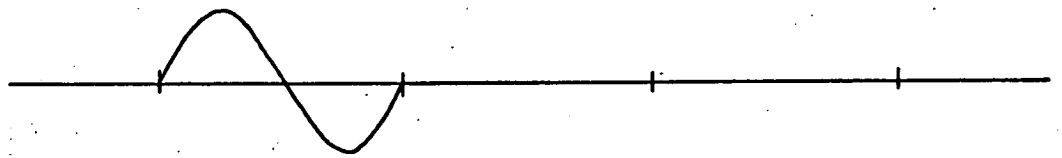
(6)



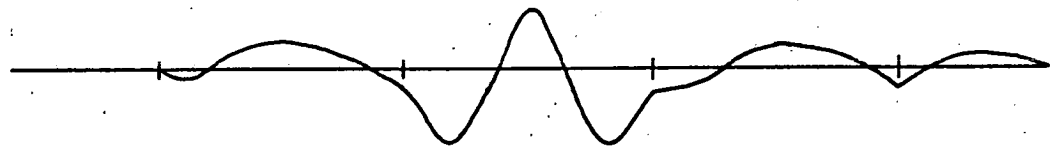
(7)



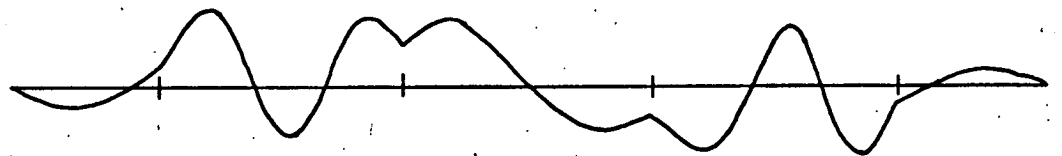
(8)



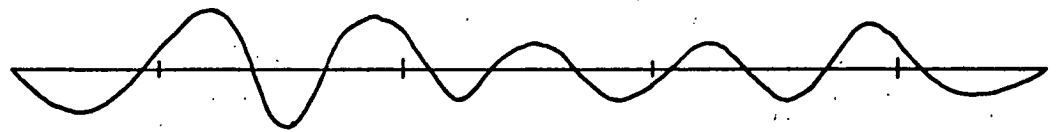
(9)



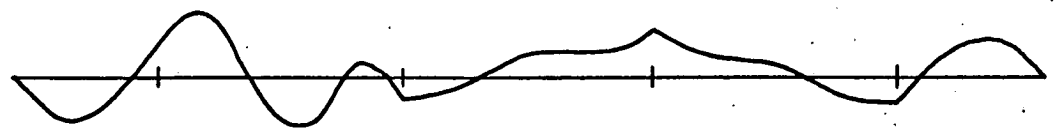
(10)



(11)

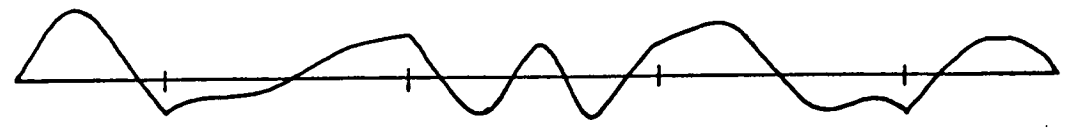


(12)

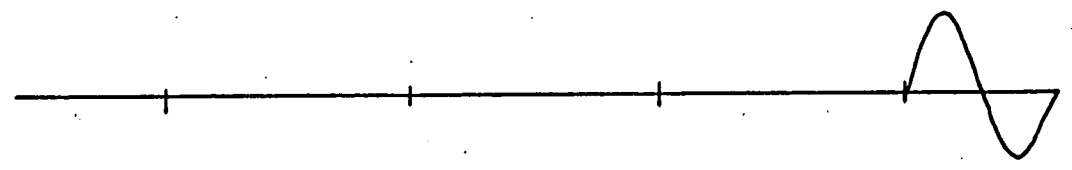


CONTD.

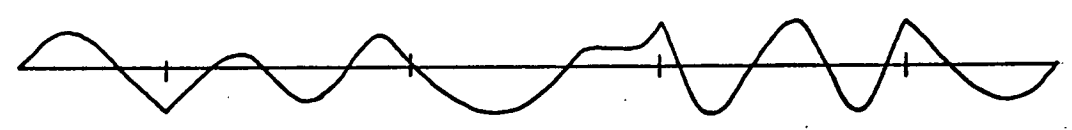
(13)



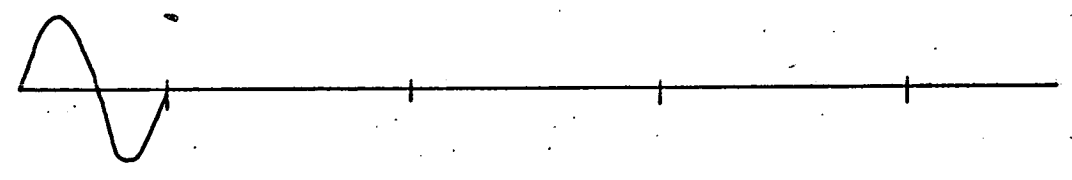
(14)



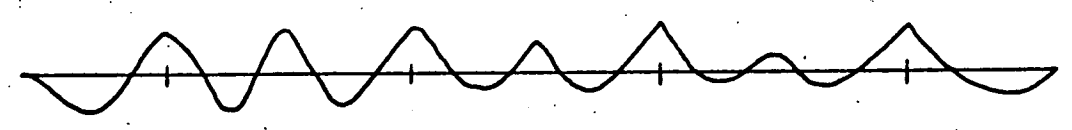
(15)



(16)



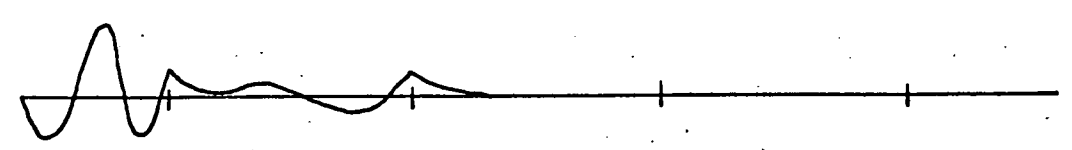
(17)



(18)



(19)



CHAPTER 4

NATURAL FREQUENCIES AND NORMAL MODES OF SYSTEMS COMPOSED
OF EQUAL SUB-SYSTEMS

4.1 COUPLING OF EQUAL SPANS THROUGH SUSPENSION ARMS

It often happens that equal spans are employed in transmission line systems passing over an open level space and hence the analysis of the present section was carried out in the research to provide some information about the coupling effects between the spans of such a system. The assumptions mentioned in the previous chapter will hold true for the following analysis.

Three Equal Spans - Inplane Motion

The system to be considered is shown in Fig. 4.1, which, when broken down into subsystems, gives the system of Fig. 4.2. Referring to the fixed-free and free-free catenaries discussed in Appendix-A, we can write the equations of motion for the broken system as -

$$\begin{bmatrix} I & & \circ \\ & I & \\ \circ & & I \end{bmatrix} \begin{bmatrix} \ddot{V}_1 \\ \ddot{V}_2 \\ \ddot{V}_3 \end{bmatrix} + \begin{bmatrix} E_1 & & \circ \\ & E_2 & \\ \circ & & E_3 \end{bmatrix} \begin{bmatrix} V_1 \\ V_2 \\ V_3 \end{bmatrix} = 0 \quad (4.1)$$

where $V_i = \{V_{i1}, V_{i3}, V_{i5}\} ; i = 1, 2, 3 \quad (4.2)$

$$E_i = \frac{\pi^2 g}{8d} \begin{bmatrix} 1 & & \circ \\ & 9 & \\ \circ & & 25 \end{bmatrix} \quad (4.3)$$

$$\text{and} \quad I = 3 \times 3 \text{ unit matrix} \quad (4.4)$$

with d being the dip of one catenary. In (4.1) - (4.4), it is understood that only three symmetrical string modes in each span are considered and that the fixed-free and free-free catenaries are represented by the stretched string mathematical model. There are however two compatibility relations which, when applied to (4.1), gives the equations of motion for the composite system. These compatibility relations require that

$$\left. \begin{aligned} U_{1R} &= U_{2L} \\ U_{2R} &= U_{3L} \end{aligned} \right\} \quad (4.5)$$

where the subscript R and L denote respectively the right and left hand ends of the i th catenary. Equations (4.5) can be expressed as one equation in the coordinates corresponding to (4.1) which is simply

$$V_{11} - V_{13/3} + V_{15/5} + V_{21} - V_{23/3} + V_{25/5} + V_{31} - V_{33/3} + V_{35/5} = 0 \quad (4.6)$$

Introducing Lagrange multiplier [1], the equations of motion for the composite system become

$$\begin{bmatrix} I & & & \\ & I & & \\ & & I & \\ & & & I \end{bmatrix} \begin{bmatrix} \ddot{V}_1 \\ \ddot{V}_2 \\ \ddot{V}_3 \end{bmatrix} + \begin{bmatrix} E_1 & & & \\ & E_2 & & \\ & & E_3 & \\ & & & \end{bmatrix} \begin{bmatrix} V_1 \\ V_2 \\ V_3 \end{bmatrix} = \lambda \begin{bmatrix} d_1 \\ d_2 \\ d_3 \end{bmatrix} \quad (4.7)$$

$$d_i = \{d_{i1}, d_{i3}, d_{i5}\} = \{1, -1/3, 1/5\}; \quad i = 1, 2, 3 \quad (4.8)$$

Let us write (4.7) as

$$I\ddot{V} + EV = \lambda d \quad (4.9)$$

To solve the equations governing free vibration, we put

$$V = \Psi \sin \omega t \text{ and } \lambda = \mu \sin \omega t \quad (4.10)$$

where Ψ is a column vector and μ is a scalar. If (4.10) is substituted in (4.9) and (4.6), we obtain respectively

$$(E - \omega^2 I) - \mu d = 0 \quad (4.11)$$

$$d' \Psi = 0 \quad (4.12)$$

In partitioned form (4.11) and (4.12) can be written as

$$\begin{bmatrix} E - \omega^2 I & -d \\ d' & 0 \end{bmatrix} \begin{bmatrix} \Psi \\ \mu \end{bmatrix} = 0 \quad (4.13)$$

The characteristic equation corresponding to (4.13) becomes

$$\begin{vmatrix} E - \omega^2 I & -d \\ d' & 0 \end{vmatrix} = 0 \quad (4.14)$$

Expanding (4.14) we arrive at

$$\frac{d_{11}^2}{\omega_{11}^2 - \omega^2} + \frac{d_{13}^2}{\omega_{13}^2 - \omega^2} + \frac{d_{15}^2}{\omega_{15}^2 - \omega^2} + \frac{d_{21}^2}{\omega_{21}^2 - \omega^2} + \dots + \frac{d_{35}^2}{\omega_{35}^2 - \omega^2} = 0 \quad (4.15)$$

Note that the frequency equation (4.15) can also be applied to systems having differing span lengths and the solutions to (4.15) can be obtained by various numerical methods.

Simplifying (4.15) and using the conditions that

$$\left. \begin{array}{l} \omega_{11}^2 = \omega_{21}^2 = \omega_{31}^2 \\ \omega_{13}^2 = \omega_{23}^2 = \omega_{33}^2 \\ \omega_{15}^2 = \omega_{25}^2 = \omega_{35}^2 \\ \omega_{15}^2 = \omega_{25}^2 = \omega_{35}^2 \end{array} \right\} \begin{array}{l} d_{11}^2 = d_{21}^2 = d_{31}^2 \\ d_{13}^2 = d_{23}^2 = d_{33}^2 \\ d_{15}^2 = d_{25}^2 = d_{35}^2 \\ d_{15}^2 = d_{25}^2 = d_{35}^2 \end{array} \quad (4.16)$$

we obtain

$$\begin{aligned} & (\omega_{11}^2 - \omega^2)^2 (\omega_{13}^2 - \omega^2)^2 (\omega_{15}^2 - \omega^2)^2 [3d_{11}^2 (\omega_{13}^2 - \omega^2) (\omega_{15}^2 - \omega^2) + \\ & + 3d_{13}^2 (\omega_{11}^2 - \omega^2) (\omega_{15}^2 - \omega^2) + 3d_{15}^2 (\omega_{11}^2 - \omega^2) (\omega_{13}^2 - \omega^2)] = 0 \end{aligned} \quad (4.17)$$

From (4.17) we get

$$(\omega_{11}^2 - \omega^2)^2 = 0 \quad (4.18)$$

$$\left. \begin{array}{l} (\omega_{13}^2 - \omega^2)^2 = 0 \\ (\omega_{15}^2 - \omega^2)^2 = 0 \end{array} \right\} \quad (4.19)$$

and

$$\begin{aligned} & d_{11}^2 (\omega_{13}^2 - \omega^2) (\omega_{15}^2 - \omega^2) + d_{13}^2 (\omega_{11}^2 - \omega^2) (\omega_{15}^2 - \omega^2) + \\ & + d_{15}^2 (\omega_{11}^2 - \omega^2) (\omega_{13}^2 - \omega^2) = 0 \end{aligned} \quad (4.20)$$

Solving (4.18) - (4.20) we obtain in increasing order of magnitude

$$\omega = \omega_{11}, \omega_{11}, \omega_1, \omega_{13}, \omega_{13}, \omega_2, \omega_{15}, \omega_{15} \text{ rad/sec}$$

where ω_{11} , ω_{13} , ω_{15} are the subsystem frequencies and since (4.20) is identical to the frequency equation of the fixed-fixed catenary, ω_1 , ω_2 are the frequencies obtained by considering an ends-fixed catenary of the same dimensions.

Considering now the Red Moss 1200 ft. span as one of the spans of the three equal span system we obtain the circular frequencies in increasing order of magnitude:

$$\omega = 1.02583, 1.02583, 2.93453, 3.07748, 3.07748, 3.07748, 5.04532 \\ 5.12913, 5.12913 \text{ rad/sec.}$$

The sketches of the possible mode shapes for repeated pairs of frequencies are shown in Fig. 4.6 where it is assumed that deformation occurs only in two adjacent spans. For the non-repeated roots the deformation occurs simultaneously in all the spans considered.

Thus it is observed that the three equal span system possesses confluent pairs of modes (i.e. modes having the same frequency). This indicates the possibility of large energy transferences between the spans, as in the case of a Wilberforce spring [11], when nearly confluent frequencies appear in a practical system.

In the above analysis, no antisymmetric modes in the spans are considered because these modes do not cause suspension arm movements and hence there are no inter-span coupling effects.

4.2 COUPLING OF EQUAL SPANS THROUGH TOWER FLEXIBILITY

The types of system dealt with in the preceding chapter is probably most characteristic of multi-span transmission line systems. In this case, the various spans interact through relatively flexible couplings in the form of suspension arms. No account of the tower flexibility had been taken. In this section we take a step forward to study the interactions of the constituent spans due to the flexibility of the towers. The system to be considered is illustrated in Fig. 4.3, which, in fact, resembles an actual transmission line system.

Inplane Motion

Strain Energy Due to Tower Flexure

We consider the i th. catenary and allow cross-span tower-arm movements h_{i1} and h_{i2} as indicated in Fig. 4.9. If the catenary is symmetrical we can write

$$\left. \begin{aligned} h_{i1} &= -h_{i2} = -h_i \\ u_{i1} &= -u_{i2} = -u_i \end{aligned} \right\} \quad (4.21)$$

Considering the right hand side suspension arm of the i th catenary Fig. 4.5, we can write the forces actingⁱⁿ the horizontal and vertical directions as follows -

$$\begin{aligned} \text{Horizontal} &: H \\ \text{Vertical} &: W - \frac{m}{2} \int_{-l}^l \ddot{v}_i dx \end{aligned}$$

where H is the horizontal component of cable tension and W is the total static weight carried by the suspension arm. W will be assumed the same for each suspension arm.

Resolving the vertical and horizontal forces on the suspension arm we obtain for the force along the suspension arm

$$F_{si} = W + H\theta_i - \frac{m}{2} \int_{-L}^L \ddot{v}_i dx \quad (4.22)$$

where θ_i is the inclination of the suspension arm to the vertical.

Resolving again we obtain the horizontal force at the i th. tower arm

$$F_i = W\theta_i \quad (4.23)$$

considering now the geometry of the inclined suspension arm we get

$$\theta_i = \frac{u_i - h_i}{l_s} \quad (4.24)$$

with l_s = length of the suspension arm.

Equation (4.23) through (4.24) becomes

$$F_i = W \frac{u_i - h_i}{l_s} \quad (4.25)$$

$$\text{or} \quad F_i + W \frac{h_i}{l_s} = W \frac{u_i}{l_s} \quad (4.26)$$

considering all the catenaries forming the system of Fig. 4.3, we can write in matrix form

$$([I] + \frac{W}{l_s} [Fl_i]) \{F\} = \frac{W}{l_s} \{u\} \quad (4.27)$$

where $[I] = 6 \times 6$ unit matrix

$[Fl_i] = 6 \times 6$ inplane tower flexibility matrix

$\{F\} = \{F_1, F_2, F_3, F_4, F_5, F_6\}$

$\{u\} = \{u_1, u_2, u_3, u_4, u_5, u_6\}$

An approximate procedure to calculate the flexibility matrices for inplane and lateral motions of any tower is given Appendix-B.

From (4.27) we obtain

$$\{F\} = \frac{W}{I} ([I] + \frac{W}{I_s} [Fl_i])^{-1} \{u\} \quad (4.28)$$

$$\text{or} \quad \{F\} = [A] \{u\} \quad (4.29)$$

Using the conditions (4.21) the strain energy for both towers can be written as

$$V_s = [F][Fl_i] \{F\} \quad (4.30)$$

$$= [u][A]' [Fl_i] [A] \{u\} \quad (4.31)$$

$$= \frac{1}{2} [u][B] \{u\} \quad (4.32)$$

$$\text{where} \quad [B] = 2 [A]' [Fl_i] [A] \quad (4.33)$$

Potential Energy in a General Inplane Displacement

Under the conditions (4.21) the total potential energy for the system is -

$$\begin{aligned}
V = & \frac{H}{2} \int_{-L}^L \left(\frac{\partial v_1}{\partial x}\right)^2 dx + \frac{H}{2} \int_{-L}^L \left(\frac{\partial v_2}{\partial x}\right)^2 dx + \dots + \frac{H}{2} \int_{-L}^L \left(\frac{\partial v_6}{\partial x}\right)^2 dx + \\
& + \frac{4mgL + M_s g}{2l_s} (u_1^2 + u_2^2 + \dots + u_6^2) + \frac{1}{2} \sum \sum b_{ij} u_i u_j \quad (4.34)
\end{aligned}$$

where b_{ij} are the elements of the matrix $[B]$ and M_s is the mass of the suspension arm. The kinetic energy becomes

$$\begin{aligned}
T = & \frac{m}{2} \int_{-L}^L \dot{v}_1^2 dx + \frac{m}{2} \int_{-L}^L \dot{v}_2^2 dx + \dots + \frac{m}{2} \int_{-L}^L \dot{v}_6^2 dx + \\
& + \frac{M_s}{4} (\dot{u}_1^2 + \dot{u}_2^2 + \dots + \dot{u}_6^2) \quad (4.35)
\end{aligned}$$

If the cables are assumed inextensible, we have six equations of constraint given by

$$U_i = \frac{mg}{2H} \int_{-L}^L v_i dx, \quad i = 1, 2, \dots, 6 \quad (4.36)$$

Solution by Rayleigh-Ritz Method

Let us assume for v_i a linear combination of symmetrical string modes and write

$$v_i = V_{i1} \cos \frac{\pi x}{2L} + V_{i3} \cos \frac{3\pi x}{2L} \quad (4.37)$$

The antisymmetrical string modes are not considered in (4.37) because these modes do not cause any tower arm deflection. Substituting (4.37) in (4.34) - (4.36) we obtain respectively

$$\begin{aligned}
V = & \frac{\pi^2 H}{8L} (V_{11}^2 + 9V_{13}^2 + V_{21}^2 + 9V_{23}^2 + \dots + V_{61}^2 + 9V_{63}^2) + \\
& + \frac{k_1}{2} (U_1^2 + U_2^2 + \dots + U_6^2) + \frac{1}{2} \sum \sum b_{ij} U_i U_j \quad (4.38)
\end{aligned}$$

For the numerical results the Red Moss 1200 ft. span was considered and using only the fundamental mode in each span the equations of motion were formed and solved. The results are given in Table - 4.1. The procedure can be easily applied to the motion in the lateral plane.

Frequencies of Six Lowest Modes (HZ)

Table 4.1

Flexibility Matrix Multiplied by			
1	10	100	1000
0.17010	0.17011	.17027	.17047
0.17010	0.17013	.17039	.17129
0.17010	0.17018	.17081	.17141
0.17011	0.17024	.17115	.17166
0.17012	0.17032	.17148	.17171
0.17022	0.17104	.17180	.17192

Note that the flexibility matrix is only a crude estimate. However, even when multiplied by a large scalar, the effect is minimal. Hence it is concluded that in actual practice the effect of tower flexibility may probably be neglected.

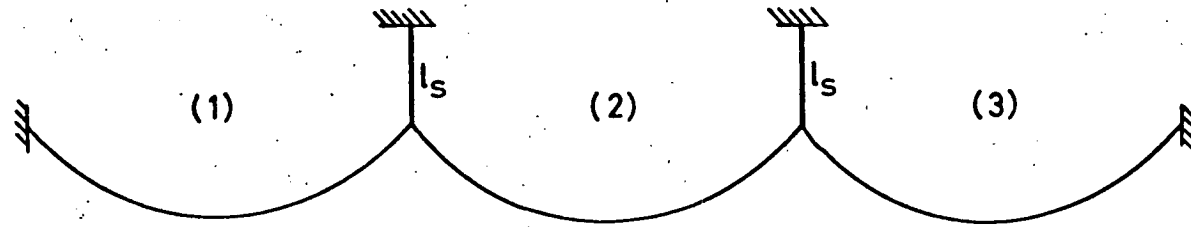


FIG. 4.1—COMPOSITE SYSTEM

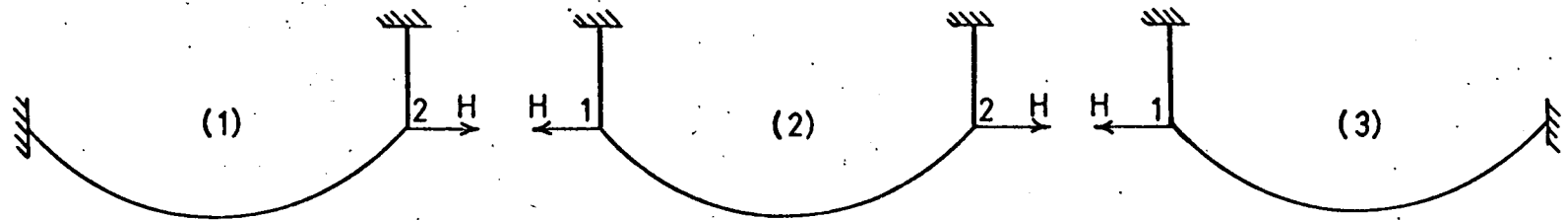


FIG. 4.2—BROKEN SYSTEM

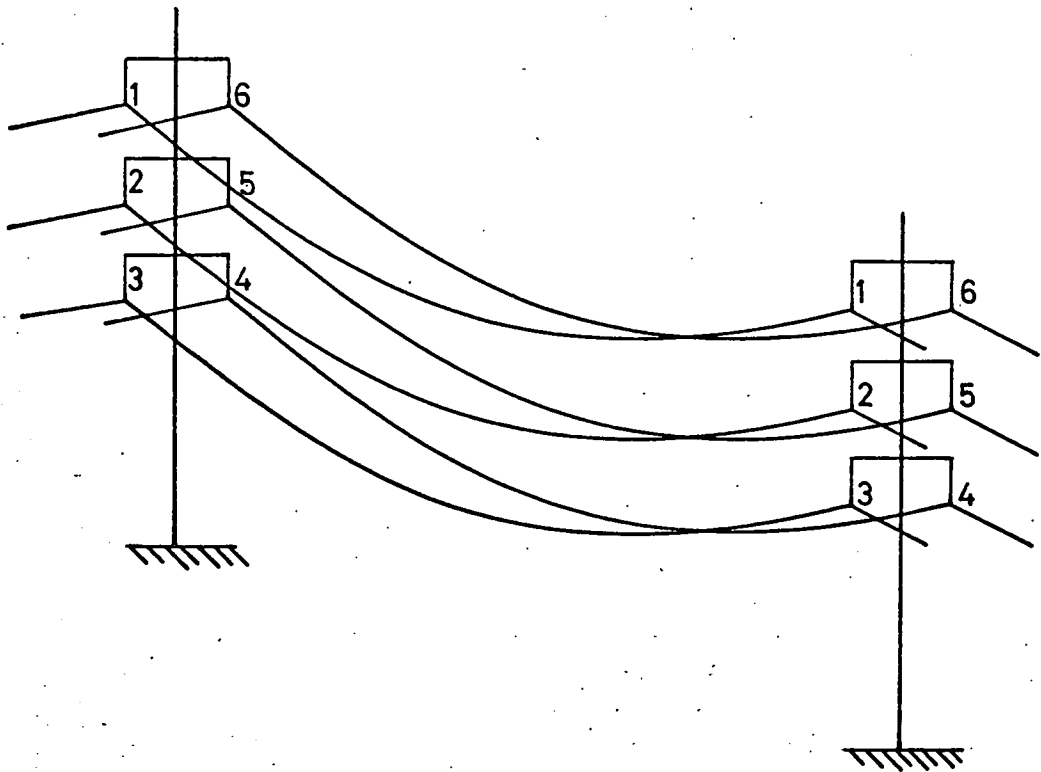


FIG. 4.3

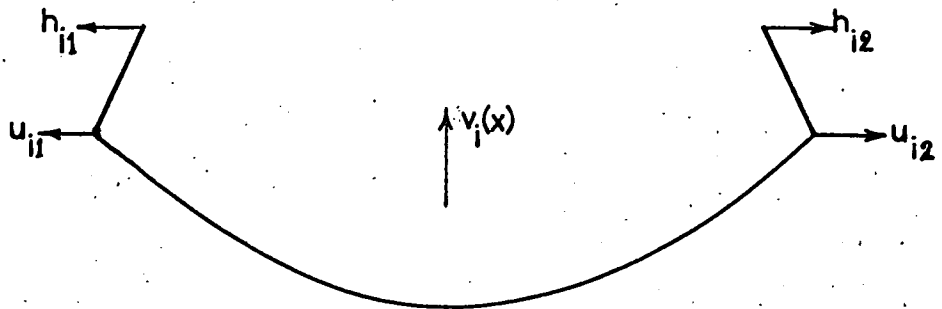


FIG. 4.4

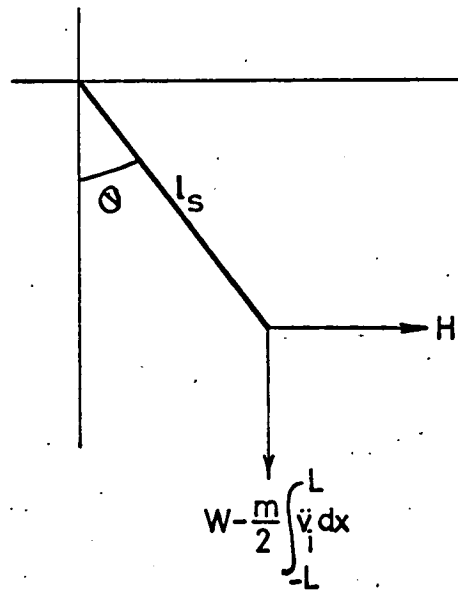


FIG. 4.5

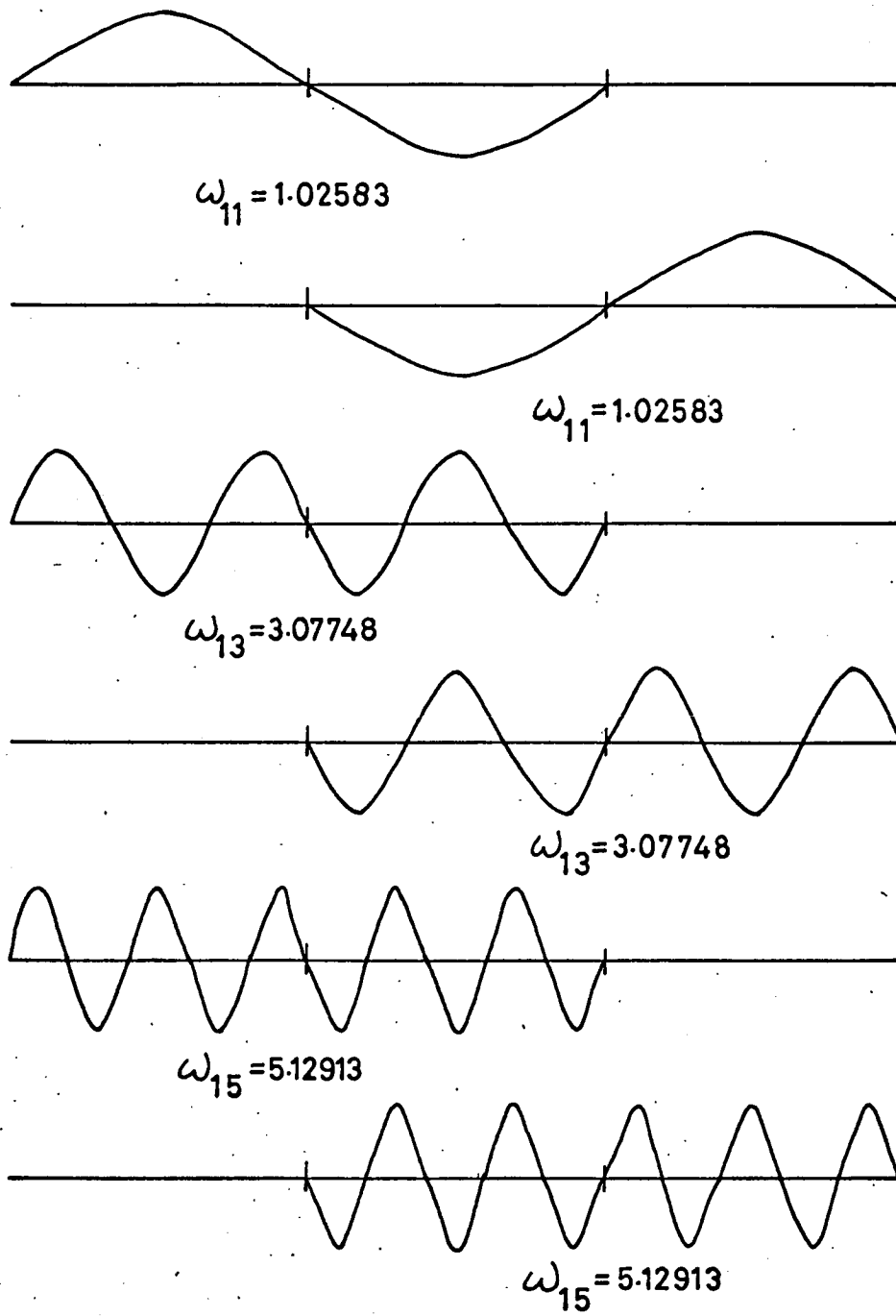


FIG. 4.6

CHAPTER 5

NONLINEAR COUPLING BETWEEN INPLANE AND LATERAL MODES
OF AN INEXTENSIBLE CATENARY

So far only the linear equations of motion of single and multi-span catenary systems have been treated and solved. Probably the assumption of linearity in the equations of motion is well justified provided that the motion takes place in the vicinity of the equilibrium position and line span/dip ratio is large. But clashing of conductors occurs at large amplitudes on shallow catenaries and nonlinear effects are bound to be important in this case. A well known example of nonlinear coupling is that between the first antisymmetric inplane and lateral modes of the single span ends fixed catenary. In order to proceed with the study of the possible nonlinear coupling between inplane and lateral modes of a uniform inextensible catenary, we undertake the analysis of the present chapter and resort to the Simpson's Lumped Mass Catenary because in this case nonlinear equations are easily formed. For simplicity it will be assumed that the catenary hangs in the vertical plane at equilibrium (i.e. no steady wind forces). To form the equations of motion in three-dimensions, let us consider the link as shown in Fig. 5.1 and assume that the ends of this link undergo displacements $(h_1, v_1, z_1), (h_2, v_2, z_2)$ measured from the equilibrium position. Then if the link is not extended or contracted during the general displacement, we must have

$$l \cos \theta_1 (H_1 - H_2) + l \sin \theta_1 (V_1 - V_2) + \frac{1}{2} [(H_1 - H_2)^2 + (V_1 - V_2)^2 + (Z_1 - Z_2)^2] = 0 \quad (5.1)$$

where l is the length of the link, θ_i is the inclination of the link to the horizontal at equilibrium and $H_i = h_i/l$, $V_i = \frac{v_i}{l}$ etc.

Solving (5.1) for $(H_i - H_j)$, up to cubic order, we obtain

$$H_i - H_j = -t_i(V_i - V_j) - \frac{S_i^3}{2}(V_i - V_j)^2 - \frac{S_i}{2}(Z_i - Z_j)^2 - \frac{t_i S_i^4}{2}(V_i - V_j)^3 - \frac{t_i S_i^2}{2}(V_i - V_j)(Z_i - Z_j)^2 \quad (5.2)$$

where $t_i = \tan\theta_i$ and $S_i = \sec\theta_i$.

An important deduction, regarding the coupling between the inplane and lateral modes of the complete catenary, can be made at this stage. Since the potential energy of the linear system is composed of quadratic terms, such as the second order terms of (5.2), there will be no statical coupling between inplane and lateral modes. Also $(H_i - H_j)$ contains no first order terms in $(Z_i - Z_j)$ and hence when the kinetic energy function for the linear system is formed by squaring the linear terms \dot{H}_i , \dot{V}_i , \dot{Z}_i , multiplying by the appropriate mass values and summing, no $\dot{Z}_i \dot{V}_j$, $\dot{Z}_i \dot{H}_j$ terms are involved. Therefore it can be concluded that the linear equations of motion of a catenary, which hangs vertically at equilibrium, will contain no coupling terms between the inplane and lateral coordinates.

For simplicity, we consider the two-mass catenary shown in Fig. 5.2 and apply (5.2) to each link. Note that (5.2) holds true for the links on the left hand side of the line of symmetry. On the right hand side of the line of symmetry we must change the sign of $\tan\theta_i$. Thus for the links forming the system of Fig. 5.2 we obtain -

$$\left. \begin{aligned}
 H_1 &= -t_1 v_1 - \frac{s_1^3}{2} v_1^2 - \frac{s_1}{2} z_1^2 - \frac{t_1 s_1^4}{2} v_1^3 - \frac{t_1 s_1^2}{2} v_1 z_1^2 \\
 H_2 - H_1 &= -\frac{1}{2} (v_2 - v_1)^2 - \frac{1}{2} (z_2 - z_1)^2 \\
 -H_2 &= -t_1 v_2 - \frac{s_1^3}{2} v_2^2 - \frac{s_1}{2} z_2^2 - \frac{t_1 s_1^4}{2} v_2^3 - \frac{t_1 s_1^2}{2} v_2 z_2^2
 \end{aligned} \right\} (5.3)$$

Adding (5.3) to give

$$\begin{aligned}
 t_1(v_1 + v_2) + \frac{1}{2}[s_1^3 v_1^2 + (v_2 - v_1)^2 + s_1^3 v_2^2 + s_1 z_1^2 + (z_2 - z_1)^2 + s_1 z_2^2] + \\
 + \frac{t_1}{2} [s_1^4 (v_1^3 + v_2^3) + s_1^2 (v_1 z_1^2 + v_2 z_2^2)] = 0
 \end{aligned} \quad (5.4)$$

Solving (5.3) for v_2 up to cubic order, we obtain

$$\begin{aligned}
 v_2 = -v_1 - \frac{1}{2t_1} \left[\left\{ 1 + \frac{2 + s_1^3}{t_1} v_1 \right\} \left\{ 2(2 + s_1^3) v_1^2 + s_1 z_1^2 + (z_2 - z_1)^2 + \right. \right. \\
 \left. \left. + s_1 z_2^2 \right\} + t_1 s_1^2 (v_1 z_1^2 - v_1 z_2^2) \right]
 \end{aligned} \quad (5.5)$$

As the system has no spring stiffnesses the potential energy is wholly due to gravity and is given by

$$V = -mgl \sum v_i \quad (5.6)$$

Substituting (5.5) in (5.6) we obtain for the potential energy

$$\begin{aligned}
 V = \frac{mg1}{2t_1} \left[\left\{ 1 + \frac{2 + s_1^3}{t_1} v_1 \right\} \left\{ 2(2 + s_1^3) v_1^2 + s_1 z_1^2 + (z_2 - z_1)^2 + s_1 z_2^2 \right\} + \right. \\
 \left. + t_1 s_1^2 (v_1 z_1^2 - v_1 z_2^2) \right]
 \end{aligned} \quad (5.7)$$

The kinetic energy of the system is given by

$$T = \frac{ml^2}{2} \left[2S_1^2 \dot{v}_1^2 + \dot{z}_1^2 + \dot{z}_2^2 + \frac{4S_1^2(2 + S_1^3)}{t_1} v_1 \dot{v}_1^2 + \left\{ \frac{2S_1^2(1 + S_1)}{t_1} + \right. \right. \\ \left. \left. + 2t_1 S_1 \right\} \dot{v}_1 z_1 \dot{z}_1 + \frac{2S_1(1 + S_1)}{t_1} \dot{v}_1 z_2 \dot{z}_2 - \frac{2S_1^2}{t_1} (\dot{v}_1 z_2 \dot{z}_1 + \dot{v}_1 z_1 \dot{z}_2) \right] \quad (5.8)$$

The equations of motion may now be formed by using Lagrange's equations.

In order to reduce the complexity of problem we transfer to normal coordinates. The linear equations of motion are obtained by keeping only the second order terms in (5.7) and (5.8). The modal matrix for the lateral motion is

$$[\Psi_z] = \begin{bmatrix} 1 & 1 \\ 1 & -1 \end{bmatrix} \quad (5.9)$$

If we use the linear transformation

$$z = [\Psi_z] \{y\} \quad (5.10)$$

The potential energy, (5.7) becomes

$$V = \frac{mgL}{2t_1} \left[2(2 + S_1^3)x_1^2 + 2S_1 y_1^2 + 2(2 + S_1)y_2^2 + \frac{2(2 + S_1^3)^2}{t_1} x_1^3 + \right. \\ \left. + \frac{2S_1(2 + S_1^3)}{t_1} x_1 y_1^2 + \frac{2(2 + S_1)(2 + S_1^3)}{t_1} x_1 y_2^2 + 4t_1 S_1^2 x_1 y_1 y_2 \right] \quad (5.11)$$

and the kinetic energy, (5.8), becomes

$$T = \frac{ml^2}{2} \left[2S_1^2 \dot{x}_1^2 + 2\dot{y}_1^2 + 2\dot{y}_2^2 + \frac{4S_1^2(2+S_1^3)}{t_1} x_1 \dot{x}_1^2 + \frac{4S_1^3}{t_1} \dot{x}_1 y_1 \dot{y}_1 + \right. \\ \left. + \frac{4S_1^2(2+S_1)}{t_1} \dot{x}_1 y_2 \dot{y}_2 + 4t_1 S_1 \dot{x}_1 (y_1 \dot{y}_2 + y_2 \dot{y}_1) \right] \quad (5.12)$$

For convenience, V_1 in (5.11) and (5.12) is replaced by x_1 .

Using Lagrange's equations, the nonlinear equations of motion in normal coordinates, for the system of Fig. 5.2, can now be written as -

$$\ddot{x}_1 + \Omega^2 x_1 + a_1 x_1^2 + a_2 y_1^2 + a_3 y_2^2 + a_4 y_1 y_2 + a_5 (x_1 \ddot{x}_1 + \dot{x}_1^2) + \\ + a_6 (\dot{y}_1^2 + y_1 \ddot{y}_1) + a_7 (\dot{y}_2^2 + y_2 \ddot{y}_2) + a_8 (y_1 \ddot{y}_2 + y_2 \ddot{y}_1 + 2\dot{y}_1 \dot{y}_2) = 0 \quad (5.13)$$

$$\ddot{y}_1 + \omega_1^2 y_1 + b_1 x_1 y_1 + b_2 x_1 y_2 + b_3 \ddot{x}_1 y_1 + b_4 \ddot{x}_1 y_2 = 0$$

$$\ddot{y}_2 + \omega_2^2 y_2 + c_1 x_1 y_2 + c_2 x_1 y_1 + c_3 \ddot{x}_1 y_2 + c_4 \ddot{x}_1 y_1 = 0$$

Where the natural frequencies of the linear system are given by

$$\Omega^2 = \frac{g(2+S_1^3)}{lt_1 S_1^2}, \quad \omega_1^2 = \frac{gS_1}{lt_1}, \quad \omega_2^2 = \frac{g(2+S_1)}{lt_1}$$

The normal mode shapes corresponding to these frequencies are shown in Fig. 5.5.

Also

$$a_1 = \frac{3g(2 + s_1^3)^2}{21t_1^2 s_1^2} \quad b_1 = \frac{gs_1(2 + s_1^3)}{1t_1^2} \quad c_1 = \frac{g(2 + s_1)(2 + s_1^3)}{1t_1^2}$$

$$a_2 = \frac{g(2 + s_1^3)}{21t_1^2 s_1} \quad b_2 = \frac{gs_1^2}{1} \quad c_2 = \frac{gs_1^2}{1}$$

$$a_3 = \frac{g(2 + s_1)(2 + s_1^3)}{21t_1^2 s_1^2} \quad b_3 = \frac{s_1^3}{t_1} \quad c_3 = \frac{s_1^2(2 + s_1)}{t_1}$$

$$a_4 = \frac{g}{1} \quad b_4 = t_1 s_1 \quad c_4 = t_1 s_1$$

$$a_5 = \frac{2(2 + s_1^3)}{-t_1}$$

$$a_6 = \frac{s_1}{t_1}$$

$$a_7 = \frac{(2 + s_1)}{t_1}$$

$$a_8 = \frac{t_1}{s_1}$$

Some Comments on the Coupled Nonlinear Equations

From (5.13) we can classify the coupling terms as follows -

- (i) statical coupling force in the inplane mode deriving from the lateral modes of the form $y_i y_j$
- (ii) dynamical coupling force in the inplane mode deriving from the lateral modes of the forms $\dot{y}_i \dot{y}_j$ and $y_i \ddot{y}_j$
- (iii) statical coupling force in the lateral modes deriving from the inplane mode of the form $x_1 y_i$

(iv) dynamical coupling force in the lateral modes deriving from the inplane mode of the form $\ddot{x}_1 y_i$

Most of the above couplings are proportional to the factors $1/t_1^2$ and $1/t$ which are very large when the dip/ratio is small. Thus the nonlinear coupling effects become more prominent in flat than in deep catenaries.

If the system is given an initial lateral displacement and released, there will be forces proportional to $y_i y_j$, $\dot{y}_i \dot{y}_j$ and $y_i \ddot{y}_j$ which will tend to produce inplane motion. The resulting inplane motion will have an amplitude depending on the tuning of the inplane and lateral natural frequencies. If θ is small for the system of Fig. 5.2, we get

$$\Omega^2 = \omega_2^2 \quad (5.14)$$

Hence it would appear that the vertical amplitude resulting from the second lateral mode will be most significant. As the amplitude in the excited vertical mode builds up, the lateral amplitude will be decreased, since the system is assumed conservative. Also when the vertical amplitude becomes significant, energy commences to be transferred back to the lateral modes through coupling (iii) and (iv). Thus the lateral mode builds up due to forces which are y_i -dependent, as in the case of a "Mathieu-Type Instability". The vertical motion consequently decays and the status-quo is restored, provided no damping forces have acted through the process. The above reasonings are the same as those of Minorsky's elastic pendulum [18, 20, 21].

If the system is given an initial vertical displacement and released, there will be no resultant lateral exciting force provided there is no initial lateral motion.

The above comments will be clear in the following paragraphs where (5.13) is given more attention.

Experimental Observation of Nonlinear Coupling Effects

For this purpose, a simple two-mass catenary was built in the laboratory from 0.011 inch diameter piano wire. A photographic view of this simple system is given in Fig. 5.6. No external excitation was arranged in the beginning. The system possesses three degrees of freedom - one vertical and two lateral. The natural frequencies and the normal modes were observed which agreed with those of the theoretical calculation. The following observations were made on this simple experimental model -

(i) the system was given an initial displacement in the vertical mode and released. The system vibrated vertically in the natural frequency. No lateral motion was noticed.

(ii) the system was given an initial displacement in the first lateral mode and released. The system swung like a pendulum and no vertical motion seemed to be excited.

(iii) the system was now given an initial displacement in the second lateral mode and released. The catenary firstly vibrated in the second lateral mode, gradually exciting the vertical mode. As the amplitude in the vertical mode built up, the amplitude of the lateral mode decreased. At one time the motion was purely vertical. Vertical motion was transferred back to the lateral plane and status-quo was restored.

Considering one mass only, the motion seemed to follow a pattern as shown in Fig. 5.3.

The conclusions concerning the coupling and absence of coupling between the various modes were confirmed by these simple laboratory tests. In particular the experimental observations confirmed that strong coupling exists between the inplane and lateral modes which have nearly equal frequencies and similar mode shapes.

External excitation was arranged by putting an electro-magnet under one of the masses. In addition to the linear resonance, the system possessed - subharmonic resonance of order 2 and superharmonic resonance of order 2. The excitation was in the vertical plane and it was thought that the nonlinearity in the exciter led to superharmonic resonance of order 2.

Analytical Methods Applied to (5.13)

The following analytical methods were applied to (5.13) but with no satisfactory solutions.

- (1) Averaging Method [4, 33, 34]
- (2) Asymptotic Method [4, 39]

The above methods as applied to (5.13) are given in Appendix-C.

Qualitative Consideration of (5.13)

If the system is given an initial displacement in one of the lateral modes, we obtain at the start

$$y_i = Y_i \cos \omega_i t, \quad i = 1 \text{ or } 2 \quad (5.15)$$

Substituting (5.15) into the first of (5.13) we get

$$\ddot{x}_1 + \Omega^2 x_1 + a_1 x_1^2 + a_5 (x_1 \ddot{x}_1 + \frac{\dot{x}_1^2}{2}) = F_{11} \cos 2\omega_1 t - F_{21} \quad (5.16)$$

we will consider (5.16) separately for initial y_1 or y_2 .

Initial Displacement in y_1

In this case we obtain

$$\ddot{x}_1 + \Omega^2 x_1 + a_1 x_1^2 + a_5 (x_1 \ddot{x}_1 + \frac{\dot{x}_1^2}{2}) = F_{11} \cos 2\omega_1 t - F_{21} \quad (5.17)$$

where $F_{11} = (a_2/2 - \omega_1^2 a_6) Y_1^2$ and $F_{21} = a_2 Y_1^2 / 2$

$$\text{Since } \omega_1^2 = \frac{1}{3} \Omega^2 \quad (5.18)$$

we get neither the conditions of linear nor subharmonic resonance in (5.17).

Initial Displacement in y_2

In this case we get

$$\ddot{x}_1 + \Omega^2 x_1 + a_1 x_1^2 + a_5 (x_1 \ddot{x}_1 + \frac{\dot{x}_1^2}{2}) = F_{12} \cos 2\omega_2 t - F_{22} \quad (5.19)$$

where $F_{12} = (a_3/2 - \omega_2^2 a_7) Y_2^2$ and $F_{22} = a_3 Y_2^2 / 2$

Since $\omega_2^2 \approx \Omega^2$, the right hand side of (5.19) is now a periodic function of frequency nearly equal to 2Ω . The condition of subharmonic resonance probably exists in this case because of the quadratic stiffness. In order to elucidate further the phenomenon of subharmonic resonance of order 2, we consider a simpler system which contains the essential terms in (5.19).

This is "A mass on two elastic bands" described below.

A Mass on Two Elastic Bands

The system to be considered is shown in Fig. 5.4. Let l be the length of each band in the static equilibrium position. Then if r is the extension of each band corresponding to a vertical displacement, x , of the mass we must have

$$(l\sin\theta + x)^2 + (l\cos\theta)^2 = (l + r)^2 \quad (5.20)$$

$$\text{or} \quad r = x\sin\theta + \frac{1}{2l}(x^2 - r^2) \quad (5.21)$$

Non-dimensionalising (5.21) by writing $R = r/l$ and $X = \frac{x}{l}$ we obtain

$$R = X\sin\theta + \frac{1}{2}(X^2 - R^2) \quad (5.22)$$

Solving (5.22) for R , up to cubic order, we get

$$R = X\sin\theta + \frac{X^2}{2}\cos^2\theta - \frac{X^3}{2}\sin\theta\cos^2\theta \quad (5.23)$$

The potential energy in a displacement, x , is given by

$$V = -mglX + kl^2(R^2 + 2RR_0) \quad (5.24)$$

where $R_0 = (\text{Equilibrium extension of each band})/l$

$$\text{Now} \quad T_e = \frac{mg}{2\sin\theta} \quad (5.25)$$

$$\text{Hence} \quad R_0 = \frac{mg}{2kl\sin\theta} \quad (5.26)$$

where T_e is the equilibrium tension in each band and K is the stiffness of each band.

Substituting (5.23) and (5.26) in (5.24) we obtain

$$V = \frac{A}{2} X^2 + \frac{B}{2} X^3 \quad (5.27)$$

$$\text{where } A = 2\sin^2\theta + \frac{mgl\cos\theta}{\tan\theta}$$

$$\text{and } B = 2\sin\theta\cos^2\theta - mgl\cos^2\theta$$

The kinetic energy is simply given by

$$T = \frac{ml^2}{2} \dot{X}^2 \quad (5.28)$$

Applying Lagrange's equations we get the equation of motion for undamped free vibration of the system

$$\ddot{X} + aX + hX^2 = 0 \quad (5.29)$$

$$\text{with } a = \frac{2K}{m}\sin\theta + \frac{g\cos^2\theta}{l\sin\theta} \quad (5.30)$$

$$h = \frac{3}{2} \left(\frac{2K}{m} - a \right) \sin\theta \quad (5.31)$$

The equation of motion for undamped forced vibration can be simply written as

$$\ddot{X} + aX + hX^2 = \frac{f(t)}{ml} \quad (5.32)$$

Equation (5.32) can now be compared to (5.19) in the context that \dot{x}_1 and \ddot{x}_1 are proportional to x_1 and $f(t)$ is some periodic function of frequency nearly equal to $2a^{1/2}$. In (5.32) let us assume that h is small. In order to obtain the equation in a standard form [18], let us introduce damping such that the equation of motion becomes

$$\ddot{X} + 2K\dot{X} + aX + hX^2 = F\cos 2\omega t \quad (5.33)$$

Let $\omega t = Z$, $2K = \epsilon h^2$, $F = h\bar{F}$, with $a > 0$, $h, K > 0$ small and (5.33) becomes

$$\omega^2 X'' + \omega^2 \epsilon h^2 X + aX' + hX^2 = h\bar{F}\cos 2Z \quad (5.34)$$

where the primes denote differentiation with respect to Z . Assuming

$$X = X_0 + hX_1 + h^2X_2 + \dots \quad (5.35)$$

$$\omega = \omega_0 + h\omega_1 + h^2\omega_2 + \dots \quad (5.36)$$

the perturbation solutions are to order 2 in h

$$\omega^2 = a - 5h^2(A^2 + B^2)/6a \pm \left\{ (h\bar{F}/3a)^2 - 4K^2a \right\}^{1/2} \quad (5.37)$$

the amplitude of the subharmonics

$$Y = (A^2 + B^2)^{1/2} = \pm \left\{ (6a/5b^2) [(a - \omega^2) \pm \left\{ (h\bar{F}/3a)^2 - 4K^2a \right\}^{1/2}] \right\}^{1/2} \quad (5.38)$$

and to order 1 in h

$$X = A\sin Z + B\cos Z + (hAB/3a)\sin 2Z - (h/3a) \left\{ F + (A^2 - B^2)/2 \right\} \cos 2Z - (h/a) (A^2 + B^2)/2 \quad (5.39)$$

$$\text{or } X = \left(\frac{h}{2a}\right)Y^2 + Y\cos(Z - \theta_1) - \left(\frac{h}{6a}\right)Y^2\cos(2Z + \theta_2) - \left(\frac{F}{3a}\right)\cos 2Z \quad (5.40)$$

$$\text{where } \tan \theta_1 = \frac{A}{B}, \quad \tan \theta_2 = AB / \left\{ (A^2 - B^2) / 2 \right\}$$

The solution is valid only for Y real and positive. For Y to be real we must have

$$F > 6 K a^{3/2} h \quad (5.41)$$

For the complete solution and forms of oscillation, the reader is referred to [13, 18].

Observation in the Laboratory

To demonstrate experimentally the existence of the subharmonics of order 2 in the above system, a mass on two elastic bands was taken in the Laboratory. A photographic view of this simple system is given in Fig. 5.7. The natural frequency calculated from (5.30) was in good agreement with the observed natural frequency. An electro-magnet was placed under the mass and when the system was excited at double the natural frequency, the resultant motion of the mass was at the natural frequency.

It is demonstrated mathematically and experimentally that simple system having quadratic stiffness possesses subharmonic resonance of order 2. Thus we can imply the same thing for the two-mass catenary.

Initial Displacement in x_1

If the system of Fig. 5.2 is given an initial displacement in the vertical mode and released we obtain at the start

$$x_1 = X_1 \cos \Omega t \quad (5.42)$$

Substituting (5.42) into the last two equations of (5.13) we obtain

$$\begin{bmatrix} \ddot{y}_1 \\ \ddot{y}_2 \end{bmatrix} + \begin{bmatrix} \omega_1^2 & 0 \\ 0 & \omega_2^2 \end{bmatrix} \begin{bmatrix} y_1 \\ y_2 \end{bmatrix} - \frac{2gX_1}{IS_1} \begin{bmatrix} 0 & \cos\Omega t \\ \cos\Omega t & 0 \end{bmatrix} \begin{bmatrix} y_1 \\ y_2 \end{bmatrix} = 0 \quad (5.43)$$

Since $\omega_2 \approx \Omega$, it would appear that the motion in y_2 will be in linear resonance, but the magnitude of the forcing will depend on the initial displacement in the mode y_1 .

Numerical Solutions of (5.13)

Recently there has been made available at the E.R.C.C. (Edinburgh Regional Computing Centre) a computer package (i.e. program with its own language) called C.S.M.P. (Continuous Systems Modelling Process) for solving nonlinear differential equations. At first we consider (5.13) as two constituent binary systems such as

- (a) the first lateral and the inplane modes
- (b) the second lateral and the inplane modes

Both (a) and (b) were solved for different initial conditions and types of solution obtained are depicted under an appropriate heading at the end of this Chapter. An attempt was also made to consider all the equations of (5.13) together and the solutions obtained are shown at the back of the present Chapter under the appropriate heading. The program as applied to one of the above cases is also given in Appendix-D.

Results demonstrate the physical qualities described above such as -

- (i) there is no vertical mode excited by an initial first lateral mode.
- (ii) the vertical mode builds up from an initial second lateral mode and as the vertical mode builds up in amplitude, the amplitude of the second lateral mode decreases. Also when the amplitude of the vertical mode becomes significant, energy commences to be transferred back to the lateral mode and status-quo is restored.
- (iii) there is no lateral motion resulting from an initial vertical mode provided there is no initial displacement in the lateral plane.

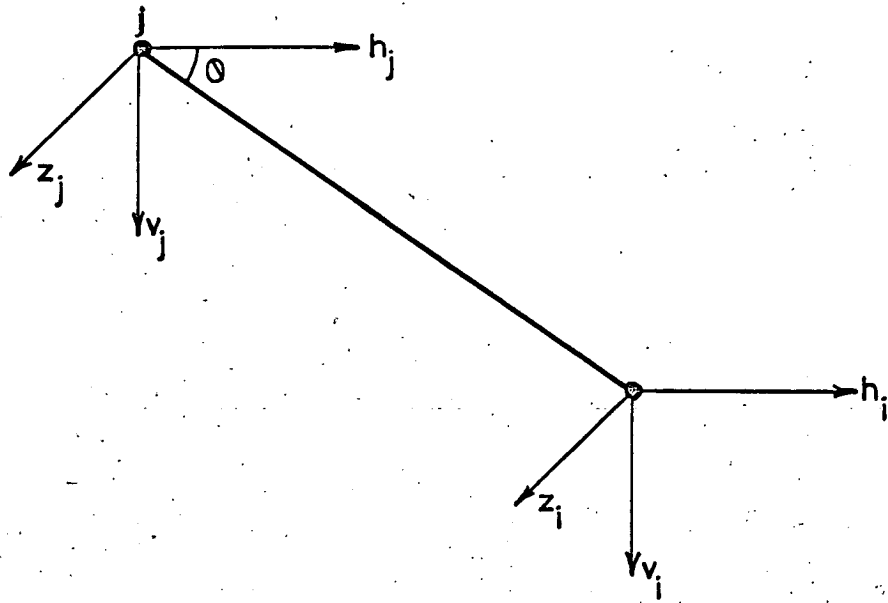


FIG. 5.1

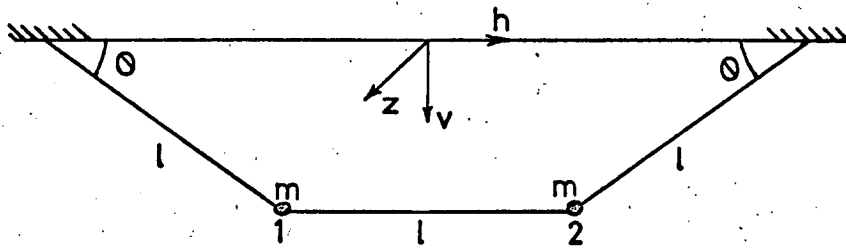


FIG. 5.2

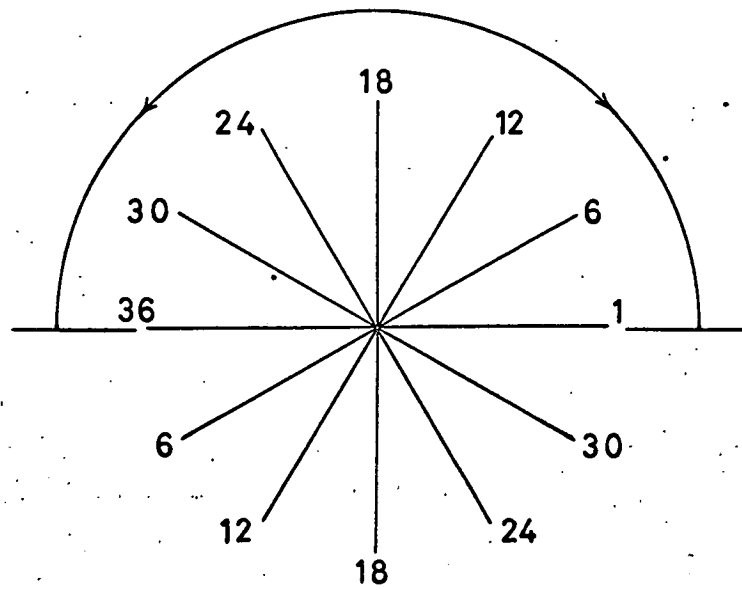


FIG. 5.3

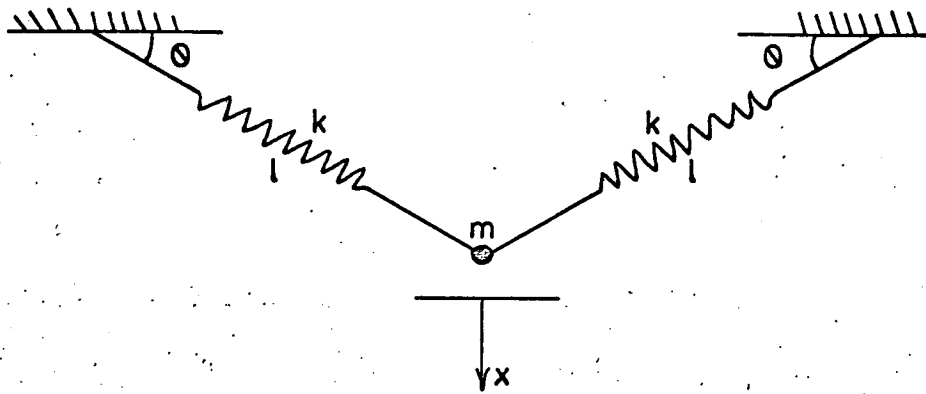
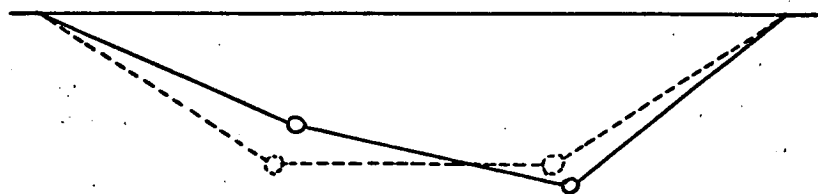
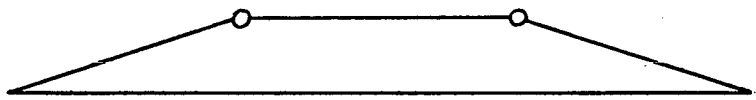


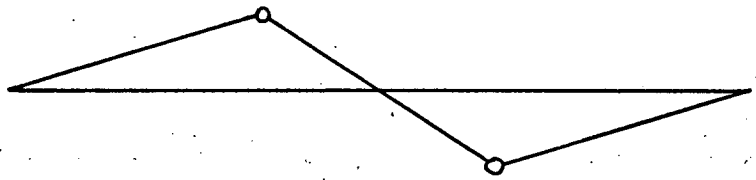
FIG. 5.4



Vertical mode (Ω)



First lateral mode (ω_1)



Second lateral mode (ω_2)

FIG. 5.5

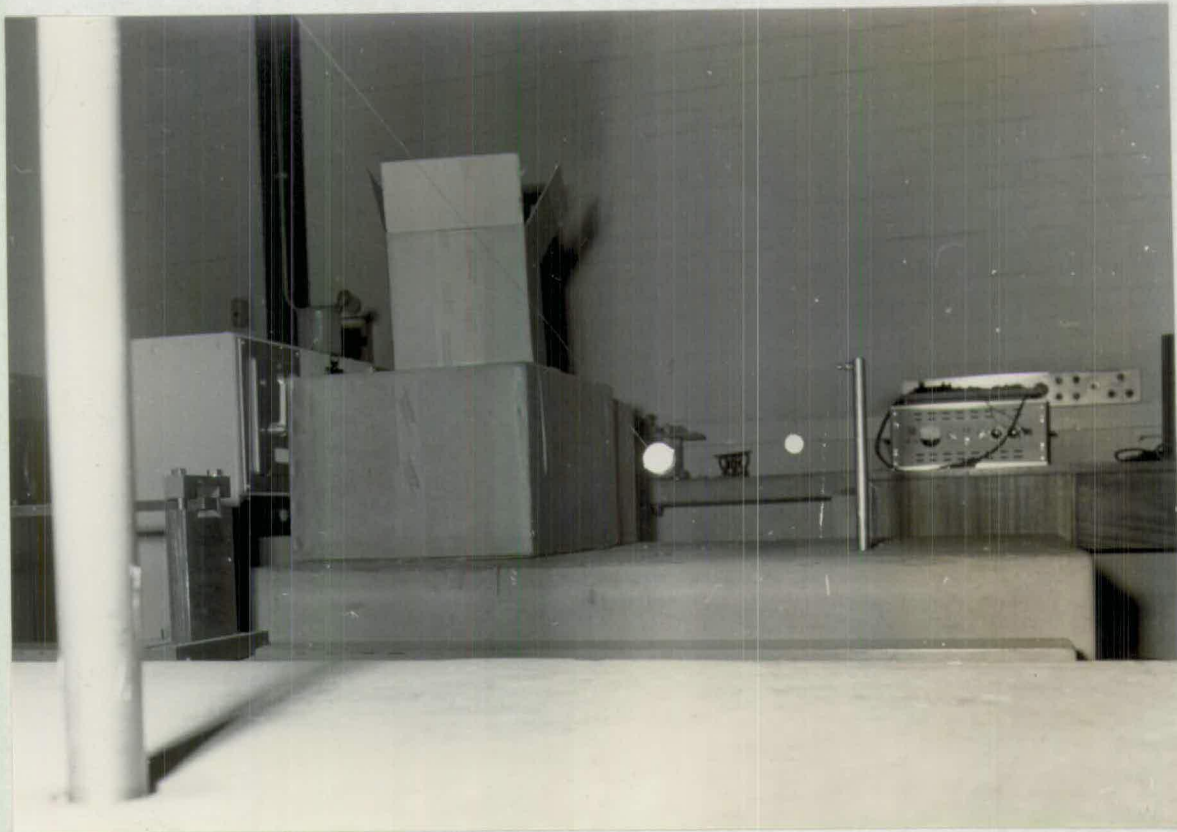


FIG. 5.6

Two Mass Catenary Model.

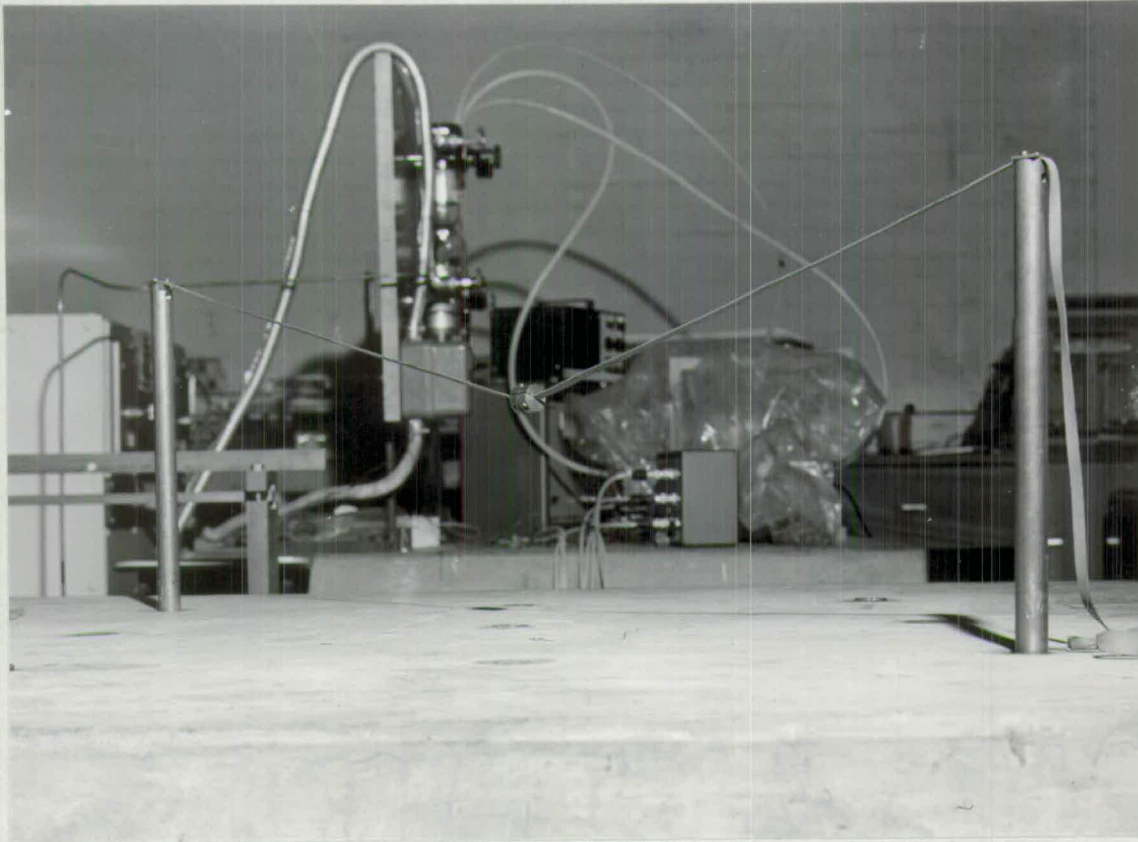
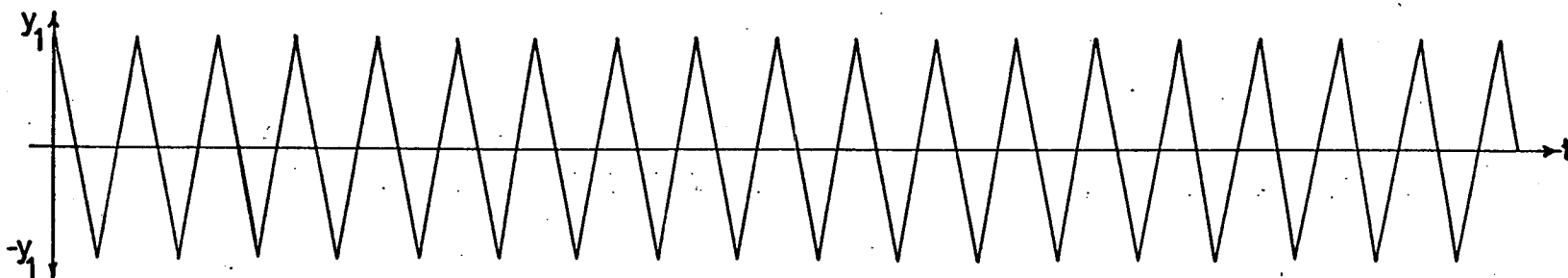
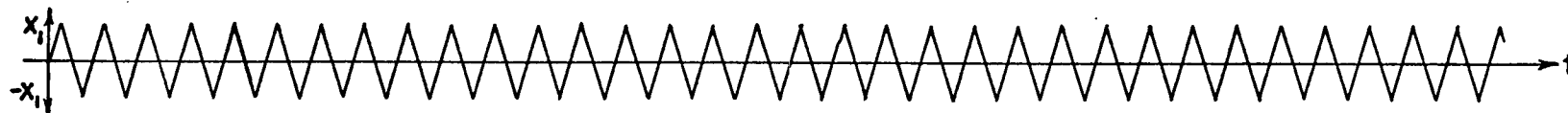


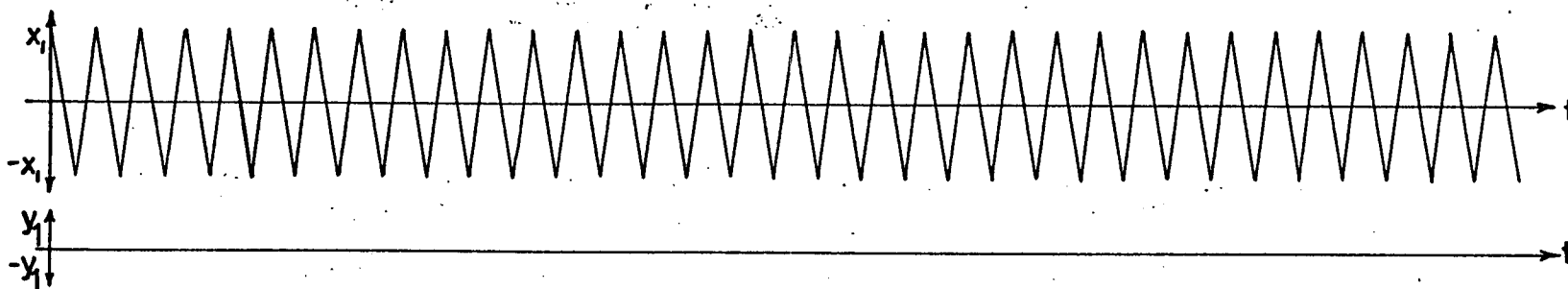
FIG. 5.7

A Mass on Two Elastic Bands

C.S.M.P. SOLUTIONS FOR BINARY SYSTEMS
(ARBITRARY AMPLITUDES)

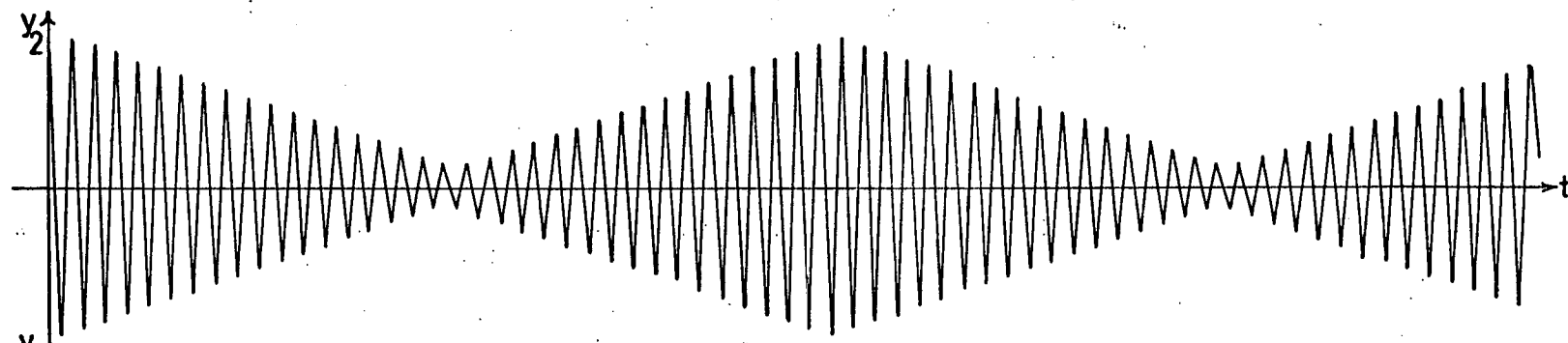
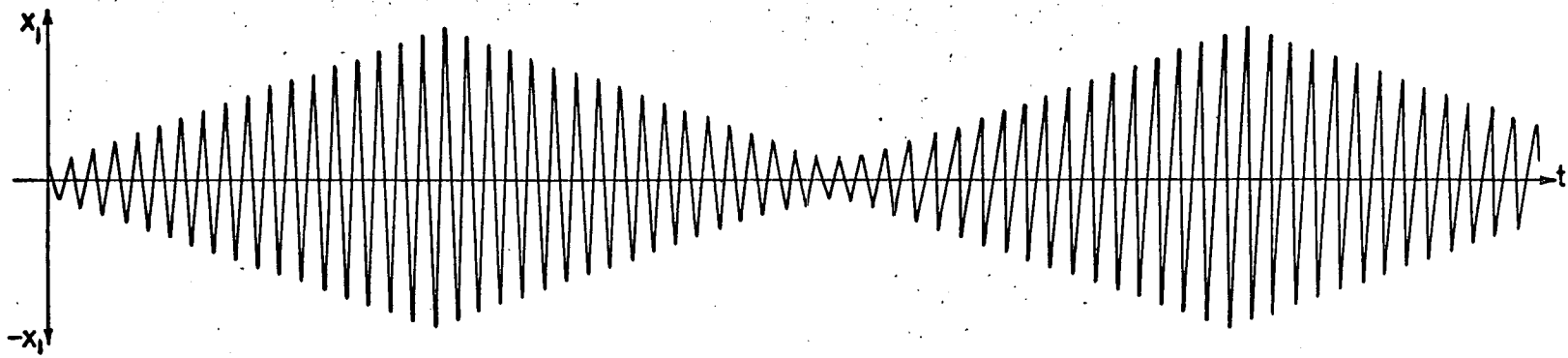


Initial conditions: $x_1 = 0, y_1 = 0.04 : x_{1max} = 0.003, y_{1max} = 0.04 : x_1\text{-period} = 0.3 \text{secs.}, y_1\text{-period} = 0.55 \text{secs.}$

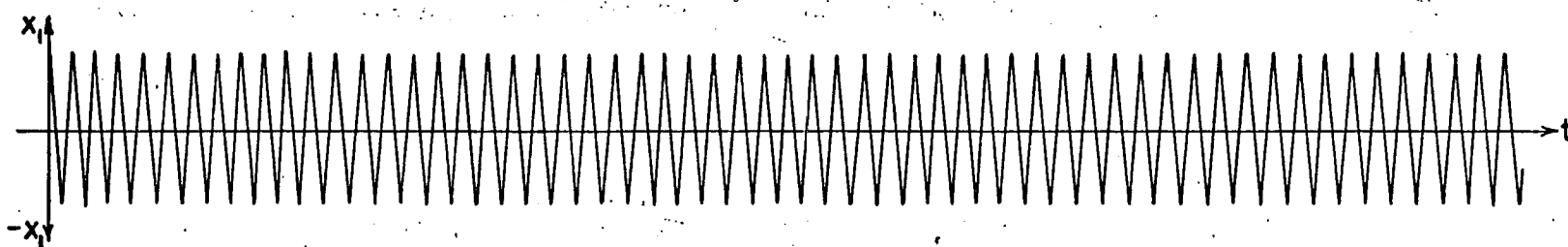


Initial conditions: $x_1 = 0.02, y_1 = 0 : x_{1max} = 0.02, y_{1max} = 0 : x_1\text{-period} = 0.32 \text{secs.}, y_1\text{-period} = 0$

CONTD/



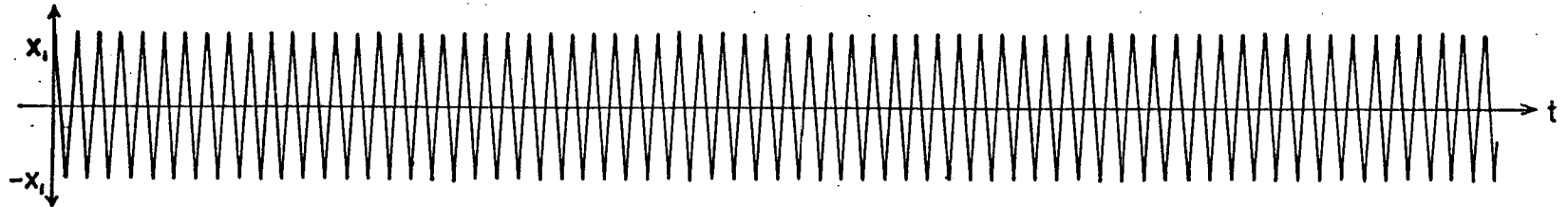
Initial conditions $x_1=0, y_2=0.03 : x_{1max}=0.023, y_{2max}=0.03 : x_1\text{-period}=0.32 \text{ secs}, y_2\text{-period}=0.32 \text{ secs}.$



Initial conditions $x_1=0.02, y_2=0 : x_{1max}=0.02, y_{2max}=0 : x_1\text{-period}=0.32 \text{ secs}, y_2\text{-period}=0$

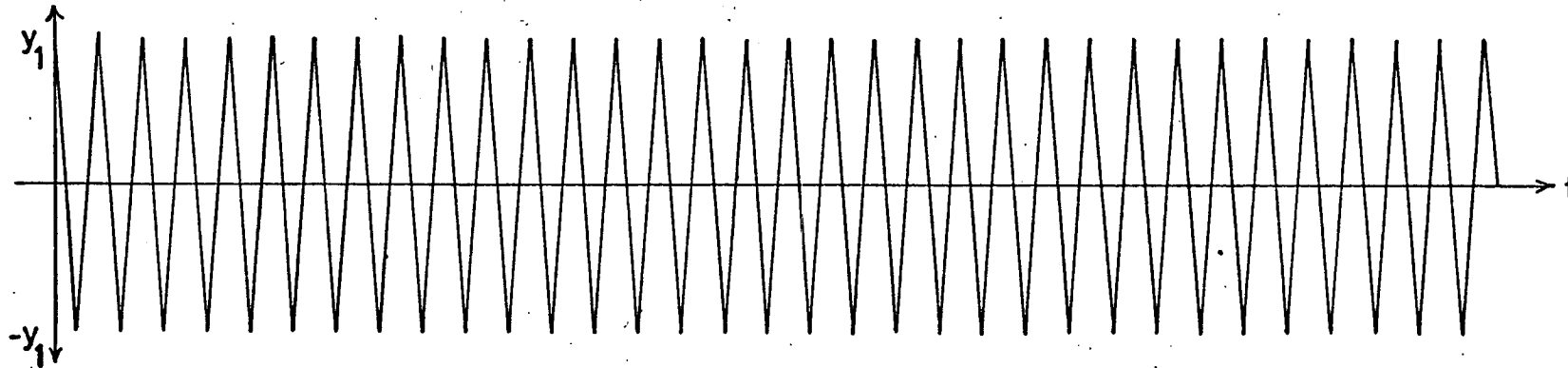
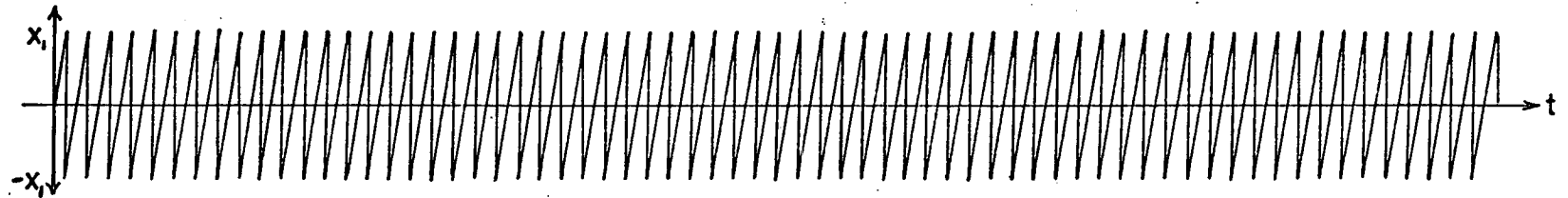
C.S.M.P. SOLUTIONS TO (5.13)

(ARBITRARY AMPLITUDES)



Initial conditions $x_1=0.02, y_1=0, y_2=0 : x_{1max.}=0.02 \quad x_1\text{-period}=0.32 \text{ secs.}$

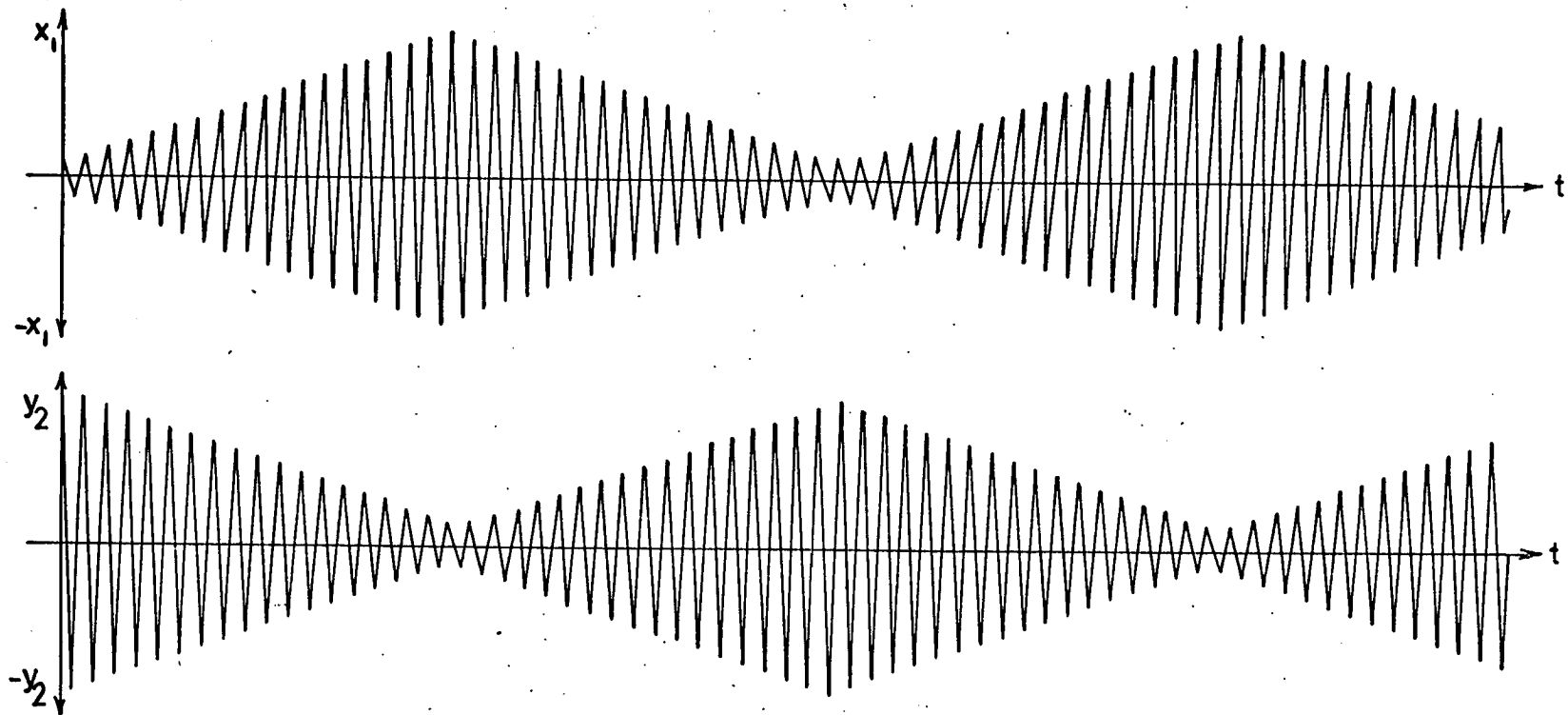
No oscillations in the modes y_1 and y_2



Initial conditions $x_1=0, y_1=0.03, y_2=0 : x_{1max.}=0.002, y_{1max.}=0.03 : x_1\text{-period}=0.32 \text{ secs, } y_1\text{-period}=0.54 \text{ secs.}$

No appreciable motion in the mode y_2

CONTD.



Initial conditions $x_1=0, y_1=0, y_2=0.03 : x_{1\max}=0.023, y_{2\max}=0.03 : x_1\text{-period}=0.32\text{ secs}, y_2\text{-period}=0.32\text{ secs}.$

No appreciable motion in the mode y_1

CHAPTER 6

NONLINEAR COUPLING BETWEEN INPLANE AND LATERAL MODES
OF MULTI-SPAN CATENARIES

In the previous Chapter we discussed qualitatively the nonlinear couplings between inplane and lateral modes of a single span fixed-fixed catenary. The study of single span fixed-fixed catenary is of academic interest only, because in actual practice a transmission line system always consists of more than one span, each span having some freedom at the ends. In the present Chapter we proceed to discuss the nonlinear effects in multi-span systems and although the following analysis is very crude, it is thought that this will provide some information about the nonlinear couplings in multi-span catenary system. The procedure outlined in the previous Chapter will again be employed. To begin with, let us consider a free-free catenary which can be obtained by releasing the ends of a fixed-fixed catenary. Moreover under certain circumstances it can be shown that the equations of motion of a free-free catenary are identical to those of the fixed-free catenary.

6.1 SINGLE SPAN FREE-FREE CATENARY

As in Chapter 5, for simplicity, we consider the two-mass catenary but this time with the ends released as shown in Fig. 6.1. Under the assumption that the horizontal displacements at the ends are equal and opposite, the potential energy can be written as

$$\begin{aligned}
 V = \frac{mg_1}{2t_1} [& s_1^3 v_1^2 + (v_2 - v_1)^2 + s_1^3 v_2^2 + s_1 z_1^2 + (z_2 - z_1)^2 + \\
 & + s_1 z_2^2 + t_1 s_1^4 v_1^3 + t_1 s_1^4 v_2^3 + t_1 s_1^2 v_1 z_1^2 + t_1 s_1^2 v_2 z_2^2] \quad (6.1)
 \end{aligned}$$

and the kinetic energy becomes

$$\begin{aligned}
 T = & \frac{ml^2}{2} [\dot{v}_1^2 + \dot{v}_2^2 + \frac{t_1^2}{4} (\dot{v}_1 + \dot{v}_2)^2 + \frac{t_1^2}{2} (\dot{v}_1 - \dot{v}_2)^2 + \\
 & + \frac{t_1(\dot{v}_1 + \dot{v}_2)}{2} \{s_1^3 v_1 \dot{v}_1 + (v_2 - v_1)(\dot{v}_2 - \dot{v}_1) + s_1^3 v_2 \dot{v}_2 + s_1 z_1 \dot{z}_1 + \\
 & + (z_2 - z_1)(\dot{z}_2 - \dot{z}_1) + s_1 z_2 \dot{z}_2\} + t_1(\dot{v}_1 - \dot{v}_2)(s_1^3 v_1 \dot{v}_1 - s_1^3 v_2 \dot{v}_2 + \\
 & + s_1 z_1 \dot{z}_1 - s_1 z_2 \dot{z}_2)] \quad (6.2)
 \end{aligned}$$

Applying Lagrange's method, the linear equations are formed and solved keeping only the second order terms in (6.1) and (6.2). Let the modal matrices for the inplane and lateral motions be respectively

$$[\Psi_V] = \begin{bmatrix} 1 & 1 \\ 1 & -1 \end{bmatrix} \quad (6.3)$$

$$\text{and} \quad [\Psi_Z] = \begin{bmatrix} 1 & 1 \\ 1 & -1 \end{bmatrix} \quad (6.4)$$

If we use the linear transformations

$$\{v\} = [\Psi_V] \{x\} \quad (6.5)$$

$$\text{and} \quad \{z\} = [\Psi_Z] \{y\} \quad (6.6)$$

the potential energy in normal coordinates becomes

$$\begin{aligned}
 v = & \frac{mgl}{2t_1} [2s_1^3 x_1^2 + 2(2 + s_1^3)x_2^2 + 2s_1 y_1^2 + 2(2 + s_1)y_2^2 + \\
 & + 2t_1 s_1^4 (x_1^3 + 3x_1 x_2^2) + 2t_1 s_1^2 (x_1 y_1^2 + x_1 y_2^2 + 2x_2 y_1 y_2)] \quad (6.7)
 \end{aligned}$$

and the kinetic energy, in normal coordinates, takes the form -

$$\begin{aligned}
 T = \frac{ml^2}{2} [& (2 + t_1^2)\dot{x}_1^2 + 2S_1^2\dot{x}_2^2 + 2\dot{y}_1^2 + 2\dot{y}_2^2 + 2t_1S_1^3x_1\dot{x}_1^2 + \\
 & + 2t_1(2 + 3S_1^3)x_2\dot{x}_1\dot{x}_2 + 2t_1S_1\dot{x}_1y_1\dot{y}_1 + 2t_1(2 + S_1)\dot{x}_1y_2\dot{y}_2 + 4t_1S_1^3x_1\dot{x}_2^2 + \\
 & + 4t_1S_1\dot{x}_2y_1\dot{y}_2 + 4t_1S_1\dot{x}_2y_2\dot{y}_1] \quad (6.8)
 \end{aligned}$$

Applying Lagrange's equations to (6.7) and (6.8), the nonlinear equations of motion can be written as follows -

$$\left. \begin{aligned}
 \ddot{x}_1 + \Omega_1^2 x_1 + a_1(x_1^2 + x_2^2) + a_2(y_1^2 + y_2^2) + a_3(x_1\dot{x}_1 + \frac{\dot{x}_1^2}{2}) + \\
 + a_4x_2\ddot{x}_2 + a_5\dot{x}_2^2 + a_6(\dot{y}_1^2 + y_1\ddot{y}_1) + a_7(\dot{y}_2^2 + y_2\ddot{y}_2) = 0 \\
 \ddot{x}_2 + \Omega_2^2 x_2 + b_1x_1x_2 + b_2y_1y_2 + b_3x_2\ddot{x}_1 + b_4x_1\ddot{x}_2 + b_5\dot{x}_1\dot{x}_2 + \\
 + b_6(y_1\ddot{y}_2 + y_2\ddot{y}_1 + 2\dot{y}_1\dot{y}_2) = 0 \\
 \ddot{y}_1 + \omega_1^2 y_1 + c_1(x_1y_1 + x_2y_2) + c_2(y_1\ddot{x}_1 + y_2\ddot{x}_2/2) = 0 \\
 \ddot{y}_2 + \omega_2^2 y_2 + d_1x_1y_2 + d_2x_2y_1 + d_3y_2\ddot{x}_1 + d_4y_1\ddot{x}_2 = 0
 \end{aligned} \right\} (6.9)$$

where the natural frequencies of the system are given by

$$\Omega_1^2 = \frac{2gS_1^3}{lt_1(2 + t_1^2)} \quad \Omega_2^2 = \frac{g(2 + S_1^3)}{lt_1S_1^2} \quad \omega_1^2 = \frac{gS_1}{lt_1} \quad \omega_2^2 = \frac{g(2 + S_1)}{lt_1}$$

and

$$\begin{aligned}
 a_1 &= \frac{3gS_1^4}{1(2+t_1^2)} & b_1 &= \frac{3gS_1^2}{1} & c_1 &= \frac{gS_1^2}{1} & d_1 &= \frac{gS_1^2}{1} \\
 a_2 &= \frac{gS_1^2}{1(2+t_1^2)} & b_2 &= \frac{g}{1} & c_2 &= t_1S_1 & d_2 &= \frac{gS_1^2}{1} \\
 a_3 &= \frac{2t_1S_1^3}{2+t_1^2} & b_3 &= \frac{t_1(2+3S_1^2)}{2S_1^2} & & & d_3 &= \frac{t_1(2+S_1)}{2} \\
 a_4 &= \frac{t_1(2+3S_1^3)}{2+t_1^2} & b_4 &= 2t_1S_1 & & & d_4 &= \frac{t_1S_1}{2} \\
 a_5 &= \frac{t_1(2+S_1^3)}{2+t_1^2} & b_5 &= 2t_1S_1 & & & & \\
 a_6 &= \frac{t_1S_1}{2+t_1^2} & b_6 &= t_1/S_1 & & & & \\
 a_7 &= \frac{t_1(2+S_1)}{2+t_1^2} & & & & & &
 \end{aligned}$$

At this stage, we consider (6.9) as four constituent binary systems such as

- (1) first inplane and first lateral mode
- (2) first inplane and second lateral mode
- (3) second inplane and first lateral mode
- (4) second inplane and second lateral mode

(1) First Inplane and First Lateral Mode

If the system is given an initial displacement in the first lateral mode and released we obtain at the start

$$y_1 = Y_1 \cos \omega_1 t \quad (6.10)$$

Substituting (6.10) into the first equation of (6.9) and remembering that $x_2, y_2 = 0$ in this case, we get

$$\ddot{x}_1 + \Omega_1^2 x_1 + a_1 x_1^2 + a_3 (x_1 \ddot{x}_1 + \frac{\dot{x}_1^2}{2}) = 0 \quad (6.11)$$

The right hand side of (6.11) being zero, it is unlikely that the first vertical mode will be excited by the first lateral mode.

When the initial displacement is in the first vertical mode we obtain in a similar manner

$$x_1 = X_1 \cos \Omega_1 t \quad (6.12)$$

$$\text{and} \quad \ddot{y}_1 + \omega_1^2 y_1 - c_1 X_1 y_1 \cos \Omega_1 t = 0 \quad (6.13)$$

where $c_1 = (c_2 \Omega_1^2 - c_1)$. Since $\Omega_1 \approx \omega_1$ it is expected that there will be 'Mathieu type' growth of y_1 provided there is initial y_1 .

(2) First Inplane and Second Lateral Mode

If the system is given an initial displacement in the second lateral mode and released, we obtain at the start

$$y_2 = Y_2 \cos \omega_2 t \quad (6.14)$$

Substituting (6.14) into the first equation of (6.9) and remembering that $x_2, y_1 = 0$ in this case we get

$$\ddot{x}_1 + \Omega_1^2 x_1 + a_1 x_1^2 + a_3 (x_1 \ddot{x}_1 + \frac{\dot{x}_1^2}{2}) = f_1 + f_2 \cos 2\omega_2 t \quad (6.15)$$

where $f_1 = -\frac{a_2 Y_2^2}{2}$ and $f_2 = (a_7 \omega_2^2 - a_2/2) Y_2^2$.

The x_1 -motion is forced at frequency $2\omega_2$. Since $\omega_2 \neq \Omega_1$ there is no possibility of x_1 being at resonance. Similarly when the system is given an initial displacement in x_1 we get for y_2 -

$$\ddot{y}_2 + \omega_2^2 y_2 = 0 \quad (6.16)$$

Equation (6.16) implies that y_2 -motion is independent of x_1 -motion.

(3) Second Vertical and First Lateral Mode

Remembering that $x_1, y_2 = 0$ in this case we obtain for the two initial displacements -

$$\ddot{x}_2 + \Omega_2^2 x_2 = 0 \quad (6.17)$$

$$\ddot{y}_1 + \omega_1^2 y_1 = 0 \quad (6.18)$$

Equations (6.17) and (6.18) are two uncoupled equations, the solutions of which depend only on initial conditions.

(4) Second Inplane and Second Lateral Mode

In this case we have $x_1, y_1 = 0$. Then following the same procedure as before we can obtain

$$x_2 + \Omega_2^2 x_2 = 0 \quad (6.19)$$

$$y_2 + \omega_2^2 y_2 = 0 \quad (6.20)$$

Equations (6.19) and (6.20) are two uncoupled equations and the solutions will depend only on initial conditions. Since $\omega_2 \simeq \Omega_2$, whirling motion of the masses may be expected under certain initial conditions.

An attempt was also made to obtain a solution to (6.9) on a digital computer using C.S.M.P. with the above initial conditions in turn; the graphs of the outputs are given under the appropriate heading at the end of the present Chapter. These show that the above qualitative explanations of (6.9) are acceptable. Hence, comparing the results with those of the previous Chapter, we may conclude that the nonlinear coupling effects are less important in free-free or fixed-free than in fixed-fixed catenaries

6.2 NONLINEAR EFFECTS IN MULTI-SPAN CATENARY SYSTEMS

In practical multi-span systems the ends of the constituent spans are joined together at a series of suspension arms which in turn are attached to the steel towers allowing certain degrees of movement at the common-span points. Since there is very little vertical movement at these points, the constituent spans can well be represented by systems like those shown in Fig. 6.1. From this viewpoint an important conclusion can be made that the nonlinear coupling effects between inplane and lateral modes are less important in multi-span catenary systems than in single span (ends fixed) catenaries. On the other hand other nonlinearities of importance are known to exist as a result of observations in the field (see section 1.2) and laboratory (these are discussed briefly below).

A multi-span catenary model having three spans but with scope for up to ten has been made from 0.011 inch diameter piano wire on which were fixed 21 masses per span. Each span is nominally 10 ft., but this can be varied; the mass density and elasticity of the model line are representative dimensionally of a full-scale line. (See Chapter 2).

The Severn Main Span was used as the constituent span. A design procedure for one of the spans is given in Appendix-F and a photographic view of the model is shown in Fig. 6.2. It has been mainly used for observing nonlinear effects which are summarised below -

- (a) a multi-span system can sustain an oscillation with differing frequencies in different spans when one part of the system receives a single frequency excitation (see also observations at Red Moss Test Line, Chapter 1).
- (b) a multi-span system can also sustain oscillation in different planes with differing frequencies when one part of the system receives a single frequency excitation in one plane.

The phenomena observed in (a) and (b) would have been, of course, impossible if the system were linear. However, these nonlinearities will be discussed in the next Chapter. At this stage, it seems worthwhile to make a few comments about the Red Moss Test Line excitation system.

6.3 COMMENTS ABOUT RED MOSS TEST LINE EXCITATION SYSTEM

As mentioned earlier in Section 1.2, Chapter 1, the suspension arm at tower 4 was fitted with a Dowty-Rotol (hydraulic) exciter for which the displacement given to the catenary was controlled to be sinusoidal. When the system was excited longitudinally the traces of force magnitude from the pen-recorder were of double the frequency of the displacement at the excited point (see Section 1.2). This was probably due to the inherent stiffness nonlinearity in the catenary.

The origin of this lies in the fact that the vertical load displacement of a point on a catenary is "hardening" downwards and "softening" upwards, which implies that the vertical nonlinear catenary stiffness is unsymmetrical about the equilibrium position. In fact, from Chapter 5 and an earlier part of the present Chapter, it is clear that a simplified equation of motion for a vertical normal mode oscillation can be written as

$$\ddot{x} + \Omega^2 x + ax^2 = F(t) \quad (6.21)$$

Since we are giving a displacement-excitation of the form

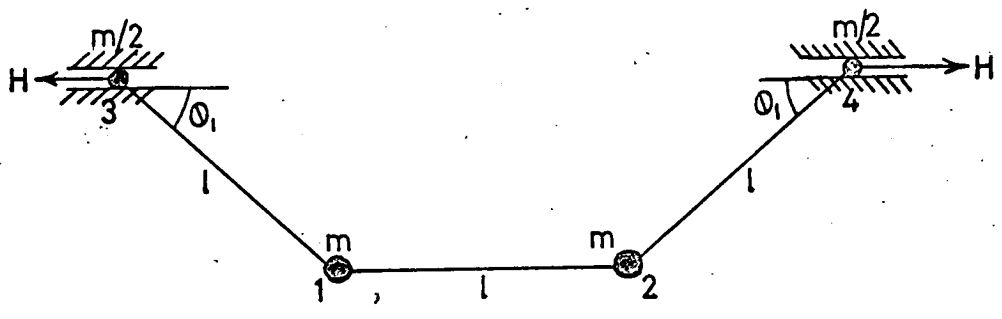
$$x = A \sin \omega t \quad (6.22)$$

the first and the second terms of (6.21) cancel each other when (6.22) is substituted in (6.21) and $\omega = \Omega$. The last term of (6.21) becomes a $A^2(1 + \cos 2\Omega t)/2$, and hence to satisfy (6.21) we must have

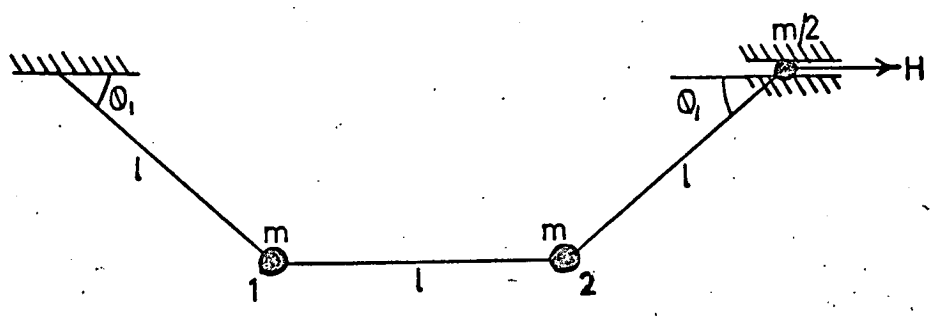
$$F(t) = aA^2(1 + \cos 2\Omega t)/2 \quad (6.23)$$

From (6.23) it is seen that $F(t)$ consists of a unidirectional part and a periodic part having double the frequency of the input displacement. This $F(t)$ is, in fact, provided by the actuator and recorded by the pen-recorder. Thus it is seen that when a span is excited by giving sinusoidal displacement, a force is produced which has double the frequency of the displacement. It also implies that an end of the span has 1 x frequency - displacement and 2 x frequency-force at the suspension point. This leads to the fact that a span vibrates at 2 x frequency when an adjacent span receives 1 x frequency excitation.

In closing up the present section it is suggested that periodic force input to the catenary system is preferable to displacement controlled input, although it is envisaged that some difficulty may be met in achieving this.



FREE FREE TWO MASS CATENARY



FIXED FREE TWO MASS CATENARY

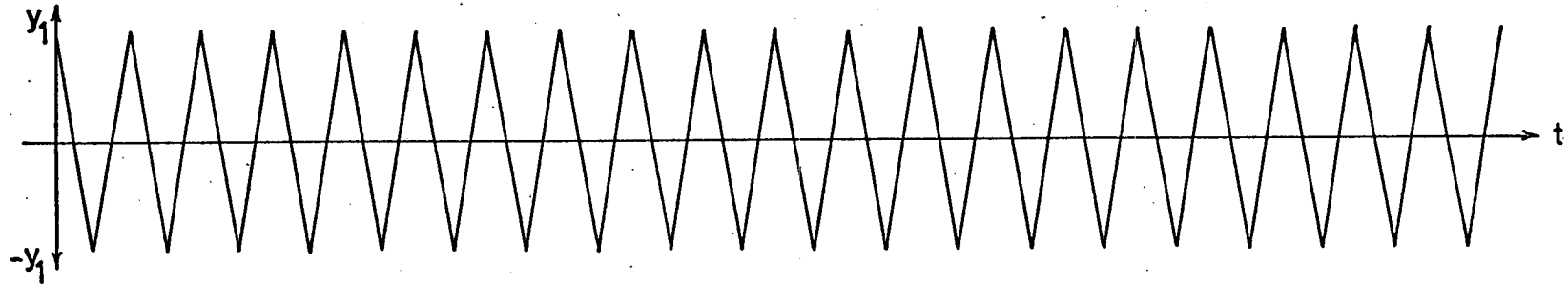
FIG. 6.1



FIG. 6.2

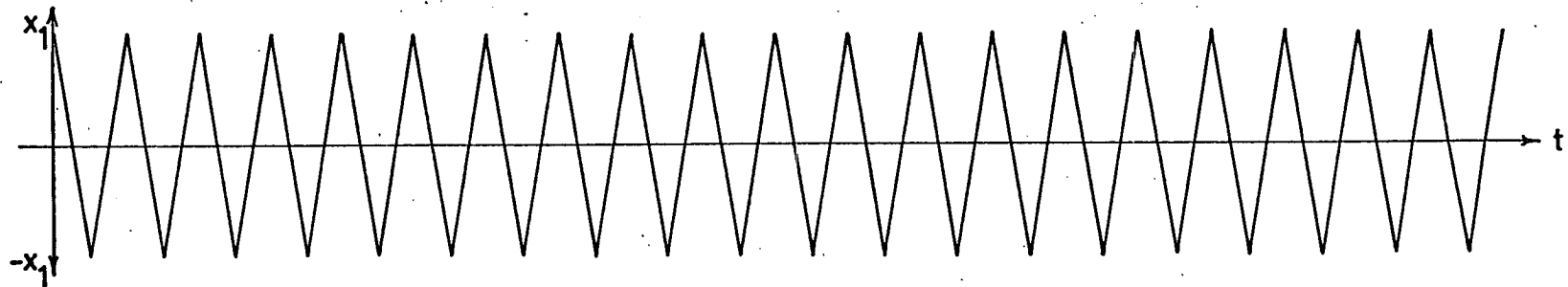
Three Span Experimental Model

C.S.M.P. SOLUTIONS TO (6-9)
(ARBITRARY AMPLITUDES)



Initial conditions $x_1=0, x_2=0, y_1=0.03, y_2=0 : y_{1\max}=0.03 : y_1\text{-period}=0.56\text{secs.}$

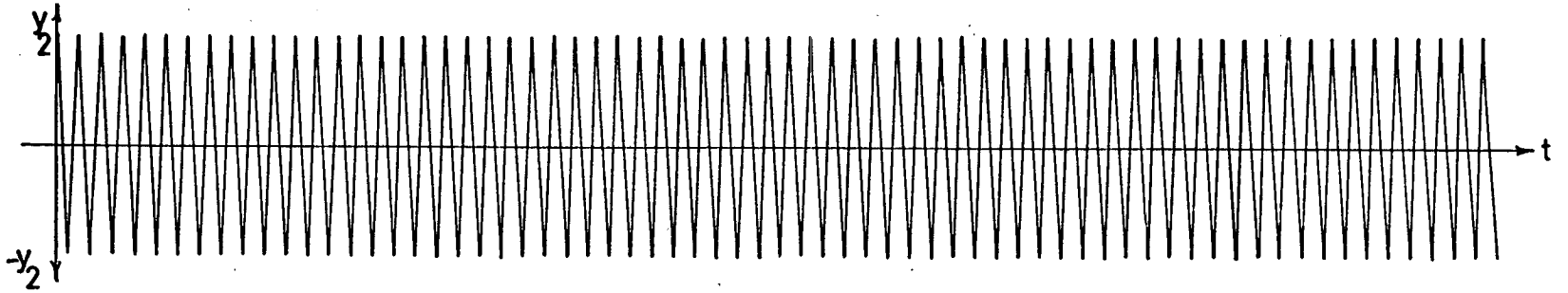
No appreciable motions in modes x_1, x_2 and y_2 .



Initial conditions $x_1=0.03, x_2=0, y_1=0, y_2=0 : x_{1\max}=0.03 : x_1\text{-period}=0.54\text{secs.}$

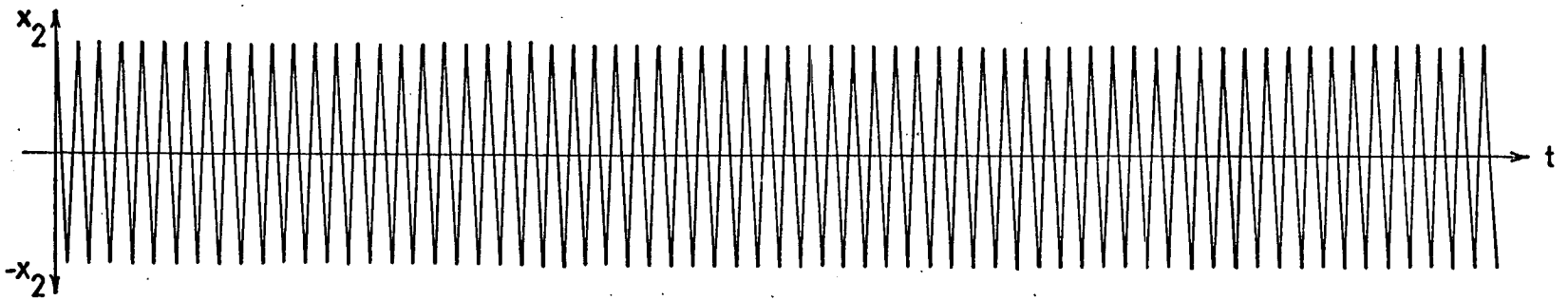
No appreciable motions in modes x_2, y_1 and y_2 .

CONTD.



Initial conditions $x_1=0, x_2=0, y_1=0, y_2=0.03 : y_{2\max}=0.03 : y_2\text{-period}=0.32$ secs.

No appreciable motions in modes x_1, x_2 and y_1 .



Initial conditions $x_1=0, x_2=0.03, y_1=0, y_2=0 : x_{2\max}=0.03 : x_2\text{-period}=0.32$ secs.

No appreciable motions in modes x_1, y_1 and y_2 .

CHAPTER 77.1 DISCUSSION

A critical survey of the literature has been given and this was intended to illustrate the previous understanding of the problem. Although the dynamics of the single span catenary were well understood, there was no easy way of applying this knowledge to the multi-span catenary systems. A technique of applying the Rayleigh-Ritz method to the oscillating catenary problem was developed and successfully applied to the single span catenary using the stretched string modes as some of the arbitrary modes and assuming that the catenary was shallow (dip/span ratio was small) and inextensible. Since in practical transmission line systems, the catenaries are shallow and the elasticity has a very slight effect on the modes and frequencies [35], the assumptions that the catenaries are shallow and inextensible are acceptable. Numerical calculations for the inplane modes of single span catenary were performed and the results were compared with those obtained experimentally and by other methods. Since there exists a good agreement, it is hoped that the method will provide an easy way of calculating the normal modes and frequencies of shallow catenaries. Also it was shown that the lateral modes and frequencies of shallow catenaries can be well represented by the stretched^{String} counterparts.

The method was also successfully applied to the inplane motion of multi-span catenary systems using single span string modes as some of the arbitrary modes and introducing appropriate constraints at the span inter-connection points. A slightly different technique was employed for the motion in the lateral plane.

In this case, the single span string modes were used in combination with "Rauscher Modes" to allow for the extra degrees of freedom at the suspension points. The natural frequencies and the normal modes were calculated for motion in both the planes for the Red Moss Test Line and the results for inplane motion were compared with those of the tests performed at the site. Coupling of equal spans through suspension arms and flexible towers were examined. For the latter case the flexibility matrices for inplane and lateral loads were required to be calculated and to this end an approximate procedure for calculating the flexibility matrices of any tower was devised.

The problem of nonlinear dynamics of catenaries was considered and found to be a very difficult one to analyse. Even simple mathematical models led to extraordinarily involved equations and computation consumed a good deal of computer time. Hence the best approach seemed to be to explain observed nonlinear effects on a physical basis. A well known example of nonlinear coupling is that between the first antisymmetric inplane and lateral modes of the single span fixed-fixed catenary. This was easily demonstrated in the laboratory by constructing a model consisting of two masses suspended on an inextensible string fixed at the two ends, but the phenomenon was in fact very difficult to analyse mathematically due to the intractable nature of the nonlinear equations of motion even though only three degrees of freedom were considered. Neglecting terms of lesser importance and with the help of an auxiliary system, the existence of the subharmonics of order 2 was demonstrated in the single span fixed-fixed catenary and this was substantiated by the solution from the computer.

As a preliminary to a study of the nonlinear couplings in multi-span catenary systems, nonlinear equations of motion for the two-mass mathematical model were formed, but this time with the ends released.

A qualitative assessment of the equations of motion was given and it was concluded from this that the nonlinear coupling between inplane and lateral modes of a catenary when the catenary is a member of a multi-span system becomes less important. But at the same time the other nonlinear effects of adjacent spans oscillating at different frequencies or in different plane cannot be neglected. We also observed a system in field sustaining phenomena which could not be attributed to linear system. The natural frequencies of the linear modes involving large movements in adjacent spans were always in a 1:1 or 1:2 ratio. Similar observations were also made in the laboratory. Now referring to Chapter 4, we saw that the systems composed of equal subsystems possess modes which have frequencies differing only superficially. The point about nearly equal frequencies is that normally stringent conditions for galloping are enhanced by having a range of similar modes and frequencies differing only over a narrow band.

Throughout the whole research, the cable elasticity, bending stiffness and other lesser effects have been ignored. In omitting to consider cable elasticity, we have not incurred significant errors anyway, because for practical values of Young's Modulus, only the high frequency symmetrical modes are affected. Also the extent to which low frequencies of long span systems are modified by bending stiffness is totally insignificant [35].

With regard to cable internal damping, this would be very small in the low frequency modes. This is because, cable distortions are small in these modes.

Also observations at Red Moss Test Line show to a small percentage of critical damping (i.e. 6.25% critical damping in the 5th normal mode). Thus in the present work we have chosen to ignore cable internal damping. However, many of the modes involve substantial suspension arm movements. In these modes, the degree of interaction between spans may be reduced by adding damping at the suspension arms connecting spans.

7.2 AREAS OF FURTHER STUDIES

Clashing amplitudes are most undesirable in transmission line systems. Instability models are linear at present and need further nonlinear theory to take amplitude from small/linear to large/nonlinear. Further analytical studies of the problem of nonlinear dynamics of catenaries would be useful. Until now most of the mathematics on nonlinear systems have been concentrated on quasi-linear cases. While computer techniques give good results they cannot yield the same insight into the behaviour of a system as an analytical approach, even though many results from different initial conditions would be obtained from the computer. A knowledge of the effect of changing relative span lengths would be useful, because field and laboratory observations have indicated that nonlinear coupling between spans is dependent on the ratio of natural frequencies in which adjacent spans have large movements at the common support point. If this can be elucidated, then calculations would need to be made on multi-span systems in which the span length ratios were varied in order to study the effect on natural frequencies. The ultimate aim of this would be to evolve a rule which determines the best ratios of span lengths for attenuation of wind excited oscillations.

To support the analysis further experiments on multi-span catenaries need to be performed and nonlinear effects observed together with whatever measurements can be taken. In closing up, tests on tower flexibilities would be worth further study.

REFERENCES

- (1) Bishop, R.E.D. 'Matrix Analysis of Vibration', Cambridge
Johnson, D.C. University Press, 1965.
Michaelson, S.
- (2) Bishop, R.E.D. 'Mechanics of Vibration', Cambridge University
Johnson, D.C. Press, 1960.
- (3) Bisplinghoff, R.L. 'Aeroelasticity', Addison-Wesley Publishing
Ashley, H. Company, Inc., 1955.
Halfman, R.L.
- (4) Bogolivbov, N.N. 'Asymptotic Methods in the Theory of Nonlinear
Mitropolsky, Y.A. Oscillations', Hindustan Publishing Corpn., 1961.
- (5) Collar, A.R. 'On Centrosymmetric and Centroskew Matrices',
Quarterly journal of mechanics and applied
mathematics. Vol. V, pp.97, 1952.
- (6) Davis, D.A. 'Investigation of Conductor Oscillation on
Richards, D.J.W. the 275-KV crossing over rivers Severn and
Scriven, R.A. Wye', Proc. I.E.E., 110(1), pp.205.
- (7) Frazer, R.A. 'Elementary Matrices', Cambridge University
Duncan, W.J. Press, 1950.
Collar, A.R.
- (8) Frazer, R.A. 'A Summarised Account of the Severn Bridge
Scruton, C. Aerodynamic Investigation', H.M.S.O.,
London, 1952.

- (9) Goldstein, S. 'Modern Developments in Fluid Dynamics',
Oxford University Press, 1952.
- (10) Goodey, W.J. 'On Natural Modes and Frequencies of Suspension
Chain', Quarterly journal of mechanics and
applied mathematics, vol. XIV, pp.118, 1961.
- (11) Hartog, D. 'Mechanical Vibrations', McGraw-Hill Book
Company, 1949.
- (12) Hartog, D. 'Transmission Line Vibration due to Sleet',
Trans. A.I.E.E., 1930, 49, 444.
- (13) Hayashi, C. 'Nonlinear Oscillations in Physical Systems',
McGraw-Hill Book Company, 1964.
- (14) Hoerner, S.F. 'Fluid Dynamic Drag', Published by the author,
1958.
- (15) Karman, I.V.
Biot, M.A. 'Mathematical Methods in Engineering',
McGraw-Hill Book Company, 1940.
- (16) Kron, G. 'Tensor Analysis of Networks', John Wiley, 1939.
- (17) Kron, G. 'Piecewise Solution of Eigenvalue Problem',
The Electrical Journal, 1958, Vol. 161,
pp. 1371.
- (18) McLachlan, N.W. 'Ordinary Nonlinear Differential Equations',
Oxford University Press, 1956.
- (19) Meirovitch, L. 'Analytical Methods in Vibration', The
Macmillan Company, 1967.

- (20) Minorsky, N. 'Nonlinear Oscillations', Van-Nostrand, 1962.
- (21) Minorsky, N. 'Nonlinear Mechanics', Edwards Bros., 1947.
- (22) Poskitt, T.J. 'Free Oscillation of Suspended Cables', The Structural Engineer, October, 1964, No. 10, Vol. 42.
- (23) Pugsley, A.G. 'On Natural Frequencies of Suspension Chain', Quarterly Journal of Mechanics and Applied Mathematics, Vol. II, 1949, pp.412.
- (24) Pugsley, A.G. 'The Theory of Suspension Bridges', Edward Arnold Ltd., 1956.
- (25) Rayleigh, J.W.S. 'The Theory of Sound', The Macmillan Company, 1926.
- (26) Reissner, H. 'Oscillation of Suspension Bridges', Journal of Applied Mechanics (ASME), Vol. 10, March, 1943.
- (27) Rohrs, J.H. 'On the Oscillation of a Suspension Chain', Trans. Phil. Soc. 9(1851).
- (28) Routh, E.J. 'Advanced Rigid Dynamics', The Macmillan Company, 1905, Sixth edition.
- (29) Saxon, D.S.
Cahn, A.S. 'Modes of Vibration of Suspension Chain' Quarterly Journal of Mechanics and Applied Mathematics, Vol. VI, pp.273, 1953.
- (30) Scriven, R.A. 'Severn Crossing : Self-excited Oscillations in a Steady Wind'. C.E.R.L. Lab. Note, RD/L/N19/63 (unpublished.)

- (31) Scriven, R.A. 'On the Equation of Motion for Finite Oscillation of an Elastic Catenary', C.E.R.l. Lab. Note, RD/L/N59/61 (unpublished).
- (32) Scriven, R.A. 'The Effect of End Conditions Upon the Natural Frequencies of a Suspended Cable', C.E.R.L. Lab. Note, RD/L/R1038 (unpublished).
- (33) Sethna, P.R. 'Transients in Certain Autonomous Multiple-degree-of-freedom Nonlinear Vibrating Systems', Journal of Applied Mechanics, Vol. 30, Trans. ASME, Series E, March, 1963.
- (34) Sethna, P.R. 'Vibrations of Dynamical Systems with Quadratic Nonlinearities', Journal of Applied Mechanics, Vol. 32, Trans. ASME, Series E. September 1965.
- (35) Simpson, A. 'Oscillations of Catenaries and Systems of Overhead Transmission Lines', Ph.D. Thesis, Vol. I, University of Bristol, 1963.
- (36) Simpson, A. 'Aerodynamic Instability of Long Span Transmission Lines, Proc. I.E.E., Vol. 112(1) pp.315.
- (37) Simpson, A. 'Determination of the Inplane Natural Frequencies of Multi-span Transmission Lines by a Transfer-Matrix Method', Proc. I.E.E., Vol.113 Jan. - June, 1966.
- (38) Simpson, A.
Lawson, T.V. 'Oscillations of Twin Power Transmission Lines', Proceedings of Symposium on Wind Effects on Buildings and Structures, Loughborough University of Technology, April, 1968.

(39) Struble, R.A.

'Nonlinear Differential Equations',

McGraw-Hill Book Company, 1962.

APPENDIX - ACATENARIES WITH VARIOUS END CONDITIONSA.1 FREE-FREE CATENARY

The free-free catenary is a physically unrealisable system which, despite its apparent impracticability, is an extremely useful building block for a multi-span catenary system. Unlike simple elastic structures, such as beams and plates, a catenary cannot exist without the gravity field and end forces. In view of this it was thought convenient to consider a catenary with end forces sufficient to maintain its equilibrium shape. The system to be considered is shown in Fig. A.1.

Referring to section 2.3, we obtain by integrating (2.85) between the limits $-L$ and L .

$$u_2 - u_1 = -\frac{mg}{H}[(xv)_{-L}^L - \int_{-L}^L v \, dx] - \frac{1}{2} \int_{-L}^L \left(\frac{\partial v}{\partial x}\right)^2 dx - \frac{1}{2} \int_{-L}^L \left(\frac{\partial w}{\partial x}\right)^2 dx \quad (\text{A.1})$$

Simplifying (A.1) to give

$$u_2 - u_1 = -\frac{mgL}{H}(v_1 + v_2) + \frac{mg}{H} \int_{-L}^L v \, dx - \frac{1}{2} \int_{-L}^L \left(\frac{\partial v}{\partial x}\right)^2 dx - \frac{1}{2} \int_{-L}^L \left(\frac{\partial w}{\partial x}\right)^2 dx \quad (\text{A.2})$$

We may now write

$$v_1 = \frac{u_1^2 + w_1^2}{2l_s} \quad (\text{A.3})$$

and

$$v_2 = \frac{u_2^2 + w_2^2}{2l_s} \quad (\text{A.4})$$

in (A.2) to give

$$\begin{aligned}
u_2 - u_1 = \frac{mgL}{2Hl_s} (u_1^2 + u_2^2 + w_1^2 + w_2^2) + \frac{mg}{H} \int_{-L}^L v \, dx - \\
- \frac{1}{2} \int_{-L}^L \left(\frac{\partial v}{\partial x}\right)^2 dx - \frac{1}{2} \int_{-L}^L \left(\frac{\partial w}{\partial x}\right)^2 dx
\end{aligned} \tag{A.5}$$

where in (A.1) - (A.5), u_1, v_1, w_1 and u_2, v_2, w_2 represent respectively the horizontal, vertical and lateral displacements of the cable corresponding to $x = -L$ and $x = L$ and l_s is the length of each suspension arm.

The potential energy due to the end forces, H ,

$$\begin{aligned}
V_H = \frac{mgL}{2l_s} (u_1^2 + w_1^2 + u_2^2 + w_2^2) - mg \int_{-L}^L v \, dx + \\
+ \frac{H}{2} \int_{-L}^L \left(\frac{\partial v}{\partial x}\right)^2 dx + \frac{H}{2} \int_{-L}^L \left(\frac{\partial w}{\partial x}\right)^2 dx
\end{aligned} \tag{A.6}$$

and the potential energy due to the gravity

$$V_G = mg \int_{-L}^L v \, dx + \frac{M_s g}{4l_s} (u_1^2 + w_1^2 + u_2^2 + w_2^2) \tag{A.7}$$

The total Potential energy becomes

$$\begin{aligned}
V = V_H + V_G \\
= \frac{2mgL + M_s g}{4l_s} (u_1^2 + w_1^2 + u_2^2 + w_2^2) + \\
+ \frac{H}{2} \int_{-L}^L \left(\frac{\partial v}{\partial x}\right)^2 dx + \frac{H}{2} \int_{-L}^L \left(\frac{\partial w}{\partial x}\right)^2 dx
\end{aligned} \tag{A.8}$$

Neglecting the small cross-span movements of the cable elements, we obtain, the kinetic energy

$$T = \frac{m}{2} \int_{-L}^L \dot{v}^2 dx + \frac{m}{2} \int_{-L}^L \dot{w}^2 dx + \frac{M_S}{8} (\dot{u}_1^2 + \dot{w}_1^2 + \dot{u}_2^2 + \dot{w}_2^2) \quad (\text{A.9})$$

where M_S = mass of each suspension arm.

In view of (A.5), the system is subject to a first order equation of constraint given by

$$u_2 - u_1 = \frac{mg}{H} \int_{-L}^L v dx \quad (\text{A.10})$$

Equations (A.8) and (A.9) through (A.10) imply that the inplane and lateral modes are uncoupled for small oscillations and can be treated separately. Moreover these expressions are in suitable forms to enable the use of the Rayleigh-Ritz method (see Chapter 2, Section 2.3).

A.2 FREE FIXED-FIXED CATENARY

The catenary is represented in the Fig. A.2. The characteristic expressions for the fixed-free catenary may be obtained from the corresponding expressions for the free-free catenary merely by putting the required end coordinates to zero for all t . In fact for the catenary of Fig. A.2, we can write

$$V = \frac{2mgL + M_S g}{4l_S} (u^2 + w^2) + \frac{H}{2} \int_{-L}^L \left(\frac{\partial v}{\partial x}\right)^2 dx + \frac{H}{2} \int_{-L}^L \left(\frac{\partial w}{\partial x}\right)^2 dx \quad (\text{A.11})$$

$$T = \frac{m}{2} \int_{-L}^L \dot{v}^2 dx + \frac{m}{2} \int_{-L}^L \dot{w}^2 dx + \frac{M_S}{8} (\dot{u}^2 + \dot{w}^2) \quad (\text{A.12})$$

and the equation of constraint becomes

$$u = \frac{mg}{H} \int_{-L}^L v dx \quad (\text{A.13})$$

For convenience the suffix has been dropped out from u and w . Here, too, the inplane and lateral modes are uncoupled and the Rayleigh-Ritz method can be easily applied.

A.3 COMPARISON WITH THE STRETCHED STRING

If in the case of the free-free catenary we assume that, in the inplane motion, the horizontal displacements at the ends of the cable are equal and opposite we can write

$$V = \frac{2mgL + M_S g}{2l_S} u^2 + \frac{H}{2} \int_{-L}^L \left(\frac{\partial v}{\partial x}\right)^2 dx \quad (\text{A.14})$$

$$T = \frac{M_S}{4} \dot{u}^2 + \frac{m}{2} \int_{-L}^L \dot{v}^2 dx \quad (\text{A.15})$$

and the equation of constraint becomes

$$u = \frac{mg}{2H} \int_{-L}^L v dx \quad (\text{A.16})$$

If in (A.16), H is large (as is usually the case in flat catenaries) then u is small and hence the terms involving u^2 and \dot{u}^2 in (A.14) and (A.15) respectively can be neglected. Then neglecting the first terms of (A.14) and (A.15) we obtain

$$V = \frac{H}{2} \int_{-L}^L \left(\frac{\partial v}{\partial x}\right)^2 dx \quad (\text{A.17})$$

$$\text{and} \quad T = \frac{m}{2} \int_{-L}^L \dot{v}^2 dx \quad (\text{A.18})$$

The expressions (A.17) and (A.18) are the familiar expressions for the stretched string with tension H . Similar arguments are also applied to the fixed-free catenary.

To supplement the analysis in the present heading, the 1200 ft. span of the Red Moss Test Line was taken and the natural frequencies were calculated considering it as a fixed-free and free-free catenary. The results together with the stretched string counterparts are tabulated as given below -

Mode Number	When used as a fixed-free catenary Hz	When used as a free-free catenary Hz	When used as a stretched string Hz
1	0.17171	0.16683	0.16320
2	0.48961	0.48945	0.48960
3	0.81558	0.81558	0.81600
4	1.14191	1.14191	1.14240
5	1.46829	1.46829	1.46880
6	1.79446	1.79446	1.79520
7	2.12027	2.12027	2.12160
8	2.44611	2.44621	2.44799
9	2.77362	2.77362	2.77439
10	3.09630	3.09630	3.10079

The values in the last column of the above Table were obtained from standard formulae [2, 19]. It should also be noted that in the above table, only the frequencies of the symmetrical modes are given. Calculations were performed for catenaries using 20 degrees of freedom and "string" modes in a Rayleigh-Ritz approach.

FREE-FREE CATENARY

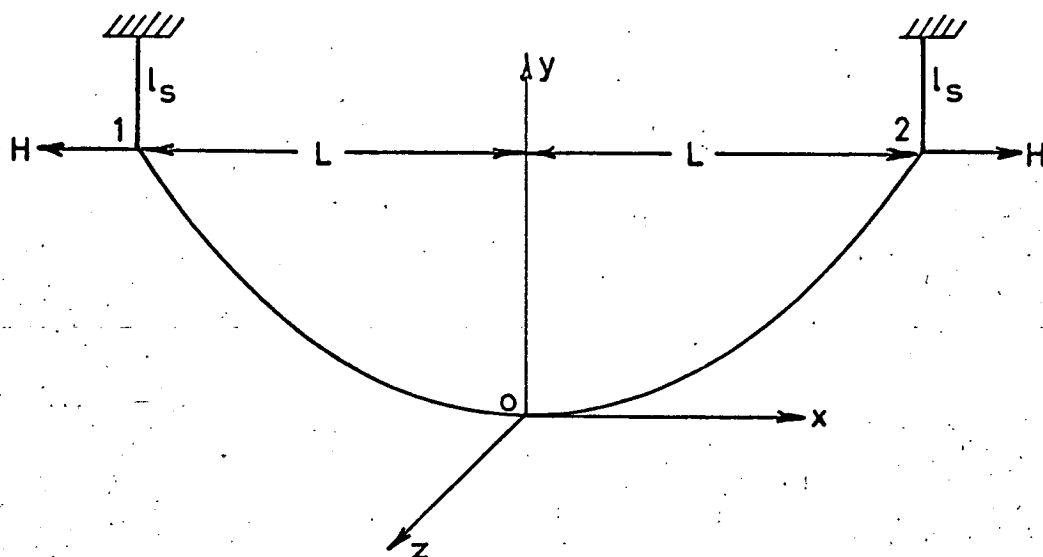


FIG. A.1

FIXED-FREE CATENARY

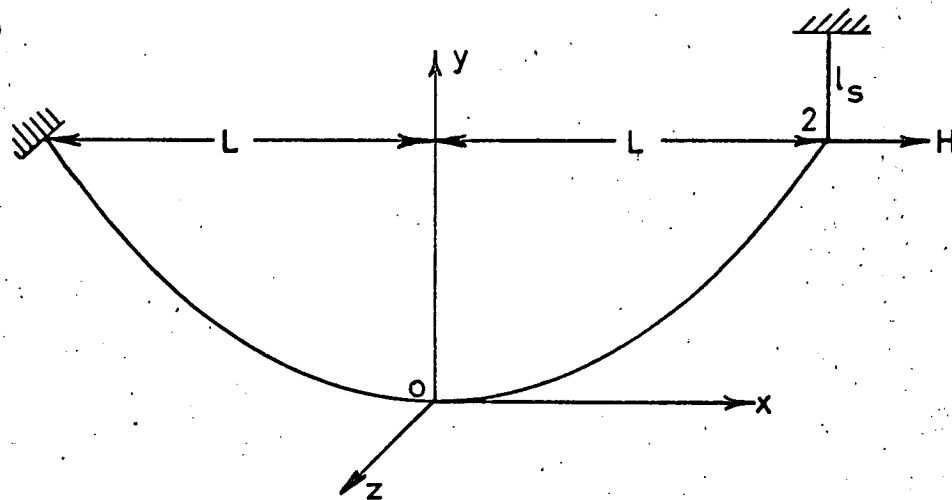


FIG. A.2

APPENDIX - BFLEXIBILITY OF TOWERS

Although there are various types of tower-structures, we will use the one which is commonly employed in transmission line systems. An actual tower is represented in Fig. B.1. No measured or standard data being readily available, we had to resort to a crude estimate e.g. the dimensions were scaled from a photograph of pylon supplied by the S.S.E.B. Although only the top part is of standard cells, we assume for simplicity that the whole tower is all made of similar cells. Such an approximate tower is represented in Fig. B.2 in which the basic cell is assumed to be a cuboid (parallel sided) cell and is as shown in Fig. B.3. This cell is subject to

- a) shear arising from overall tower and arm bending
- b) torsion

Both these, shear and torsion, lead to load inputs as shown in Fig. B.4. Deflections due to bending are neglected as the upright tower members are much more substantial in cross section than the diagonal members. If we assume that the load is equally shared between the top points as indicated in Fig. B.5, we can readily find the sideways deflection of the cell.

Referring to Fig. B.6, the load in diagonal member

$$P_d = P \sec \theta \quad (\text{B.1})$$

So the deflection (elongation) of the diagonal member

$$\delta = \frac{P_d l}{AE} = \frac{Pl \sec \theta}{AE} \quad (\text{B.2})$$

and the deflection sideways of the frame

$$\delta_S = \delta \cos \theta = \frac{Pl}{AE} \quad (\text{B.3})$$

Let $b/h = r = 1.5$ (for the Red Moss towers)

Then

$$\begin{aligned} l &= h \operatorname{cosec} \theta \\ &= h \sqrt{1 + (1.5)^2} \\ &= 1.8 h \end{aligned} \quad (\text{B.4})$$

Substituting (B.4) in (B.3) we obtain

$$\delta_S = \frac{1.8 Ph}{AE} \quad (\text{B.5})$$

The diagonals are taken to be 4 in. angles x 3/16 in. mild steel,
so that

$$A = 1.5 \text{ in}^2$$

$$E = 30 \times 10^6 \text{ lbf/in}^2$$

$$\text{and hence } AE = 0.45 \times 10^8 \text{ lbf}$$

Substituting the value of AE in the expression for δ_S we obtain

$$\delta_S = 4 \times 10^{-8} Ph \quad (\text{B.6})$$

Flexibility of Cell

In Shear:- Referring to Fig. B.7 we notice that there are four frames acting in shear and hence

$$\delta_S = 10^{-8} P_S h \quad (\text{B.7})$$

where P_S is the total force sideways in the cell.

In Torsion:- In this case, we notice from Fig. B.8 that there are eight frames acting in torsion. Or in other words, a force of magnitude $T/2b$ is acting on two triangular frames. Hence by (B.7) we obtain

$$\delta_S = 10^{-8} \frac{Th}{b} \quad (\text{B.8})$$

From Fig. B.9 we obtain the torsional displacement

$$\theta = \frac{\delta_S}{b} = 10^{-8} \frac{Th}{b^2} \quad (\text{B.9})$$

Since $b/h = 1.5$, (B.9) becomes

$$\theta = 10^{-8} \frac{T}{2.25h} \quad (\text{B.10})$$

CALCULATION OF THE INPLANE AND LATERAL FLEXIBILITY MATRICES
FOR THE RED-MOSS TOWERS

Denoting the loading points on the arms by numerics as indicated in Fig. B.2, we can calculate the flexibility matrices in the following manner.

Flexibility Matrix for Horizontal Longitudinal LoadsLoad at (1): Torque = $30 P_1$

$$\begin{aligned}
\delta_{11} &= 10^{-8} \times \frac{1}{2} \sum h_{\text{arm}} P_1 + 30 \times \frac{10^{-8}}{2.25} \sum_B^1 \frac{1}{h_{\text{tower}}} \cdot 30 P_1 \\
&= 10^{-8} P_1 \left[15 + \frac{30^2}{2.25} \left(\frac{10}{8} + \frac{3}{10} + \frac{3}{12} \right) \right] \\
&= 10^{-8} \times 736 \times P_1 \\
&= 7.36 \times 10^{-6} P_1
\end{aligned}$$

Note that the arm cellsⁱⁿ shear have only half the stiffness of tower cells. Also^{as} a preliminary check, let us apply a load of 20,000 lbf which is that given by the span on one side breaking. For this case δ_{11} is about 1.8 in., which is an acceptable figure.

$$\delta_{61} = -7.21 \times 10^{-6} P_1$$

$$\begin{aligned}
\delta_{21} &= 10^{-8} P_1 \times \frac{30 \times 40}{2.25} (5/8 + 3/10 + 3/12) \\
&= 6.27 \times 10^{-6} P_1
\end{aligned}$$

$$\delta_{51} = -6.27 \times 10^{-6} P_1$$

$$\begin{aligned}
\delta_{31} &= 10^{-8} P_1 \times \frac{30 \times 30}{2.25} (3/10 + 3/12) \\
&= 2.20 \times 10^{-6} P_1
\end{aligned}$$

$$\delta_{41} = -2.20 \times 10^{-6} P_1$$

Load at (2) : Torque = 40 P₂

$$\begin{aligned}\delta_{22} &= 10^{-8} \times \frac{1}{2} \sum h_{\text{arm } 2} P_2 + \frac{40^2 + 10^{-8}}{2.25} \sum_B^2 \frac{1}{h_{\text{tower}}} P_2 \\ &= 10^{-8} P_2 \left[20 + \frac{40^2}{2.25} \left(\frac{5}{8} + \frac{3}{10} + \frac{3}{12} \right) \right] \\ &= 8.57 \times 10^{-6} P_2\end{aligned}$$

$$\delta_{52} = - 8.37 \times 10^{-6} P_2$$

$$\begin{aligned}\delta_{32} &= 10^{-8} P_2 \times \frac{40 \times 30}{2.25} \left(\frac{3}{10} + \frac{3}{12} \right) \\ &= 2.93 \times 10^{-6} P_2\end{aligned}$$

$$\delta_{42} = - \delta_{32}$$

Load at (4) : Torque = 30 P₃

$$\begin{aligned}\delta_{33} &= 10^{-8} \times \frac{1}{2} \sum h_{\text{arm } 3} P_3 + \frac{30^2 \times 10^{-8}}{2.25} \sum_B^3 \frac{1}{h_{\text{tower}}} P_3 \\ &= 10^{-8} P_3 \left[15 + \frac{30^2 \times 10^{-8}}{2.25} \left(\frac{3}{10} + \frac{3}{12} \right) \right] \\ &= 2.23 \times 10^{-6} P_3\end{aligned}$$

$$\delta_{43} = - 2.20 \times 10^{-6} P_3$$

Hence the flexibility matrix from arm shear and tower torsion can be written as

Load at (3)

$$\begin{aligned}\delta_{33} &= 10^{-8} \sum_B^3 h_{\text{tower}} P_3 \\ &= 0.66 \times 10^{-6} P_3 = \delta_{43}\end{aligned}$$

Hence the lateral flexibility matrix is

$$[f_1] = \begin{bmatrix} 1.46 & & & & & & \\ & 1.06 & 1.06 & & & & \\ & 0.66 & 0.66 & 0.66 & & & \\ & 0.66 & 0.66 & 0.66 & 0.66 & & \\ & 1.06 & 1.06 & 0.66 & 0.66 & 1.06 & \\ & 1.46 & 1.06 & 0.66 & 0.66 & 1.06 & 1.46 \end{bmatrix} \quad \text{SYM} \quad (\text{B.12})$$

Adding (B.12) to (B.11) we obtain for the inplane flexibility matrix

$$[f1_i] = \begin{bmatrix} 8.82 & & & & & & \\ & 7.33 & 9.63 & & & & \\ & 2.86 & 3.59 & 3.01 & & & \\ & -1.54 & -2.27 & -1.54 & 3.01 & & \\ & -5.21 & -7.31 & -2.27 & 3.59 & 9.63 & \\ & -5.75 & -5.21 & -1.54 & 2.86 & 7.33 & 8.82 \end{bmatrix} \quad \text{SYM} \quad (\text{B.13})$$

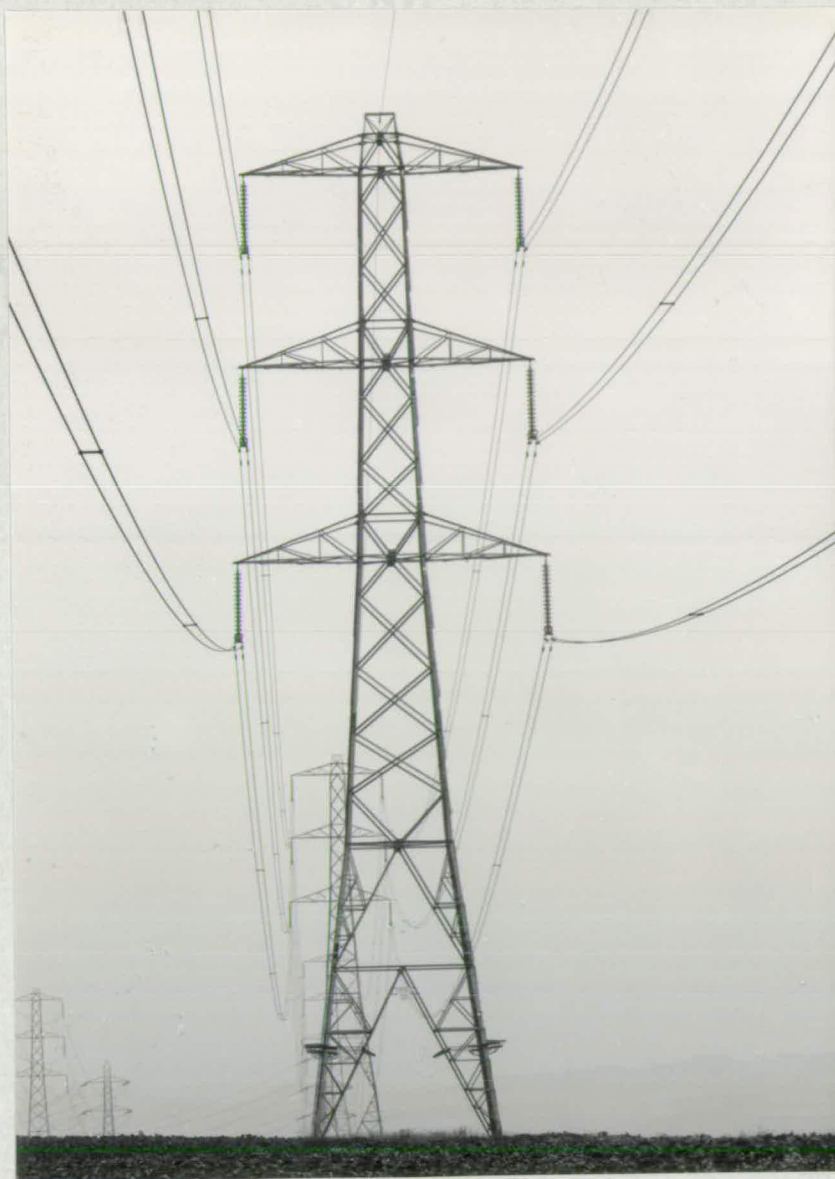


FIG. B.1

An Actual Transmission Line Tower

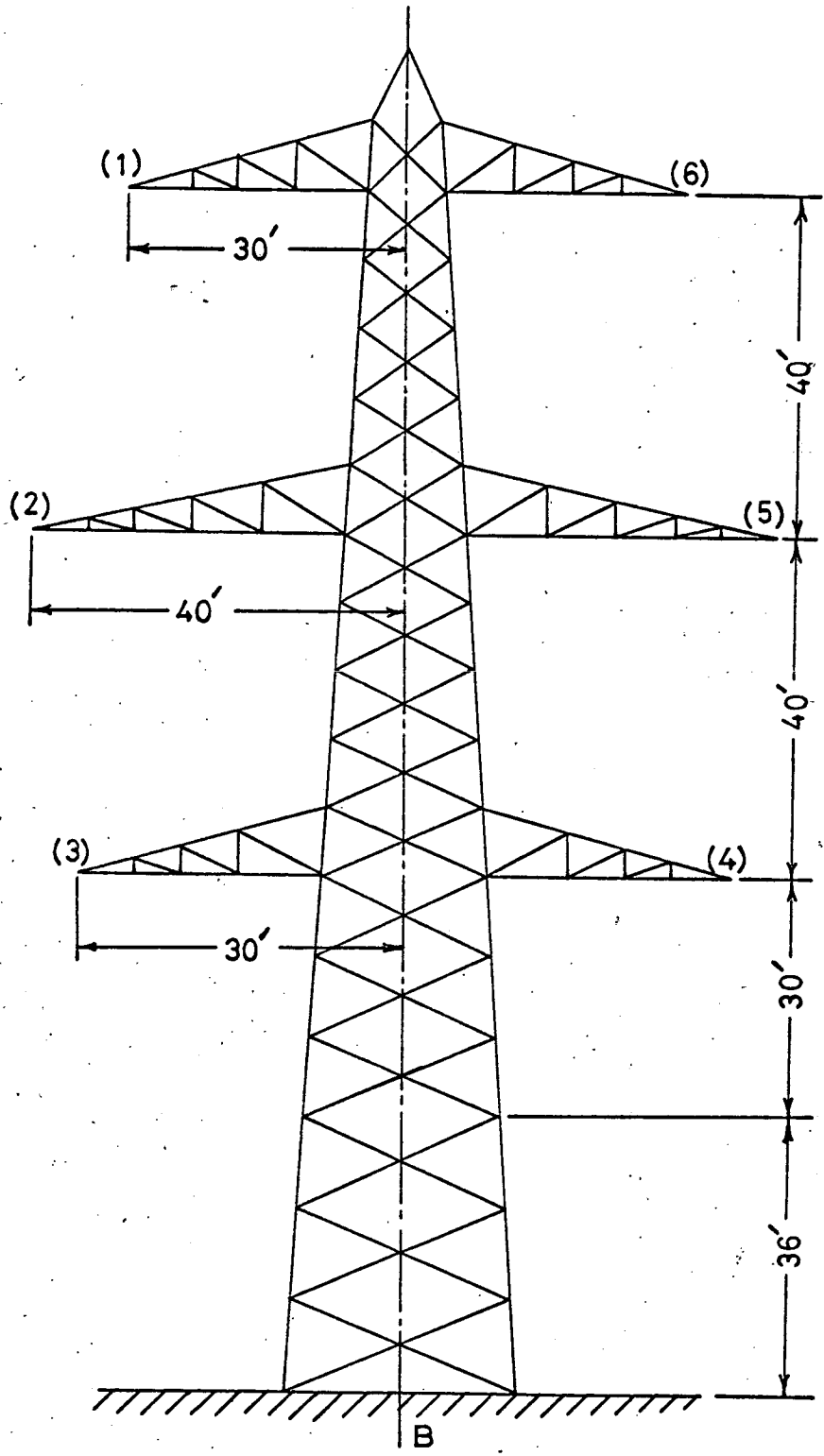


FIG. B.2

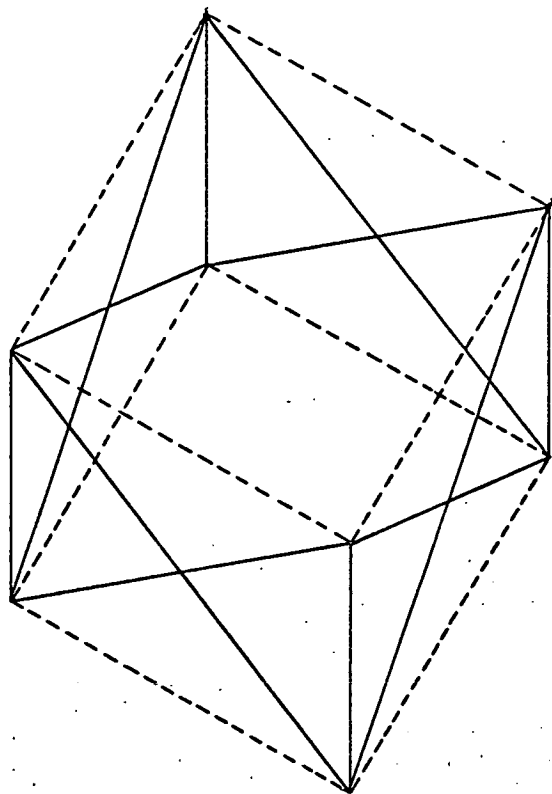


FIG. B.3

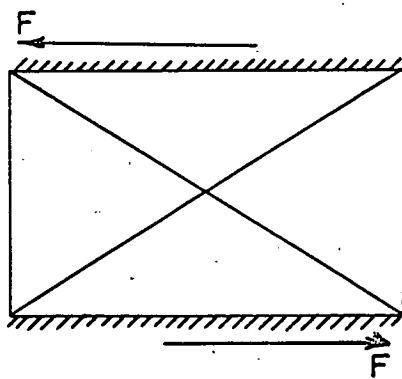


FIG. B.4

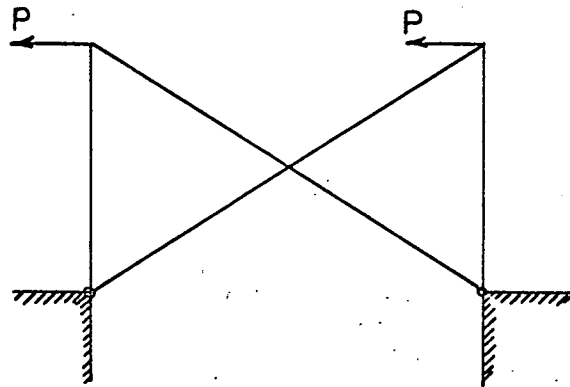


FIG. B.5

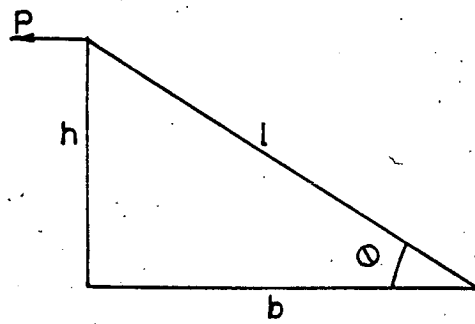


FIG. B.6

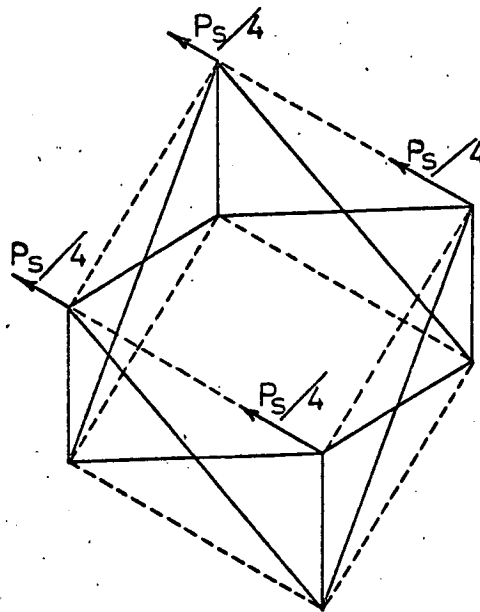


FIG. B.7

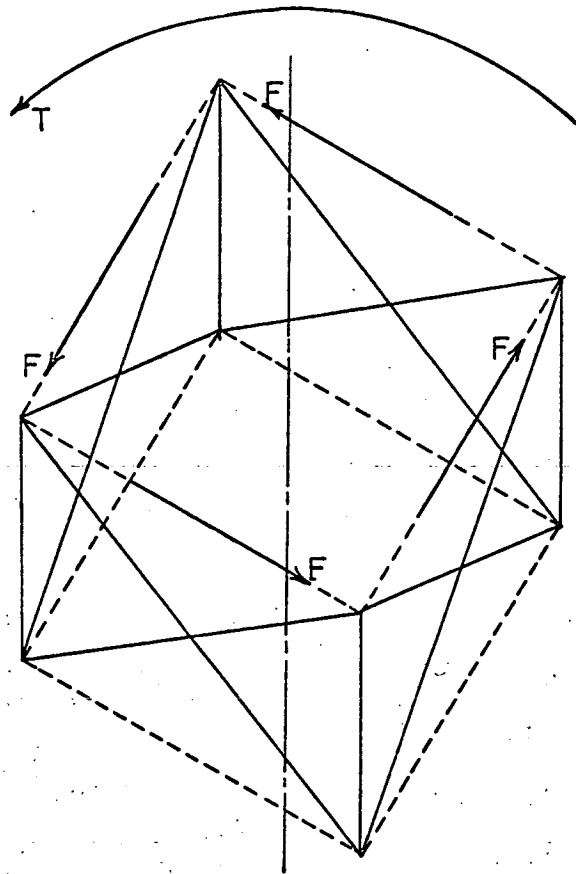


FIG. B.8

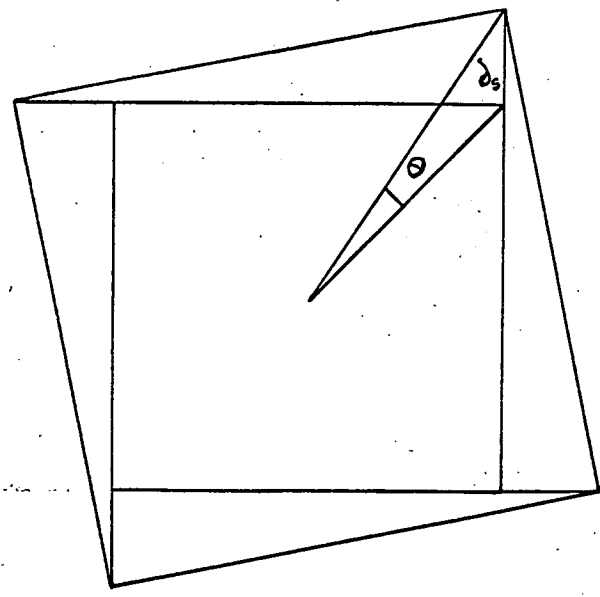


FIG. B.9

APPENDIX - CAnalytical Methods Applied to (5.13)

For convenience we rewrite (5.13) as

$$\begin{aligned}
 \ddot{q}_1 + \omega_1^2 q_1 + b_1 q_1 q_3 + b_2 q_2 q_3 + b_3 q_1 \ddot{q}_3 + b_4 q_2 \ddot{q}_3 &= 0 \\
 \ddot{q}_2 + \omega_2^2 q_2 + c_1 q_2 q_3 + c_2 q_1 q_3 + c_3 q_2 \ddot{q}_3 + c_4 q_1 \ddot{q}_3 &= 0 \\
 \ddot{q}_3 + \omega_3^2 q_3 + a_1 q_3^3 + a_2 q_1^2 + a_3 q_2^2 + a_4 q_1 q_2 + \\
 + a_5 (q_3 \ddot{q}_3 + \dot{q}_3^2/2) + a_6 (q_1 \ddot{q}_1 + \dot{q}_1^2) + a_7 (q_2 \ddot{q}_2 + \dot{q}_2^2) \\
 + a_8 (q_1 \ddot{q}_2 + q_2 \ddot{q}_1 + 2\dot{q}_1 \dot{q}_2) &= 0
 \end{aligned} \tag{C.1}$$

$$\begin{aligned}
 q_1 &= y_1 & q_3 &= x_1 \\
 q_2 &= y_2 & \omega_3^2 &= \Omega^2
 \end{aligned}$$

In order to facilitate analysis let us introduce a small parameter ϵ , $0 < \epsilon \ll 1$. Then the coordinates q_i will be taken

$$q_n = \epsilon p_n, \quad n = 1, 2, 3 \tag{C.2}$$

Substituting (C.2) in (C.1) we get

$$\begin{aligned}
 \ddot{p}_1 + \omega_1^2 p_1 + \epsilon \{b_1 p_1 p_3 + b_2 p_2 p_3 + b_3 p_1 \ddot{p}_3 + c_4 p_2 \ddot{p}_3\} &= 0 \\
 \ddot{p}_2 + \omega_2^2 p_2 + \epsilon \{c_1 p_2 p_3 + c_2 p_1 p_3 + c_3 p_2 \ddot{p}_3 + c_4 p_1 \ddot{p}_3\} &= 0 \\
 \ddot{p}_3 + \omega_3^2 p_3 + \epsilon \{a_1 p_3^3 + a_2 p_1^2 + a_3 p_2^2 + a_4 p_1 p_2 + a_5 (p_3 \ddot{p}_3 + \dot{p}_3^2/2) + \\
 + a_6 (p_1 \ddot{p}_1 + \dot{p}_1^2) + a_7 (p_2 \ddot{p}_2 + \dot{p}_2^2) + a_8 (p_1 \ddot{p}_2 + p_2 \ddot{p}_1 + 2\dot{p}_1 \dot{p}_2)\} &= 0
 \end{aligned} \tag{C.3}$$

Equations (C.3) can be written as

$$\ddot{p}_n + \omega_n^2 p_n + \epsilon f_n(p_1, p_2, p_3, \dot{p}_1, \dot{p}_2, \dot{p}_3, \ddot{p}_1, \ddot{p}_2, \ddot{p}_3) = 0$$

$$\text{where } n = 1, 2, 3 \quad (\text{C.4})$$

Averaging Method [33, 34]

To apply the averaging method, let us rewrite (C.4) as

$$\ddot{p}_n + S_n^2 \gamma^2 p_n = \epsilon [\epsilon^{-1} (S_n^2 \gamma^2 - \omega_n^2) p_n - f_n], n = 1, 2, 3 \quad (\text{C.5})$$

$$S_n = \frac{P_n}{Q_n}$$

and P_n and Q_n are positive integers and both prime and γ is some positive parameter. Let ω_1 be the lowest natural frequency and let $P_1 = Q_1 = 1$. Then γ is in the neighbourhood of ω_1 . Furthermore let us impose the conditions

$$\left| \left(\frac{P_r}{Q_r} \right)^2 \gamma^2 - \omega_r^2 \right| < \epsilon, r = 1, 2, 3 \quad (\text{C.6})$$

Introducing functions $A_n(t)$ and $\psi_n(t)$ such that

$$p_n = A_n(t) \cos(S_n \gamma t + \psi_n(t)) \quad (\text{C.7})$$

$$\dot{p}_n = -A_n(t) S_n \gamma \sin(S_n \gamma t + \psi_n(t))$$

and using the method of variation of parameters we obtain

$$\dot{A}_n = -\frac{\epsilon}{S_n \gamma} [\epsilon^{-1} (S_n^2 \gamma^2 - \omega_n^2) A_n \cos \theta_n - g_n] \sin \theta_n \quad (\text{C.8})$$

$$A_n \dot{\psi}_n = -\frac{\epsilon}{S_n \gamma} [\epsilon^{-1} (S_n^2 \gamma^2 - \omega_n^2) A_n \cos \theta_n - g_n] \cos \theta_n \quad (\text{C.9})$$

$$\text{where } \theta_n = (s_n \gamma t + \Psi_n(t)), n = 1, 2, 3 \quad (\text{C.10})$$

$$\text{and } g_1 = D_1 \cos(\theta_3 + \theta_1) + D_1 \cos(\theta_3 - \theta_1) + D_2 \cos(\theta_3 + \theta_2) + \\ + D_2 \cos(\theta_3 - \theta_2)$$

$$g_2 = E_1 \cos(\theta_3 + \theta_2) + E_1 \cos(\theta_3 - \theta_2) + E_2 \cos(\theta_3 + \theta_1) + \\ + E_2 \cos(\theta_3 - \theta_1) \quad (\text{C.11})$$

$$g_3 = F_1 + F_2 \cos 2\theta_1 + F_3 \cos 2\theta_2 + F_4 \cos 2\theta_3 + \\ + F_5 \cos(\theta_1 + \theta_2) + F_6 \cos(\theta_2 - \theta_1)$$

where D_i 's, E_i 's and F_i 's are functions A_1, A_2, A_3 and are given by

$$D_1 = A_1 A_3 (b_1 - s_3^2 \gamma^2 b_3) \quad D_2 = A_2 A_3 (b_2 - s_3^2 \gamma^2 b_4)$$

$$E_1 = A_2 A_3 (c_1 - s_3^2 \gamma^2 c_3) \quad E_2 = A_1 A_3 (c_2 - s_3^2 \gamma^2 c_4)$$

$$F_1 = \frac{1}{2} [a_2 A_1^2 + a_3 A_2^2 + (a_1 - a_5 s_3^2 \gamma^2 / 2) A_3^2]$$

$$F_2 = A_1^2 (a_2 / 2 - a_6 s_1^2 \gamma^2)$$

$$F_3 = A_2^2 (a_3 / 2 - a_7 s_2^2 \gamma^2)$$

$$F_4 = A_3^2 (a_1 / 2 - 3 a_5 s_3^2 \gamma^2 / 4)$$

$$F_5 = \frac{A_1 A_2}{2} \{a_4 - a_8 (s_1 + s_2)^2 \gamma^2\}$$

$$F_6 = \frac{A_1 A_2}{2} \{a_4 - a_8 (s_2 - s_1)^2 \gamma^2\}$$

By (C.8), \dot{A}_1 , \dot{A}_2 and \dot{A}_3 are given by

$$\begin{aligned} \dot{A}_1 = & -\frac{\epsilon}{4iS_1\gamma} [\epsilon^{-1}(S_1^2\gamma^2 - \omega_1^2) A_1 (e^{i2\theta_1 - i2\theta_1})] + \\ & + \frac{\epsilon}{4iS_1\gamma} [D_1 \left\{ e^{\frac{i(\theta_3 + 2\theta_1)}{-e}} \frac{-i(\theta_3 + 2\theta_1)}{-e} \frac{i(2\theta_1 - \theta_3)}{+e} \frac{-i(2\theta_1 - \theta_3)}{-e} \right\} + \\ & + D_2 \left\{ e^{\frac{i(\theta_1 + \theta_2 + \theta_3)}{-e}} \frac{-i(\theta_1 + \theta_2 + \theta_3)}{-e} \frac{i(\theta_1 - \theta_2 - \theta_3)}{+e} - \right. \\ & \left. \frac{-i(\theta_1 - \theta_2 - \theta_3)}{-e} \frac{i(\theta_1 - \theta_2 + \theta_3)}{+e} \frac{-i(\theta_1 - \theta_2 + \theta_3)}{-e} + \right. \\ & \left. + e^{\frac{i(\theta_1 + \theta_2 - \theta_3)}{-e}} \frac{-i(\theta_1 + \theta_2 - \theta_3)}{-e} \right\}] \end{aligned} \quad (C.12)$$

$$\begin{aligned} \dot{A}_2 = & -\frac{\epsilon}{4iS_2\gamma} [\epsilon^{-1}(S_2^2\gamma^2 - \omega_2^2) A_2 (e^{i2\theta_2 - i2\theta_2})] + \\ & + \frac{\epsilon}{4iS_2\gamma} [E_1 \left\{ e^{\frac{i(\theta_3 + 2\theta_2)}{-e}} \frac{-i(\theta_3 + 2\theta_2)}{-e} \frac{i(2\theta_2 - \theta_3)}{+e} \frac{-i(2\theta_2 - \theta_3)}{-e} \right\} + \\ & + E_2 \left\{ e^{\frac{i(\theta_1 + \theta_2 + \theta_3)}{-e}} \frac{-i(\theta_1 + \theta_2 + \theta_3)}{-e} \frac{i(\theta_2 - \theta_1 - \theta_3)}{+e} - \right. \\ & \left. \frac{-i(\theta_2 - \theta_1 - \theta_3)}{-e} \frac{i(\theta_2 - \theta_1 + \theta_3)}{+e} \frac{-i(\theta_2 - \theta_1 + \theta_3)}{-e} + \right. \\ & \left. + e^{\frac{i(\theta_1 + \theta_2 - \theta_3)}{-e}} \frac{-i(\theta_1 + \theta_2 - \theta_3)}{-e} \right\}] \end{aligned} \quad (C.13)$$

$$\begin{aligned} \dot{A}_3 = & -\frac{\epsilon}{4iS_3\gamma} [\epsilon^{-1}(S_3^2\gamma^2 - \omega_3^2) A_3 (e^{i2\theta_3 - i2\theta_3})] + \\ & + \frac{\epsilon}{4iS_3\gamma} [2F_1 \left\{ e^{\frac{i\theta_3}{-e}} \frac{-i\theta_3}{-e} \right\} + F_2 \left\{ e^{\frac{i(\theta_3 + 2\theta_1)}{-e}} \frac{-i(\theta_3 + 2\theta_1)}{-e} + \right. \\ & \left. + e^{\frac{i(\theta_3 - 2\theta_1)}{-e}} \frac{-i(\theta_3 - 2\theta_1)}{-e} \right\} + F_3 \left\{ e^{\frac{i(\theta_3 + 2\theta_2)}{-e}} \frac{-i(\theta_3 + 2\theta_2)}{-e} + \right. \\ & \left. + e^{\frac{i(\theta_3 - 2\theta_2)}{-e}} \frac{-i(\theta_3 - 2\theta_2)}{-e} \right\}] \end{aligned}$$

$$\begin{aligned}
& + e^{\frac{i(\theta_3 - 2\theta_2)}{-e}} e^{-\frac{i(\theta_3 - 2\theta_2)}{-e}} \} + F_4 \{ e^{\frac{i3\theta_3}{-e}} e^{-\frac{i3\theta_3}{-e}} + \\
& + e^{\frac{-i\theta_3}{-e}} e^{\frac{i\theta_3}{-e}} \} + F_5 \{ e^{\frac{i(\theta_1 + \theta_2 + \theta_3)}{-e}} e^{-\frac{i(\theta_1 + \theta_2 + \theta_3)}{-e}} + \\
& + e^{\frac{i(\theta_3 - \theta_1 - \theta_2)}{-e}} e^{-\frac{i(\theta_3 - \theta_1 - \theta_2)}{-e}} \} + F_6 \{ e^{\frac{i(\theta_3 + \theta_2 - \theta_1)}{-e}} e^{-\frac{i(\theta_3 + \theta_2 - \theta_1)}{-e}} - \\
& - e^{\frac{-i(\theta_3 + \theta_2 - \theta_1)}{+e}} e^{\frac{i(\theta_3 - \theta_2 + \theta_1)}{+e}} e^{-\frac{i(\theta_3 - \theta_2 + \theta_1)}{-e}} \}] \quad (C.14)
\end{aligned}$$

and $A_1 \dot{\Psi}_1$, $A_2 \dot{\Psi}_2$ and $A_3 \dot{\Psi}_3$ are given by

$$\begin{aligned}
A_1 \dot{\Psi}_1 = & -\frac{\epsilon}{4S_1 \gamma} [\epsilon^{-1} (S_1^2 \gamma^2 - \omega_1^2) A_1 (2 + e^{\frac{i2\theta_1}{+e}} e^{-\frac{i2\theta_1}{+e}})] + \\
& + \frac{\epsilon}{4S_1 \gamma} [D_1 \{ e^{\frac{i(\theta_3 + 2\theta_1)}{+e}} e^{-\frac{i(\theta_3 - 2\theta_1)}{+e}} + 2e^{\frac{i\theta_3}{+e}} e^{-\frac{i\theta_3}{+e}} + 2e^{\frac{-i\theta_3}{+e}} e^{\frac{i\theta_3}{+e}} \} \\
& + e^{\frac{i(\theta_3 - 2\theta_1)}{+e}} e^{-\frac{i(\theta_3 - 2\theta_1)}{+e}} \} + D_2 \{ e^{\frac{i(\theta_1 + \theta_2 + \theta_3)}{+e}} + \\
& + e^{\frac{-i(\theta_1 + \theta_2 + \theta_3)}{+e}} e^{\frac{i(\theta_3 + \theta_2 - \theta_1)}{+e}} e^{-\frac{i(\theta_3 + \theta_2 - \theta_1)}{+e}} + \\
& + e^{\frac{i(\theta_3 - \theta_2 + \theta_1)}{+e}} e^{-\frac{i(\theta_3 - \theta_2 + \theta_1)}{+e}} e^{\frac{i(\theta_3 - \theta_2 - \theta_1)}{+e}} e^{-\frac{i(\theta_3 - \theta_2 - \theta_1)}{+e}} \}] \quad (C.15)
\end{aligned}$$

$$\begin{aligned}
A_2 \dot{\Psi}_2 = & -\frac{\epsilon}{4S_2 \gamma} [\epsilon^{-1} (S_2^2 \gamma^2 - \omega_2^2) A_2 (2 + e^{\frac{i2\theta_2}{+e}} e^{-\frac{i2\theta_2}{+e}})] + \\
& + \frac{\epsilon}{4S_2 \gamma} [E_1 \{ e^{\frac{i(\theta_3 + 2\theta_2)}{+e}} e^{-\frac{i(\theta_3 + 2\theta_2)}{+e}} + 2e^{\frac{i\theta_3}{+e}} e^{-\frac{i\theta_3}{+e}} + \\
& + e^{\frac{i(\theta_3 - 2\theta_2)}{+e}} e^{-\frac{i(\theta_3 - 2\theta_2)}{+e}} \} + E_2 \{ e^{\frac{i(\theta_1 + \theta_2 + \theta_3)}{+e}} e^{-\frac{i(\theta_1 + \theta_2 + \theta_3)}{+e}} + \\
& + e^{\frac{i(\theta_3 - \theta_2 + \theta_1)}{+e}} e^{-\frac{i(\theta_3 - \theta_2 + \theta_1)}{+e}} e^{\frac{i(\theta_3 + \theta_2 - \theta_1)}{+e}} e^{-\frac{i(\theta_3 + \theta_2 - \theta_1)}{-e}} + \\
& + e^{\frac{i(\theta_3 - \theta_2 - \theta_1)}{+e}} e^{-\frac{i(\theta_3 - \theta_2 - \theta_1)}{+e}} \}] \quad (C.16)
\end{aligned}$$

$$\begin{aligned}
A_3 \dot{\Psi}_3 = & -\frac{\epsilon}{4S_3 \gamma} [\epsilon^{-1} (S_3^2 \gamma^2 - \omega_3^2) A_3 (2 + e^{i2\theta_3} + e^{-i2\theta_3})] + \\
& + \frac{\epsilon}{4S_3 \gamma} [2F_1 \{e^{i\theta_3} + e^{-i\theta_3}\} + F_2 \{e^{i(\theta_3 + 2\theta_1)} + e^{-i(\theta_3 + 2\theta_1)}\} + \\
& + e^{i(\theta_3 - 2\theta_1)} + e^{-i(\theta_3 - 2\theta_1)}\} + F_3 \{e^{i(\theta_3 + 2\theta_2)} + e^{-i(\theta_3 + 2\theta_2)}\} + \\
& + e^{i(\theta_3 - 2\theta_2)} + e^{-i(\theta_3 - 2\theta_2)}\} + F_4 \{e^{i3\theta_3} + e^{-i3\theta_3} + e^{i\theta_3} + e^{-i\theta_3}\} + \\
& + F_5 \{e^{i(\theta_1 + \theta_2 + \theta_3)} + e^{-i(\theta_1 + \theta_2 + \theta_3)} + e^{i(\theta_1 + \theta_2 - \theta_3)} + \\
& + e^{-i(\theta_1 + \theta_2 - \theta_3)}\} + \\
& + F_6 \{e^{i(\theta_3 + \theta_2 - \theta_1)} + e^{-i(\theta_3 + \theta_2 - \theta_1)} + e^{i(\theta_2 - \theta_1 - \theta_3)} + \\
& + e^{-i(\theta_2 - \theta_1 - \theta_3)}\}] \tag{C.17}
\end{aligned}$$

Thus it is seen that

$$\left. \begin{aligned}
\dot{A}_n &= \epsilon F_n(A_1, A_2, A_3, \Psi_1, \Psi_2, \Psi_3, t) \\
A_n \dot{\Psi}_n &= \epsilon G_n(A_1, A_2, A_3, \Psi_1, \Psi_2, \Psi_3, t)
\end{aligned} \right\} n = 1, 2, 3 \tag{C.18}$$

Following the method of averaging let us introduce new variables a_n and ψ_n such that

$$\left. \begin{aligned}
A_n &= a_n + \epsilon \bar{F}_n(a_1, a_2, a_3, \psi_1, \psi_2, \psi_3, t) \\
\psi_n &= \psi_n + \epsilon \bar{G}_n(a_1, a_2, a_3, \psi_1, \psi_2, \psi_3, t)
\end{aligned} \right\} n = 1, 2, 3, \tag{C.19}$$

where \bar{F}_n and \bar{G}_n are the indefinite integrals of F_n and G_n respectively, excluding those terms that are independent of t in F_n and G_n .

The integration is performed regarding A_r and Ψ_r ($r = 1, 2, 3$) as constants and these quantities are then replaced by the new variables a_r, ψ_r . The a_n and ψ_n ($n = 1, 2, 3$) satisfy the following differential equations of the first approximation:

$$\dot{a}_n = \epsilon M_t \{ F_n \} \quad (C.20)$$

$$\dot{\psi}_n = \epsilon M_t \{ G_n \} \quad (C.21)$$

where the operator M_t operating on a function Q is defined as

$$M_t \{ Q \} = \lim_{T \rightarrow \infty} \frac{1}{T} \int_0^T Q dt \quad (C.22)$$

The above integration is to be performed with respect to explicitly occurring t in Q . Thus the equation of the first approximation becomes

$$\dot{a}_n = 0 \quad (C.23)$$

$$a_n \dot{\psi}_n = - \frac{\epsilon}{2S_n \gamma} [\epsilon^{-1} (S_n^2 \gamma^2 - \omega_n^2) a_n] \quad (C.24)$$

Since P_n and Q_n are arbitrary they can be chosen such that

$$S_n^2 \gamma^2 - \omega_n^2 = 0 \quad (\epsilon^2) \quad n = 1, 2, 3 \quad (C.25)$$

$$\text{Hence} \quad a_n \dot{\psi}_n = 0 \quad (C.26)$$

Therefore it is seen that

$$a_n = \text{constant} \quad (C.27)$$

$$a_n \psi_n = \text{constant} \quad (C.28)$$

Thus, to the first order approximation there is no change in amplitude and phase angle i.e. the method does not provide any information beyond that given by the linear theory.

Asymptotic Method

Let us assume that

$$\left. \begin{aligned} p_1 &= A_1 \cos(\omega_1 t - \theta_1) + \epsilon p_{11} + \epsilon^2 p_{12} + \dots \\ p_2 &= A_2 \cos(\omega_2 t - \theta_2) + \epsilon p_{21} + \epsilon^2 p_{22} + \dots \\ p_3 &= A_3 \cos(\omega_3 t - \theta_3) + \epsilon p_{31} + \epsilon^2 p_{32} + \dots \end{aligned} \right\} \quad (C.29)$$

where A_n , θ_n , p_{ni} , $n = 1, 2, 3$; $i = 1, 2, \dots, N$ are functions of time.

Substituting (C.29) in (C.5) we obtain to order t

$$\begin{aligned} & \cos \Psi_1 [\ddot{A}_1 - A_1(\omega_1 - \dot{\theta}_1)^2] + \sin \Psi_1 [A_1 \ddot{\theta}_1 - 2\dot{A}_1(\omega_1 - \dot{\theta}_1)] + \epsilon \ddot{p}_{11} + S_1^2 \gamma^2 A_1 \cos \Psi_1 \\ & + S_1^2 \gamma^2 \epsilon p_{11} = \epsilon [\epsilon^{-1} (S_1^2 \gamma^2 - \omega_1^2) A_1 \cos \Psi_1] + \epsilon (S_1^2 \gamma^2 - \omega_1^2) p_{11} - \\ & - \epsilon b_1 A_1 A_3 \cos \Psi_1 \cos \Psi_3 - \epsilon b_2 A_2 A_3 \cos \Psi_2 \cos \Psi_3 - \epsilon b_3 A_1 \cos \Psi_1 \\ & \cos \Psi_3 [\ddot{A}_3 - A_3(\omega_3 - \dot{\theta}_3)^2] - \epsilon b_3 A_1 \cos \Psi_1 \sin \Psi_3 [A_3 \ddot{\theta}_3 - 2\dot{A}_3(\omega_3 - \dot{\theta}_3)] - \\ & - \epsilon b_4 A_2 \cos \Psi_2 \cos \Psi_3 [\ddot{A}_3 - A_3(\omega_3 - \dot{\theta}_3)^2] - \epsilon b_4 A_2 \sin \Psi_2 \cos \Psi_3 [A_3 \ddot{\theta}_3 - 2\dot{A}_3(\omega_3 - \dot{\theta}_3)] \quad (C.30) \end{aligned}$$

$$\begin{aligned}
& \cos \Psi_2 [\ddot{A}_2 - A_2 (\omega_2 - \dot{\theta}_2)^2] + \sin \Psi_2 [A_2 \ddot{\theta}_2 - 2\dot{A}_2 (\omega_2 - \dot{\theta}_2)] + \epsilon \ddot{p}_{21} + S_2^2 \gamma^2 A_2 \cos \Psi_2 \\
& + S_2^2 \gamma^2 \epsilon p_{21} = \epsilon [\epsilon^{-1} (S_2^2 \gamma^2 - \omega_2^2) A_2 \cos \Psi_2] + \epsilon (S_2^2 \gamma^2 - \omega_2^2) p_{21} \\
& - \epsilon C_1 A_2 A_3 \cos \Psi_2 \cos \Psi_3 - \epsilon C_2 A_1 A_3 \cos \Psi_1 \cos \Psi_3 - \epsilon C_3 A_2 \cos \Psi_2 \\
& \cos \Psi_3 [\ddot{A}_3 - A_3 (\omega_3 - \dot{\theta}_3)^2] - \epsilon C_3 A_2 \cos \Psi_2 \sin \Psi_3 [A_3 \ddot{\theta}_3 - 2\dot{A}_3 (\omega_3 - \dot{\theta}_3)] \\
& - \epsilon C_4 A_1 \cos \Psi_1 \cos \Psi_3 [\ddot{A}_3 - A_3 (\omega_3 - \dot{\theta}_3)^2] - \epsilon C_4 A_1 \sin \Psi_1 \sin \Psi_3 [A_3 \ddot{\theta}_3 - 2\dot{A}_3 (\omega_3 - \dot{\theta}_3)]
\end{aligned} \tag{C.31}$$

$$\begin{aligned}
& \cos \Psi_3 [\ddot{A}_3 - A_3 (\omega_3 - \dot{\theta}_3)^2] + \sin \Psi_3 [A_3 \ddot{\theta}_3 - 2\dot{A}_3 (\omega_3 - \dot{\theta}_3)] + \epsilon \ddot{p}_{31} + S_3^2 \gamma^2 A_3 \cos \Psi_3 \\
& + S_3^2 \gamma^2 \epsilon p_{31} = \epsilon [\epsilon^{-1} (S_3^2 \gamma^2 - \omega_3^2) A_3 \cos \Psi_3] + \epsilon (S_3^2 \gamma^2 - \omega_3^2) p_{31} \\
& - \epsilon a_1 A_3^2 \cos^2 \Psi_3 - \epsilon a_2 A_1^2 \cos^2 \Psi_1 - \epsilon a_3 A_2^2 \cos^2 \Psi_2 - \epsilon a_4 A_1 A_2 \cos \Psi_1 \cos \Psi_2 \\
& - \epsilon a_5 A_3 \cos \Psi_3 \cos \Psi_3 [\ddot{A}_3 - A_3 (\omega_3 - \dot{\theta}_3)^2] - \epsilon a_5 A_3 \cos \Psi_3 \sin \Psi_3 [A_3 \ddot{\theta}_3 - 2\dot{A}_3 (\omega_3 - \dot{\theta}_3)] \\
& - \frac{\epsilon a_5}{2} [A_3^2 \cos^2 \Psi_3 + (\omega_3 - \dot{\theta}_3)^2 A_3^2 \sin^2 \Psi_3 - 2A_3 \dot{A}_3 (\omega_3 - \dot{\theta}_3) \sin \Psi_3 \cos \Psi_3] \\
& - \epsilon a_6 A_1 \cos \Psi_1 \cos \Psi_1 [\ddot{A}_1 - A_1 (\omega_1 - \dot{\theta}_1)^2] - \epsilon a_6 A_1 \cos \Psi_1 \sin \Psi_1 [A_1 \ddot{\theta}_1 - 2\dot{A}_1 (\omega_1 - \dot{\theta}_1)] \\
& - \epsilon a_6 [\dot{A}_1^2 \cos^2 \Psi_1 + (\omega_1 - \dot{\theta}_1)^2 A_1^2 \sin^2 \Psi_1 - 2A_1 \dot{A}_1 (\omega_1 - \dot{\theta}_1) \sin \Psi_1 \cos \Psi_1] \\
& - \epsilon a_7 A_2 \cos \Psi_2 \cos \Psi_2 [\ddot{A}_2 - A_2 (\omega_2 - \dot{\theta}_2)^2] - \epsilon a_7 A_2 \cos \Psi_2 \sin \Psi_2 [A_2 \ddot{\theta}_2 - 2\dot{A}_2 (\omega_2 - \dot{\theta}_2)] \\
& - \epsilon a_7 [\dot{A}_2^2 \cos^2 \Psi_2 + (\omega_2 - \dot{\theta}_2)^2 A_2^2 \sin^2 \Psi_2 - 2A_2 \dot{A}_2 (\omega_2 - \dot{\theta}_2) \sin \Psi_2 \cos \Psi_2] \\
& - \epsilon a_8 A_1 \cos \Psi_1 \cos \Psi_2 [\ddot{A}_2 - A_2 (\omega_2 - \dot{\theta}_2)^2] - \epsilon a_8 A_1 \cos \Psi_1 \sin \Psi_2 [A_2 \ddot{\theta}_2 - 2\dot{A}_2 (\omega_2 - \dot{\theta}_2)] \\
& - \epsilon a_8 A_2 \cos \Psi_2 \cos \Psi_1 [\ddot{A}_1 - A_1 (\omega_1 - \dot{\theta}_1)^2] - \epsilon a_8 A_2 \cos \Psi_2 \sin \Psi_1 [A_1 \ddot{\theta}_1 - 2\dot{A}_1 (\omega_1 - \dot{\theta}_1)] -
\end{aligned}$$

$$\begin{aligned}
-2 \in a_8 [\dot{A}_1 \dot{A}_2 \cos \Psi_1 \cos \Psi_2 - \dot{A}_1 (\omega_2 - \dot{\theta}_2) A_2 \cos \Psi_1 \sin \Psi_2 - \dot{A}_2 (\omega_1 - \dot{\theta}_1) A_1 \sin \Psi_1 \cos \Psi_2 \\
+ (\omega_1 - \dot{\theta}_1) (\omega_2 - \dot{\theta}_2) A_1 A_2 \sin \Psi_1 \sin \Psi_2] \quad (C.32)
\end{aligned}$$

$$\text{where } \Psi_n = (\omega_n t - \theta_n) \quad ; \quad n = 1, 2, 3 \quad (C.33)$$

Equating the coefficients of $\cos \Psi_n$ and $\sin \Psi_n$ for $n = 1, 2, 3$ on both sides of (C.30)-(C.32) we obtain

$$\cos \Psi_1 : \ddot{A}_1 - A_1 (\omega_1 - \dot{\theta}_1)^2 + S_1^2 \gamma^2 A_1 = (S_1^2 \gamma^2 - \omega_1^2) A_1 \quad (C.34)$$

$$\cos \Psi_2 : \ddot{A}_2 - A_2 (\omega_2 - \dot{\theta}_2)^2 + A_2^2 \gamma^2 A_2 = (S_2^2 \gamma^2 - \omega_2^2) A_2 \quad (C.35)$$

$$\cos \Psi_3 : \ddot{A}_3 - A_3 (\omega_3 - \dot{\theta}_3)^2 + S_3^2 \gamma^2 A_3 = (S_3^2 \gamma^2 - \omega_3^2) A_3 \quad (C.36)$$

$$\sin \Psi_1 : A_1 \ddot{\theta}_1 - 2\dot{A}_1 (\omega_1 - \dot{\theta}_1) = 0 \quad (C.37)$$

$$\sin \Psi_2 : A_2 \ddot{\theta}_2 - 2\dot{A}_2 (\omega_2 - \dot{\theta}_2) = 0 \quad (C.38)$$

$$\sin \Psi_3 : A_3 \ddot{\theta}_3 - 2\dot{A}_3 (\omega_3 - \dot{\theta}_3) = 0 \quad (C.39)$$

We shall not treat the variational equations (C.34) - (C.39) precisely. It is sufficient at this point to obtain solutions correct to first order in ϵ . Hence we reduce (C.34) - (C.39) to

$$\frac{d\theta_n}{dt} = 0 \quad , \quad n = 1, 2, 3 \quad (C.40)$$

$$\frac{dA_n}{dt} = 0 \quad , \quad n = 1, 2, 3 \quad (C.41)$$

merely by dropping terms $d^2 A_n / dt^2$, $(d^2 \theta_n / dt^2)$, $(\frac{d\theta_n}{dt})^2$ $dA_n / dt \times d\theta_n / dt$.

Equations (C.40) and (C.41) imply that to order one in ϵ , the amplitudes and phase angles remain constant.

If a solution for p_{11} , p_{21} , p_{31} is required then the first order terms in ϵ can be collected and solved from (C.30) - (C.32). Hence as in the case of averaging method no advance is made over straightforward linear theory.

APPENDIX - DDIGITAL COMPUTER PROGRAM FOR SOLVING
NONLINEAR DIFFERENTIAL EQUATIONS

Referring to Chapter 5, we consider (5.13) for numerical solution.

For convenience (5.13) are rewritten as -

$$(1 + A_6 x_1) \ddot{x}_1 + A_1 x_1 + A_2 x_1^2 + A_3 y_1^2 + A_4 y_2^2 + A_5 y_1 y_2 + A_6 \dot{x}_1^2 +$$

$$+ A_7 (\dot{y}_1^2 + y_1 \ddot{y}_1) + A_8 (\dot{y}_2^2 + y_2 \ddot{y}_2) + A_9 (y_1 \ddot{y}_2 + y_2 \ddot{y}_1 + 2\dot{y}_1 \dot{y}_2) = 0$$
(D.1)

$$- \ddot{y}_1 + B_1 y_1 + B_2 x_1 y_1 + B_3 x_1 y_2 + B_4 \ddot{x}_1 y_1 + B_5 \ddot{x}_1 y_2 = 0$$

$$\ddot{y}_2 + C_1 y_2 + C_2 x_1 y_2 + C_3 x_1 y_1 + C_4 \ddot{x}_1 y_2 + C_5 \ddot{x}_1 y_1 = 0$$

where the constants Ai's, Bi's and Ci's replace those of the original equations. At this stage we take an arbitrary system, with length of link and dip of the catenary equal to 1ft. and $\frac{1}{4}$ ft. respectively, and calculate the constants in (D.1). The values of these constants are given in the main body of the program.

```
//MEE006 JOB (0000,,,5), "BORGOHAIN SYS SIM", CLASS = D
/* HOLD ***** MOUNT DISC RCA329 *****
//JOB LIB DD DSN=CSMP.SIMLOAD, DISP=(OLD,PASS), VOL=SER=RCA329
// UNIT = 2311
//G EXEC PGM = DEJCSMP2, TIME=5
//FTO2FOO1 DD SYSOUT=B, DCB = (RECFM=F, BLKSIZE=80)
//FTO6FOOL DD SYSOUT=A
```

```

//FT07FOOL DD UNIT=2311, VOL=SER=RCA329, SPACE=(TRK,(40,10))
//FT08FOOL DD UNIT=2311, VOL=SER=RCA329, SPACE=(TRK,(40,10))
//FT13FOOL DD UNIT=2311, VOL=SER=RCA329, SPACE=(TRK,(40,10)),
//          DCB= (RECFM=V, LRECL=200, BLKSIZE=204)
//FT14FOOL DD UNIT=2311, VOL=SER=RCA329, SPACE=(TRK,(40,10)),
//          DCB= (RECFM=V, LRECL=200, BLKSIZE=204)
//FT15FOOL DD DUMMY
//SYSPRINT DD SYSOUT=A
//COMPRINT DD SYSOUT=A
//SYSUT1   DD UNIT=2311, VOL=SER=RCA329, SPACE=(TRK,(40,10))
//SYSUT2   DD UNIT=2311, VOL=SER=RCA329, SPACE=(TRK,(40,10))
//SYSLIN   DD UNIT=2311, VOL=SER=RCA329, SPACE=(TRK,(30,10))
//SYSLINK  DD DSN=*.SYSLIN, DISP=(OLD,PASS), UNIT=2311, VOL=SER=RCA329
//          DD DSN=CSMP.SYMBM(CTLCDS), VOL=SER=RCA329, UNIT=2311
//          DISP=(OLD,KEEP)
//SYSLIB   DD DSN=CSMP.SIMLOAD, VOL=SER=RCA329, DISP=(OLD,KEEP),
//          UNIT=2311
//          DD DSN = SYS1.FORTLIB, DISP=SHR
//SYSLMOD  DD DSN=&NOSET(DEJEZE), UNIT=2311, VOL=SER=RCA329,
//          SPACE=(TRK,(50,201))
//FT01FOOL DD *

```

TITLE CATENARY

$$\begin{aligned}
 X12DOT = & -(A1 * X1 + A2 * (X1**2) + (A3 - A7 * B1 - A7 * B2 * X1 - A9 * C3 * \\
 & X1) * (Y1 ** 2) + (A4 - A8 * C1 - A8 * C2 * X1 - A9 * B3 * X1) * \\
 & (Y2 ** 2) + (A5 - A7 * B3 * X1 - A8 * C3 * X1 - A9 * C1 - A9 * C2 * \\
 & X1 - A9 * B1 - A9 * B2 * X1) * Y1 * Y2 + A6 * (X1DOT ** 2)/2 + A7 *
 \end{aligned}$$

$$\begin{aligned} & (Y1DOT ** 2) + A8 * (Y2DOT ** 2) + 2 * A9 * Y1DOT * Y2DOT) / (1 + A6 * \\ & X1 - (A7 * B4 + A9 * C5) * (Y1 ** 2) - (A8 * C4 + A9 * B5) * (Y2 ** 2) \\ & - (A7 * B5 + A8 * C5 + A9 * C4 + A9 * B4) * Y1 * Y2) \end{aligned}$$

$$X12DOT = \text{INTGRL}(0.0, X12DOT)$$

$$X1 = \text{INTGRL}(0.0, X12DOT)$$

$$\begin{aligned} Y12DOT = & -(B1 * Y1 + B2 * X1 * Y1 + B3 * X1 * Y2 + B4 * X12DOT * Y1 + \\ & B5 * X12DOT * Y2) \end{aligned}$$

$$Y12DOT = \text{INTGRL}(0.0, Y12DOT)$$

$$Y1 = \text{INTGRL}(0.0, Y12DOT)$$

$$\begin{aligned} Y22DOT = & -(C1 * Y2 + C2 * X1 * Y2 + C3 * X1 * Y1 + C4 * X12DOT * Y2 + \\ & C5 * X12DOT * Y1) \end{aligned}$$

$$Y22DOT = \text{INTGRL}(0.0, Y22DOT)$$

$$Y2 = \text{INTGRL}(0.02, Y22DOT)$$

$$\text{PARAM A1} = 362.33862$$

$$\text{PARAM A2} = 6528.96484$$

$$\text{PARAM A3} = 724.67822$$

$$\text{PARAM A4} = 2128.00952$$

$$\text{PARAM A5} = 32.17400$$

$$\text{PARAM A6} = 24.02527$$

$$\text{PARAM A7} = 4.00000$$

$$\text{PARAM A8} = 11.74597$$

$$\text{PARAM A9} = 0.25000$$

$$\text{PARAM B1} = 128.69589$$

$$\text{PARAM B2} = 1545.97705$$

$$\text{PARAM B3} = 34.31982$$

```
PARAM B4 = 4.26667
PARAM B5 = 0.26667
PARAM C1 = 377.91455
PARAM C2 = 4539.75000
PARAM C3 = 34.31892
PARAM C4 = 12.52903
PARAM C5 = 0.26667
```

```
TIMER DELT=0.01, FINTIM=20.0, OUTDEL=0.01
```

```
METH RKAFX
```

```
PRTPLT X1, Y1, Y2
```

```
LABEL CATENARY
```

```
END
```

```
STOP
```

```
END JOB
```

```
/*
```

It is to be noted in the above program that integrations are performed using Runge-Kutta fixed integral method. The computer prints and plots the variables X1, Y1 and Y2 at the interval 0.01 sec upto the maximum of 20 sec.

APPENDIX - ENORMAL MODES AND NATURAL FREQUENCIES OF A CATENARY
WITH THREE EXTRA POINT MASSES

The analysis of this section is not of direct relevance but was carried out at the request of Dr. Rowbottom of the C.E.R.L., Leatherhead. The point masses represent extra masses due to aero-dampers proposed. The system considered is a twin-conductor transmission line span having the following specifications:-

Span/dip	=	1000/23
Mass/unit length	=	2 x 0.57 lbm/ft.
Discrete mass	=	25 lbm each
No. of discrete mass	=	3

The system is shown in Fig. E.1.

Assumptions

- (1) The linearised equations of motion apply
- (2) The cable is suspended from the same horizontal level
- (3) The cable is inextensible
- (4) There is no bending stiffness in the cable
- (5) Equilibrium shape of the cable remains unchanged when the discrete masses are added.

Theory

Referring to the Section 2.3, the potential energy,

$$V = \frac{H}{2} \int_{-L}^L \left(\frac{\partial v}{\partial x} \right)^2 dx \quad (\text{E.1})$$

and the kinetic energy

$$T = \frac{m}{2} \int_{-L}^L \dot{v}^2 dx + \frac{1}{2} \sum_{i=1}^3 M \dot{v}_{Mi}^2 \quad (E.2)$$

As the cable is assumed inextensible, there is an equation of constraint given by

$$\int_{-L}^L v dx = 0 \quad (E.3)$$

It is to be noted that in the potential energy expression the extra masses are distributed uniformly along the cable whereas in the kinetic energy expression they are left as they are placed. Also in (E.2), M is the mass of each point mass.

A Rayleigh-Ritz technique will be used by using six arbitrary sinusoidal deformation modes giving altogether five modes. Thus let us write

$$v = V_1 \cos \frac{\pi x}{2L} + V_2 \sin \frac{\pi x}{L} + \dots + V_5 \cos \frac{5\pi x}{2L} + V_6 \sin \frac{3\pi x}{L} \quad (E.4)$$

Substituting (E.4) in (E.1) - (E.3) we obtain

$$V = \frac{\pi H}{8L} (V_1^2 + 4V_2^2 + \dots + 25V_5^2 + 36V_6^2) \quad (E.5)$$

$$\begin{aligned} T = & \frac{mL}{2} (\dot{V}_1^2 + \dot{V}_2^2 + \dots + \dot{V}_5^2 + \dot{V}_6^2) + \frac{M}{2} [(1 + 2f_1^2) \dot{V}_1^2 + (1 + 2f_3^2) \dot{V}_3^2 + \\ & + (1 + 2f_5^2) \dot{V}_5^2 + 2f_2^2 \dot{V}_2^2 + 2f_4^2 \dot{V}_4^2 + 2f_6^2 \dot{V}_6^2 + 2(1 + 2f_1 f_3) \dot{V}_1 \dot{V}_3 + \\ & + 2(1 + 2f_1 f_5) \dot{V}_1 \dot{V}_5 + 2(1 + 2f_3 f_5) \dot{V}_3 \dot{V}_5 + 4f_2 f_4 \dot{V}_2 \dot{V}_4 + 4f_2 f_6 \dot{V}_2 \dot{V}_6 + \\ & + 4f_4 f_6 \dot{V}_4 \dot{V}_6] \end{aligned} \quad (E.6)$$

$$\text{where} \quad \left. \begin{array}{l} f_1 = \cos \frac{\pi}{12} \\ f_3 = \cos \frac{\pi}{4} \\ f_5 = \cos \frac{5\pi}{12} \end{array} \right\} \left. \begin{array}{l} f_2 = \sin \frac{\pi}{6} \\ f_4 = \sin \frac{\pi}{2} \\ f_6 = \sin \frac{5\pi}{6} \end{array} \right\} \quad (\text{E.7})$$

The equation of constraint becomes

$$v_1 - \frac{v_3}{3} + \frac{v_5}{5} = 0 \quad (\text{E.8})$$

From (E.5) and (E.6) through (E.8) it is observed that symmetrical and antisymmetrical modes are uncoupled and hence can be treated separately.

Symmetrical Modes

$$V_S = \frac{1}{2} D'_{VS} E_{VS} D_{VS} \quad (\text{E.9})$$

$$T_S = \frac{1}{2} \dot{D}'_{VS} M_{VS} \dot{D}_{VS} \quad (\text{E.10})$$

$$\text{where} \quad D_{VS} = \{v_1 \ v_3 \ v_5\} \quad (\text{E.11})$$

$$E_{VS} = \begin{bmatrix} 1 & & 0 \\ & 9 & \\ 0 & & 25 \end{bmatrix} \times \frac{\pi^2 H}{4L}$$

$$M_{VS} = mL \begin{bmatrix} 1 & & 0 \\ & 1 & \\ 0 & & 1 \end{bmatrix} + M \begin{bmatrix} 1 + 2f_1^2 & 1 + 2f_1 f_3 & 1 + 2f_1 f_5 \\ 1 + 2f_1 f_3 & 1 + 2f_3^2 & 1 + 2f_3 f_5 \\ 1 + 2f_1 f_5 & 1 + 2f_3 f_5 & 1 + 2f_5^2 \end{bmatrix} \quad (\text{E.12})$$

and the transformation matrix from (E.8)

$$D_{VS} = \begin{bmatrix} V_1 \\ V_3 \\ V_5 \end{bmatrix} = \begin{bmatrix} 1/3 & -1/5 \\ 1 & 0 \\ 0 & 1 \end{bmatrix} \begin{bmatrix} V_3 \\ V_5 \end{bmatrix} = Q D_{VSt} \quad (\text{E.13})$$

By singular transformation of (E.9) and (E.10) with the help of (E.13)

we obtain

$$V_S = \frac{1}{2} D_{VSt}' Q' E_{VS} Q D_{VSt} = \frac{1}{2} D_{VSt}' E_{VSt} D_{VSt} \quad (\text{E.14})$$

$$T_S = \frac{1}{2} \dot{D}_{VSt}' Q' M_{VS} Q \dot{D}_{VSt} = \frac{1}{2} \dot{D}_{VSt}' M_{VSt} \dot{D}_{VSt} \quad (\text{E.15})$$

Applying Lagrange's equations to (E.14) and (E.15) the equations of symmetrical motion can be easily formed and solved.

Anti-symmetrical Modes

$$V_{AS} = \frac{1}{2} D_{VAS}' E_{VAS} D_{VAS} \quad (\text{E.16})$$

$$T_{AS} = \frac{1}{2} \dot{D}_{VAS}' M_{VAS} \dot{D}_{VAS} \quad (\text{E.17})$$

where

$$D_{VAS} = \{ V_2 \ V_4 \ V_6 \} \quad (\text{E.18})$$

$$E_{VAS} = \begin{bmatrix} 1 & 0 \\ & 4 \\ 0 & 9 \end{bmatrix} \times \frac{\pi^2 H}{L}$$

$$M_{VAS} = \begin{bmatrix} 1 & & 0 \\ & 1 & \\ 0 & & 1 \end{bmatrix} x mL + 2M \begin{bmatrix} f_2^2 & f_2 f_4 & f_2 f_6 \\ f_2 f_4 & f_4^2 & f_4 f_6 \\ f_2 f_6 & f_4 f_6 & f_6^2 \end{bmatrix} \quad (E.19)$$

No reducing relation of the type (E.13) is required in this case and hence applying Lagrange's equations to (E.16) and (E.17) the equations for antisymmetrical motion can be easily formed and solved.

Results

Normal mode shapes and natural frequencies of vibration of the catenary of Fig. E.1 were calculated and compared with those of a catenary without the masses. The sketches of the approximate normal mode shapes are shown in Fig. E.2 in increasing order of frequencies. The number on the left represent frequencies (radians/sec) with the masses and numbers on the right represent the frequencies without the masses. The normal mode shapes were not altered appreciably when the extra masses were introduced. From Fig. E.2 it can be concluded that the addition of the discrete masses makes little difference to the natural frequencies and the normal modes.

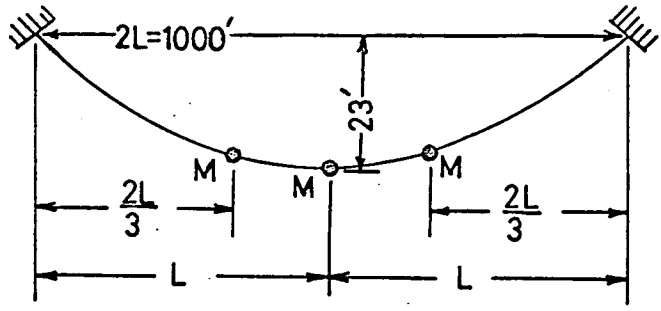


FIG. E.1

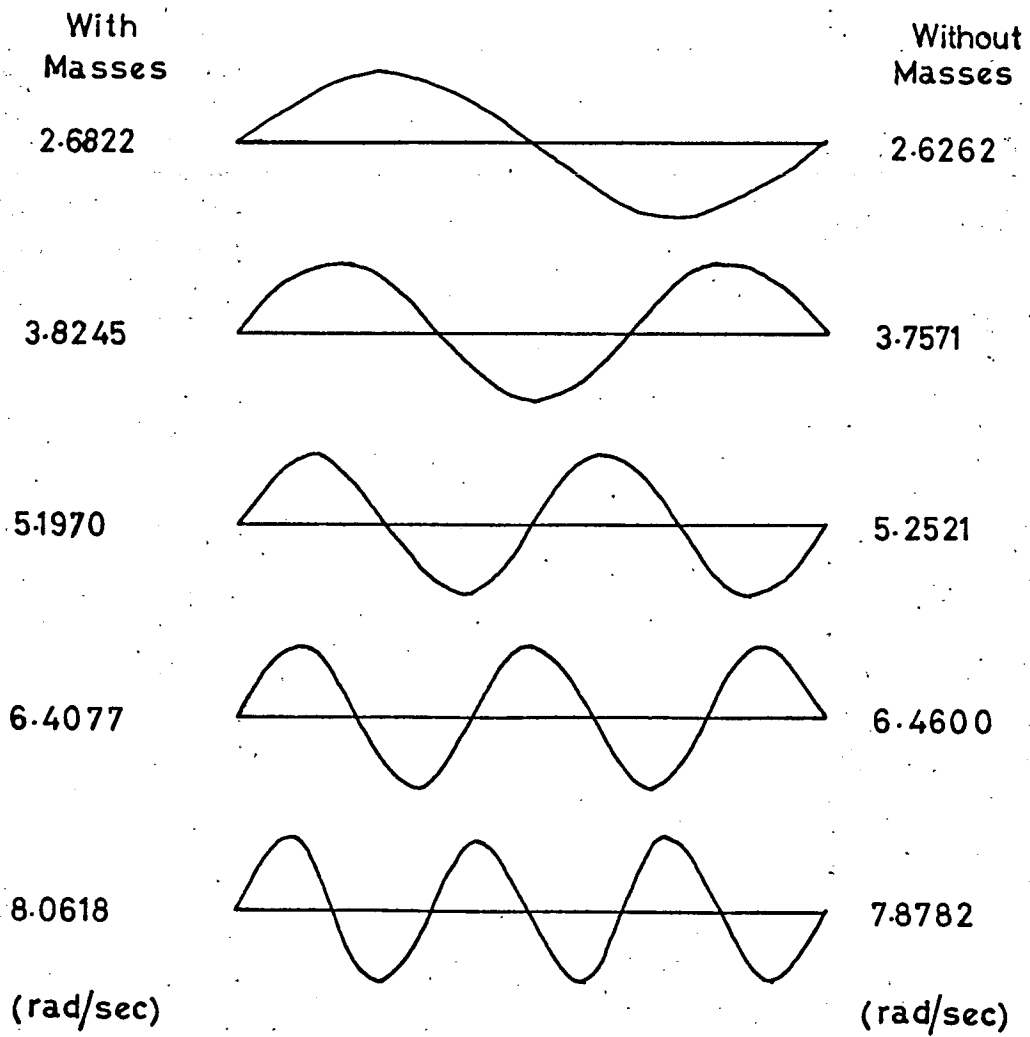


FIG. E.2

APPENDIX - FDESIGN OF THE CATENARY MODEL

The fixed-fixed catenary model on which the experiments were performed is shown in Fig. F.1. The model proportions are those of the Severn Crossing Mainspan (see Chapter 2). To gain insight into the design procedure, we perform an elementary dimensional analysis of the problem of elastic catenary oscillation. We assume that

$$\omega^2 = f(L, d, A, \rho, E, g) \quad (\text{F.1})$$

where L is the span of the catenary; d , the dip; A , the cross-sectional area; ρ , the density of the cable material; E , the Young's Modulus of the cable material and g , the acceleration due to gravity. In the usual manner we obtain

$$\omega^2 = \frac{g}{d} f_1\left(\frac{L}{d}, \frac{A}{d^2}, \frac{\rho g d}{E}\right) \quad (\text{F.2})$$

From (F.2) it is seen that $\omega^2 \propto \frac{1}{d}$ which can also be observed from Chapter 2. Now if a model of the system is built and it is required that this model should represent accurately any kind of oscillation we must have

$$\frac{L_m}{d_m} = \frac{L}{d} \quad (\text{F.3})$$

$$\frac{A_m}{d_m^2} = \frac{A}{d^2} \quad (\text{F.4})$$

$$\frac{\rho_m d_m}{E_m} = \frac{\rho d}{E} \quad (\text{F.5})$$

Using (F.3) in (F.5) we obtain

$$\frac{\rho_m L_m}{E_m} = \frac{\rho L}{E} \quad (\text{F.6})$$

In another form (F.6) can be written as

$$\frac{E_m A_m}{W_m} = \frac{EA}{W} \quad (\text{F.7})$$

where W is the total weight of the actual span.

Calculation for the Catenary Model

We choose a model span of 10 ft. By (F.3) the dip of the model span is given by

$$d_m = \frac{L_m d}{L} = \frac{10 \times 265}{5310} = 0.5 \text{ ft.} = 6 \text{ ins.} \quad (\text{F.8})$$

Mass and stiffness requirements need to be satisfied independently.

Hence we adopt the lumped mass catenary and select a 0.011 inch diameter piano wire on which the lumped masses are to be hung. Then by (F.7) we obtain

$$W_m = \frac{E_m A_m W}{EA} \quad (\text{F.9})$$

where $A_m = \frac{\pi}{4} (0.011)^2 = 0.000095 \text{ in}^2$

$$A = 2.23 \text{ in}^2$$

$$E_m = 30 \times 10^6 \text{ lb/in}^2$$

$$E = 25.5 \times 10^6 \text{ lb/in}^2$$

$$W = 22850 \text{ lbs.}$$

For the above values of Severn Main span the reader is referred to reference [35]. Substituting the required values in (F.9) we obtain

$$W_m = 1.145 \text{ lbs}$$

Before determining the size of the masses, we adopt the Lagrangian type of mass distribution in which the mass of a link is equally divided and concentrated at the two ends of the link. Also we decide arbitrarily to represent the catenary by 20 degrees of freedom in the vertical plane. In this case we obtain for the weight of each lumped mass

$$\omega = \frac{1.145}{22} = 0.0521 \text{ lbs.}$$

For the ease of manufacture, the lumped masses were made cylindrical having a diameter of 0.75 inch. Then the length of each mass is given by

$$\frac{\pi}{4} (0.75)^2 \times l_m \times 0.289 = 0.0521$$

$$\text{or } l_m = 0.408 \approx 13/32 \text{ inch}$$

To facilitate fastening of the masses to the piano wire each mass was made of two semi-cylindrical halves with a small groove in one half. This small groove was provided only to position mass on the piano wire. The two halves of the mass could be put together with the help of tightening screws as shown in Fig. F.2.

To determine the length, l , of the piano wire in between two masses we use the formulae [35] which are given below.

$$t_1 = \frac{2d_m}{L_m} \frac{\sum_{i=1,3}^{21} (1 + i^2 t_1^2)^{-\frac{1}{2}}}{\sum_{i=1,3}^{21} i (1 + i^2 t_1^2)^{-\frac{1}{2}}} \quad (\text{F.10})$$

and

$$\frac{L_m}{2} = \sum_{i=1,3}^{21} l \cos \theta_i \quad (\text{F.11})$$

where $t_1 = \tan \theta_1$ and θ_i ($i = 1, 3 \dots 21$) are the inclinations of the portions of the piano wire in between masses (see Chapter 2).

For the multi-span catenary model (Chapter 6) the proportions of each span are the same as those of the single span fixed-fixed catenary (see Fig. 6.2). A suspension arrangement at the common point of two adjacent spans was devised which, shown in Fig. F.3, allowed certain degrees of freedom at this point. This suspension device also allowed variation of the span/dip ratio of the constituent spans. No attempt was made to represent dimensionally the mass of the suspension arm.

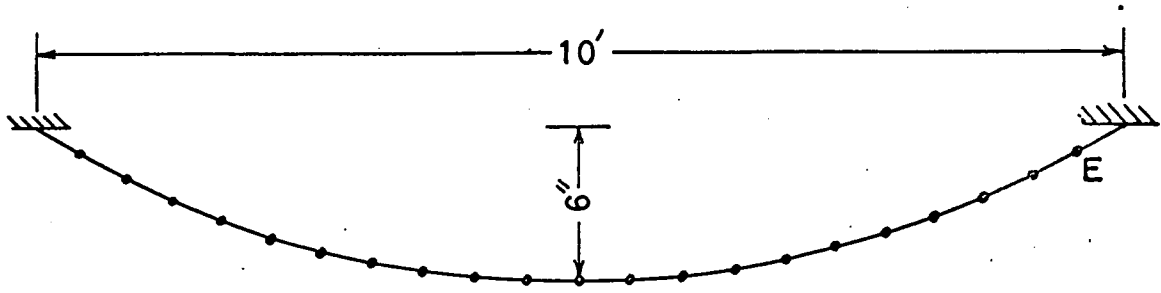
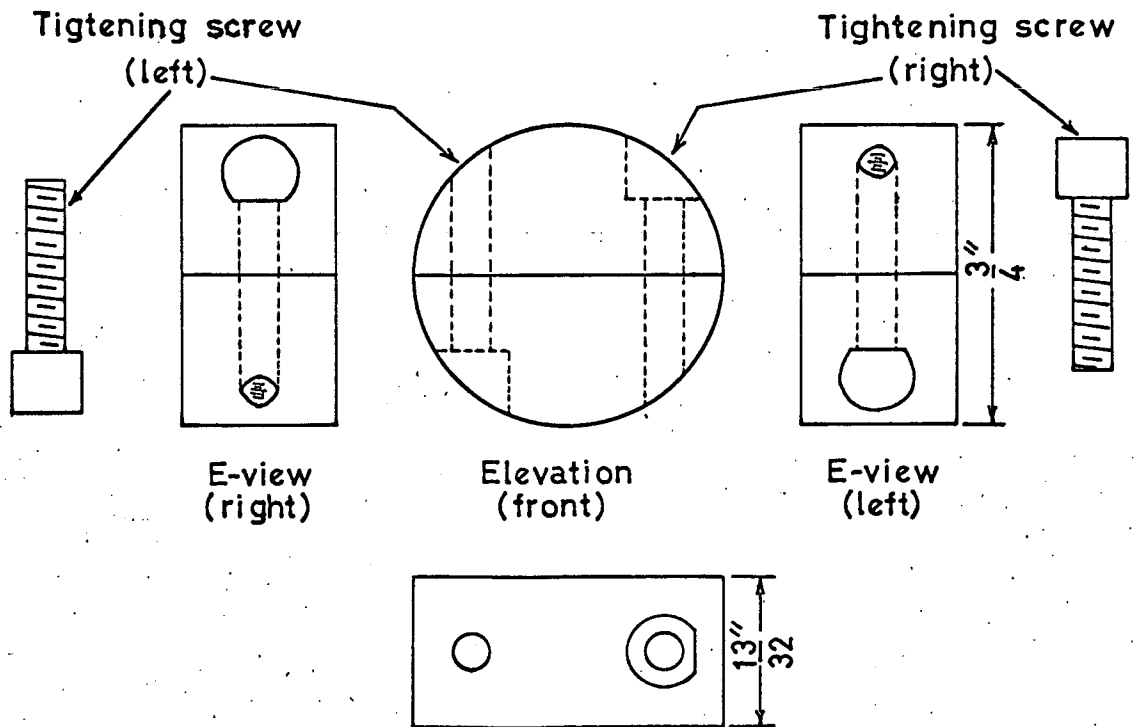


FIG. F.1

E DENOTES POINT OF EXCITATION



PLAN

FIG. F.2

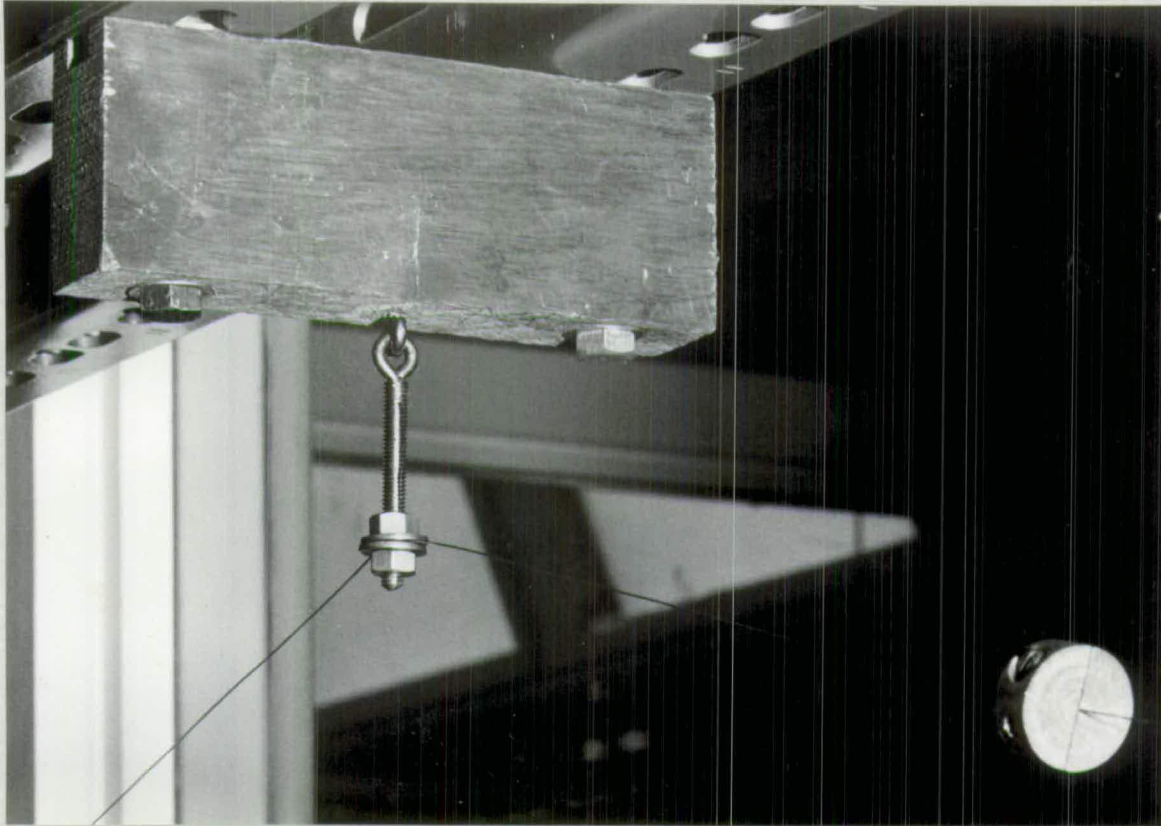


FIG. F.3

A Suspension Device for Three Span
Experimental Model.